

Effects of Large Amphiphilic Ligands upon
the Spectra and Kinetics of
Cytochrome *c* Oxidase

1

by

Jia He

A thesis
submitted to the Department of Biological Sciences
in partial fulfillment of the requirements
for the degree of
Master of Science

August 1992
Brock University
St. Catharines, Ontario

© Jia He, 1992

LIST OF ABBREVIATIONS

2

ATP	: adenosine triphosphate
COV	: sonicated cytochrome <i>c</i> oxidase-containing vesicles
EDTA	: ethylenediamine tetraacetic acid
EPR:	: electronic paramagnetic resonance
FCCP	: <i>p</i> -trifluoromethoxycarbonylcyanide phenylhydrazone
HEPES	: 4-(2-hydroxyethyl)-piperazine-ethanesulphonic acid
K_m	: Michaelis constant
MCD	: magnetic circular dichroism
SMP	: submitochondrial particles
TMPD	: N, N, N,' N,' -tetramethyl-p-phenylenediamine
TMPD ⁺	: Würster's blue
TN	: turnover (μ equivalents per second per μ mol enzyme)
V_{max}	: maximum rate of the reaction

TABLE OF CONTENTS

3

	Page.no
Title page	1
List of Abbreviations	2
Table of contents	3
List of figures	5
List of tables	9
Abstract	10
Acknowledgements	11
Introduction	12
General features of cytochrome oxidase	12
Conformations of cytochrome oxidase	19
Ligands of cytochrome oxidase	21
Ionophores	28
Local anesthetics	33
Materials and Methods	39
List of reagents	39
Purification of enzyme and SMP	40
Preparation of 'pulsed' enzyme	41
Preparation of cyanide- and formate-liganded enzyme	42
Preparation of COV	42
Polarography	43
Spectrophotometry	44
Fluorescence and phosphorescence spectrophotometry	48

Results	5 0	4
Part I : Valinomycin-cytochrome oxidase interaction	50	
A. Spectroscopic effects of valinomycin	50	
B. Kinetic effects of valinomycin	60	
C. Protein fluorescence and phosphorescence study	70	
Part II : Dibucaine-cytochrome oxidase interaction	79	
A. Spectroscopic effects of dibucaine	79	
B. Kinetic effects of dibucaine	99	
Discussion	1 2 0	
Conclusions	1 2 9	
References	1 3 0	

LIST OF FIGURES

5

Fig. no.		Page no.
1.	A model for cytochrome <i>c</i> oxidase function in membrane	13
2.	Membrane orientation of cytochrome <i>c</i> oxidase	15
3.	(a) Structural formula of valinomycin	29
	(b) conformational change of valinomycin upon binding of K ⁺	29
4.	Spectra of high and low spin forms of cytochrome oxidase	51,52
5.	Spectra of the resting and valinomycin-liganded enzyme.	53
6.	Progressive appearance of valinomycin-oxidase complex: Difference spectra(valinomycin-liganded minus resting enzyme)	54
7.	Effect of valinomycin concentration upon the spectral shift of cytochrome oxidase at high & low ionic strengths.	56
8.	Kinetics of valinomycin binding to resting cytochrome oxidase.	57, 58
9.	Effect of cation composition upon the valinomycin- induced spectral shift of cytochrome oxidase	62
10.	Effect of valinomycin upon steady state enzyme activity.	64

11.	Kinetic analysis of the effects of valinomycin upon the ascorbate-cytochrome <i>c</i> -cytochrome <i>aa3</i> -O ₂ steady state.	66	6
12.	Steady state reduction of cytochrome <i>a</i> induced by TMPD: action of valinomycin.	68	
13.	Respiration rates of cytochrome oxidase-containing proteoliposomes: influence of different valinomycin concentrations in presence and absence of FCCP and nigericin.	69	
14.	Fluorescence spectra of cytochrome oxidase ± valinomycin	71, 72	
15.	Phosphorescence spectra of the deoxygenated cytochrome oxidase ± valinomycin	74,75	
16.	NaNO ₂ quenching of phosphorescence of cytochrome oxidase ± valinomycin	76	
17.	Spectral characteristics of dibucaine.	81,82	
18.	Absolute spectra of resting enzyme and dibucaine-liganded enzyme.	83	
19.	Difference spectra of dibucaine-liganded species minus resting enzyme.	84	
20(A).	Time course of dibucaine binding to resting cytochrome oxidase: comparison with formate binding.	86	
20(B).	Analysis of dibucaine binding kinetics : logarithmic plots of the differential absorbance changes.	87	
20(C).	Analysis of formate binding kinetics : logarithmic plots of the differential absorbance changes (±dibucaine).	87	

21.	Effect of the dibucaine concentration on the magnitude of the cytochrome oxidase spectral shift	89
22.	Effect of ionic strength upon the dibucaine-induced enzyme spectral shift	90
23.	The early and late steady state behaviour of cytochrome oxidase in the presence of dibucaine, valinomycin and formate.	93-96
24.	Cytochrome <i>a</i> steady state in the presence of different ligands	98
25.	Effect of dibucaine upon steady state enzyme activity.	100
26.	Kinetic analysis of the effects of dibucaine upon the ascorbate-cytochrome <i>c</i> -cytochrome <i>aa3</i> -O ₂ steady state.	101
27(A).	Fast and slow phases of dibucaine inhibition of cytochrome oxidase	103
27(B).	Kinetics of dibucaine inhibition monitored by the cytochrome <i>c</i> steady state.	104
28.	Effect of dibucaine on the steady state of cytochrome oxidase	105, 106
29.	Effect of dibucaine on the steady states of <i>a</i> and CuA.	108,109
30.	Effect of dibucaine on the steady state behaviour of submitochondrial particles.	111,112
31.	Effect of dibucaine on cytochrome oxidase turnover at high and low ionic strengths: Polarographic study	114
32.	Dibucaine effect on V _{max} values for cytochrome	116

oxidase at high and low ionic strengths.	8
33. Dibucaine effect on K_M values for cytochrome <i>c</i> and cytochrome oxidase at high and low ionic strengths.	118
34. The dibucaine effect on the respiration of reconstituted cytochrome oxidase .	119
35. A scheme for inhibition of electron transport through cytochrome <i>c</i> oxidase to molecular oxygen.	128

LIST OF TABLES

9

Table no.	Page no.
1. Rate constants for valinomycin - cytochrome oxidase interaction	61
2. Comparative study of valinomycin-cytochrome oxidase interaction in different media	63
3. Nitrite quenching of phosphorescence of cytochrome <i>c</i> oxidase \pm valinomycin	78
4. Dibucaine-induced spectral changes in different media	91
5. Comparison of valinomycin- and dibucaine-cytochrome <i>c</i> oxidase interactions	127

ABSTRACT

10

Cytochrome *c* oxidase (ferrocytochrome *c* : O₂ oxidoreductase ; EC 1.9. 3.1) is the terminal enzyme in the mitochondrial electron transport chain, catalyzing the transfer of electrons from ferrocytochrome *c* to molecular oxygen. The effects of two large amphiphilic molecules - valinomycin and dibucaine upon the spectra of the isolated enzyme and upon the activity of both isolated enzyme and enzyme in membrane systems are investigated by using spectrophotometric and oxygen electrode techniques.

The results show that both valinomycin and dibucaine change the Soret region of the spectrum and cause a partial inhibition in a concentration range higher than that in which they act as ionophores. It is concluded that both valinomycin and dibucaine binding induce a conformational change of the protein structure which modifies the spectrum of the *a*₃ Cu_B centre and diminishes the rate of electron transfer between cytochrome *a* and the binuclear centre.

ACKNOWLEDGEMENTS

11

" I once spent a whole day without food and drink, and a whole night without sleep, in order to meditate. I found no advantage in it. It is better to learn. "

Confucius

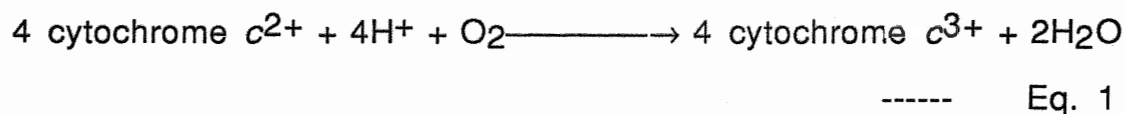
I wish to express my sincere thanks to all those people who have helped me one way or another , both on campus and out of campus during my study in Brock University , especially to my supervisor, Dr. Peter Nicholls and the Department of Biological Science , Brock University. Without their financial support it would have been impossible to start this project, not to mention finish it . Thanks again to Dr. Peter Nicholls. He has opened up an area of science to me that I didnot know before and for that I thank him. I am also grateful for the Differential Foreign Fee Scholarship which I received for one term from the Ontario government. Many thanks to my family that I left behind so far away for so long (22 months). Finally I would like to say " Thank you, you are great !" to those people who have shared a laboratory and its equipment with me during these experiments .

INTRODUCTION

12

I. General features of cytochrome oxidase

Cytochrome *c* oxidase (ferrocytochrome *c* : O₂ oxidoreductase; EC 1.9.3.1) is the terminal enzyme of the electron transport chain located in the eukaryotic inner mitochondrial membrane and the plasma membrane of some prokaryotes. It catalyzes a four-electron reduction of oxygen to water and the oxidation of ferrocytochrome *c*. As the diagram in Fig.1 shows, electrons flow from cytochrome *c* bound at the external("C") face to an oxygen reduction site(Mitchell 1966a) and at the same time a proton electrochemical potential is generated across the membrane by a combination of the consumption of matrix protons during the reduction of oxygen and the translocation of protons from matrix to intermembrane space(Wikström 1977, Chan and Li 1990). The overall reaction can be described as follows :



This proton electrochemical potential is composed of a pH gradient(alkaline inside) and a membrane potential (negative inside), and is utilized to drive the thermodynamically unfavourable synthesis of ATP , via the F₁F₀ ATP synthetase.

Cytochrome *c* oxidase can be purified from many sources, such as bacteria , yeast and mammals. Cytochrome oxidase from

Fig. 1

out (intermembrane space)

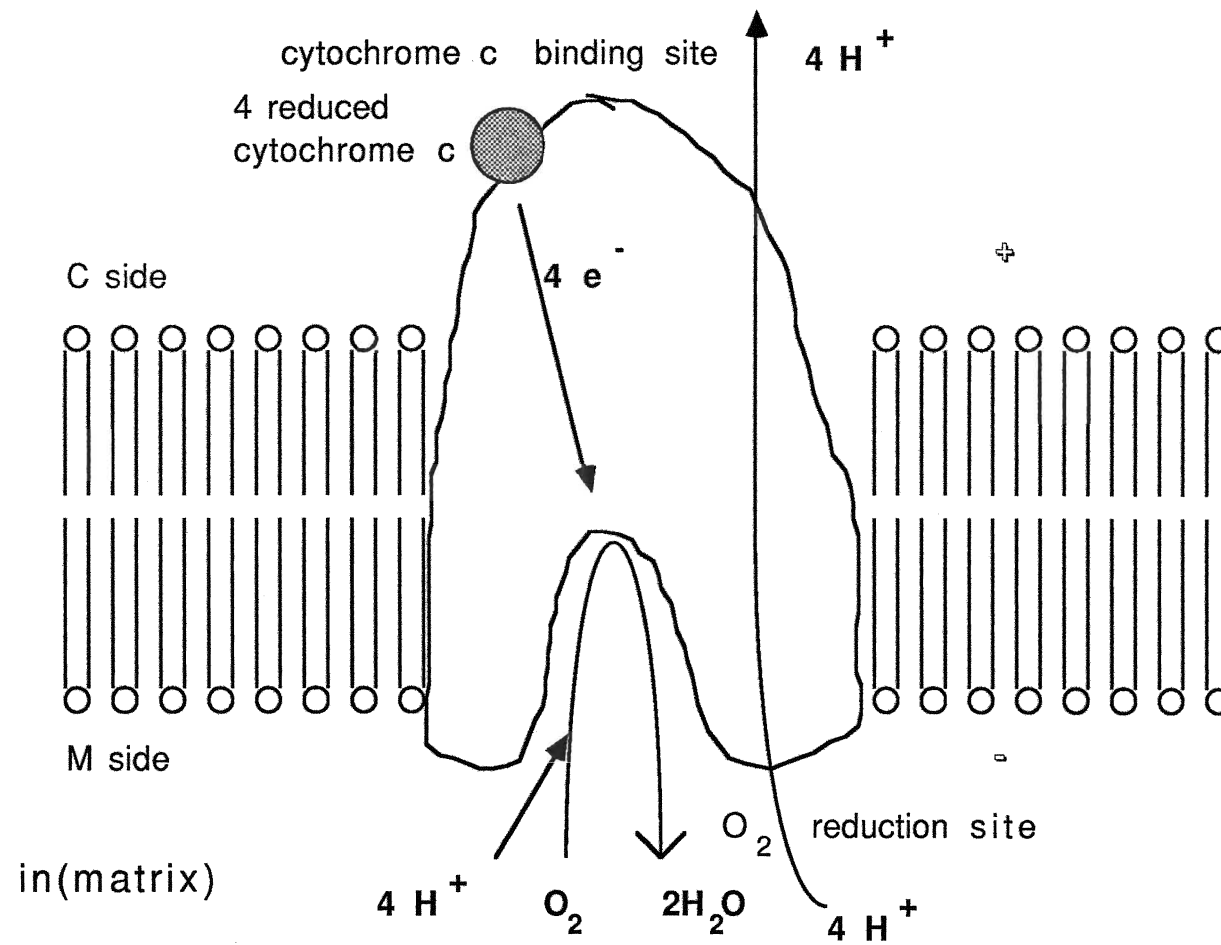


Fig. 1. A model for cytochrome c oxidase function in membranes 13

Adopted from Fig. 1(Cooper 1990). C and M sides are referring to cytosol side and mitochondrial matrix side respectively. The "+" side refers to positively charged side , which in this case is the "C" side. The "-" side refers to negatively charged side, which in this case is the "M" side.

mammals , especially that from bovine heart, has been most extensively studied. It contains 13 polypeptide subunits (Kadenbach et al 1983) and has a molecular weight of 200,000 per monomer. It can also exist as a dimer (Wikström et al 1981). The three heaviest polypeptides , subunits I , II and III are coded by mitochondrial DNA . The smaller polypeptides are coded by nuclear DNA. Chemical labelling , cross-linking and antibody binding have been used to probe subunit structure, orientation in the membrane and interrelationships . The results as reviewed by Cooper et al (1991) are summarized in the scheme of Fig. 2.

Fig. 2 shows how subunits I and III are buried in the hydrophobic membrane and subunit II binds *c* . All the subunits are transmembranous , except for subunit V which faces the matrix and subunits VI and VII which face the cytoplasm.

The eukaryotic enzyme contains two iron-containing haem A groups and two functional copper atoms, Cu_A and Cu_B (Wikström et al 1981). . The two haems are in very different environments (Keilin and Hartree 1939) : haem *a* is usually low spin and does not bind ligands while haem *a*₃ is usually high spin and reacts with various ligands. The two copper atoms are integral parts of the electron transfer apparatus: Cu_A accepts electrons directly from cytochrome *c* (Hill 1990) and Cu_B forms part of the O₂ reduction site with haem *a*₃. The stoichiometry and function of a possible third copper atom "Cu_X" (Steffens et al 1987) are uncertain. The roles of one zinc and one magnesium atom (Einarsdottir and Caughey 1984, 1985) have also not been determined, although Yewey and Caughey (1987) suggested that

Fig. 2

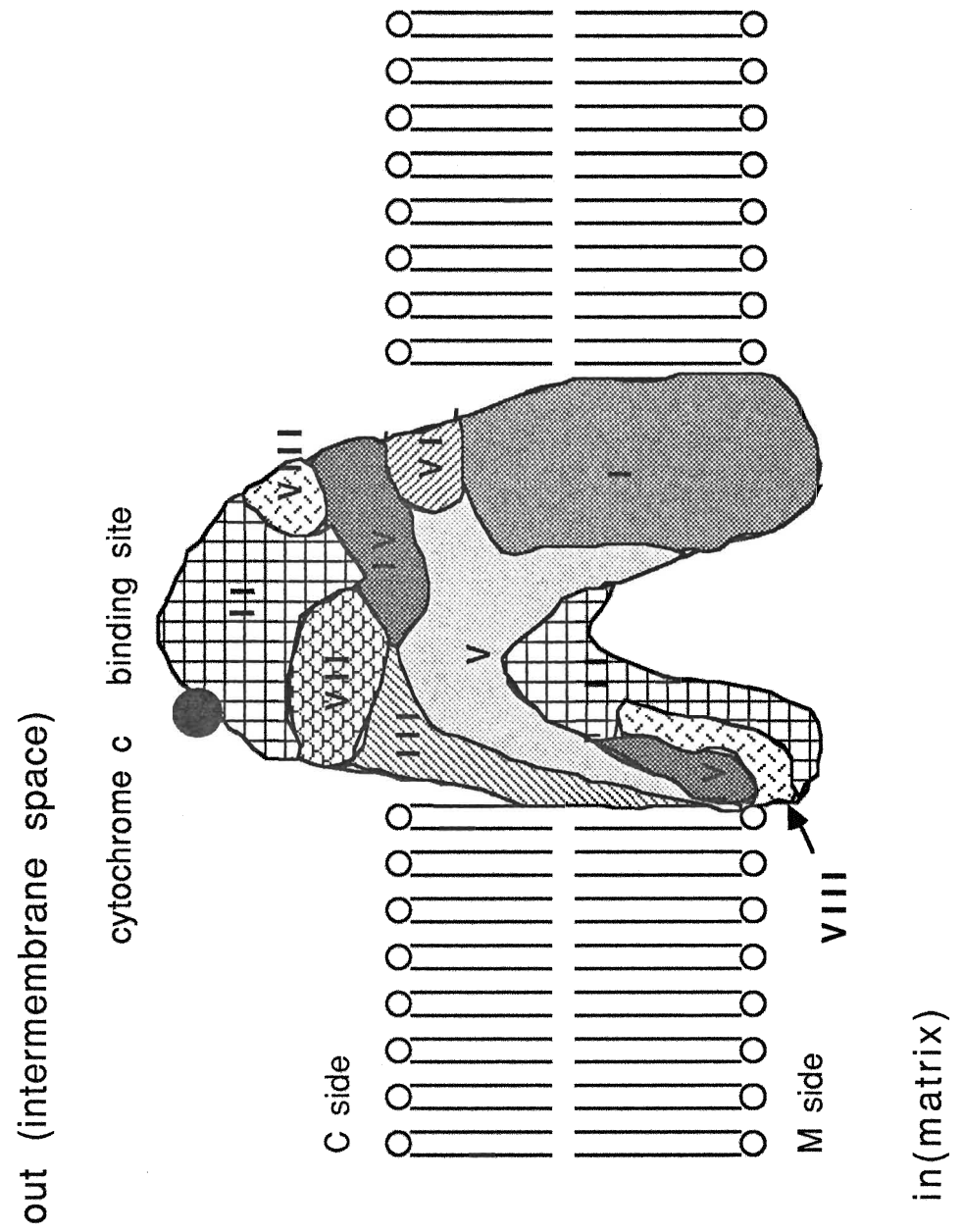


Fig. 2. Membrane orientation of cytochrome c oxidase

15

Adopted from Fig.1(Cooper et al 1991). Different patches represent different subunits and their relative positions when the enzyme is located in membrane. Subunits IX, X, XI, XII and XIII are omitted for clarity.

the intrinsic magnesium might be essential for ATP binding.

16

Direct localization of the prosthetic groups has been harder to achieve as the haems and coppers are labile under the dissociating conditions used to separate subunits via SDS PAGE or similar means. But several pieces of evidence indicate that subunits I and II contain all four redox centers. Firstly, subunit II has an amino acid sequence homologous to that of copper proteins of the plastocyanin type in plant photosynthesis (Colman et al 1978). So the binding site for CuA is presumably in subunit II. This leaves cytochrome *a* and the binuclear center on subunit I. Secondly, bacterial *aa3*-type cytochrome oxidases have a relatively simple subunit composition. In all the bacteria from which such an oxidase has been isolated, no more than four subunits have been found (Poole 1988). The isolated *Paracoccus* oxidase has two subunits which resemble the two largest subunits in the mitochondrial oxidase in their hydrophobicity, immunological cross-reactivity (Ludwig 1982) and sequence homology (Steffens et al 1987). This enzyme is identical or closely similar to the mitochondrial enzyme with respect to electron transfer activity and spectroscopic parameters (Albracht et al 1980). A third loosely associated subunit in the *Paracoccus* enzyme resembles subunit III of mammalian enzyme.

Chemically modified cytochrome *c* derivatives bind covalently to subunit II (Bisson et al 1980). The haem *c* binding subunits of *Thermus thermophilus* (Buse et al 1989) and of PS3 (Ishizuka et al 1990) are also partially homologous with eukaryotic subunit II. So apparently subunit II contains a high

affinity cytochrome *c* binding site . Cytochrome *c* protects subunit II from labelling with water-soluble carbodiimides(Bisson and Montecucco 1982, Kadenbach and Stroh 1984) However , there was also some protection of subunits VII, X, XI, and XIII . This could indicate substrate-induced conformational change or that nuclear subunits play a facilitatory role in cytochrome *c* binding.

Kinetic studies (Cooper 1990) reveal that the reaction does not obey conventional Michaelis-Menten kinetics at low ionic strength. Non-linear Lineweaver-Burk or Eadie-Hofstee plots are obtained which consist of a 'high-affinity, low turnover' phase and a 'low-affinity , high turnover 'phase . That led to the suggestion that there was a second low affinity site for cytochrome *c* on cytochrome *c* oxidase. Erecinska(1977) suggested that subunits V and VI provide a low affinity site. But as both the PS3 (Nicholls and Sone 1984)and *Nitrobacter agilis* enzymes(Fukumori and Yamanaka 1984) possess a kinetically measurable low affinity site, it appears likely that nuclear -coded subunits are not essential parts of the binding site for a second cytochrome *c* molecule. The low affinity site may be comprised of phospholipid, perhaps involving cardiolipin(Trivedi et al 1986).

Subunit III removal does not affect metal content or enzyme turnover(Yewey and Caughey 1987). It also does not dramatically change electron transport or the optical spectrum(Penttila et al 1979, Saraste et al 1980) . Complete removal of subunit III by α -chymotrypsin treatment of the bovine enzyme(Wilson and Prochaska 1990), or cytochrome *c* affinity chromatography of rat

liver enzyme in the presence of lauryl maltoside(Thompson et al 1985) showed that the proton translocation was cut by 50%. The *aa3*-type cytochrome *c* oxidase from *Paracoccus* ,which was originally purified as a two subunit enzyme, had a proton translocation stoichiometry of 0.6 H⁺/e⁻ (Poole 1988). DCCD, the carboxyl-specific protein modifying reagent which binds a glutamic acid residue in a part of the presumed proton translocation channel in ATP synthetase(Hoppe and Sebald 1984), also binds Glu-90, a conserved subunit III residue(Prochaska et al 1981). It is far more effective in inhibiting proton translocation than electron transfer(Azzi et al 1984). This evidence indicates that subunit III is important in modulation of proton translocation . It is also suggested by Haltia et al (1989) to be necessary for the correct assembly of subunit I and II.

The functions of the nuclear coded subunits are less clearly understood. Bisson et al (1987) showed that millimolar concentrations of ATP abolish the high affinity K_m and linearize the Eadie-Hofstee plots. But labelling experiments with carbodiimides showed no ATP-induced change in cytochrome *c* binding to subunit II , the presumed high-affinity *c* binding site , and photo-affinity labelling showed that ATP binds to sites on subunits IV and VII. These results indicate that nuclear subunits may undergo conformational change upon binding ATP. Kadenbach(1986) suggests that allosteric effectors such as ATP can change the activity of cytochrome *c* oxidase by binding to specific sites on nuclear-coded subunits.

In addition to fully oxidized 'resting' enzyme and fully reduced enzyme, cytochrome c oxidase can exist in transient forms, such as 'pulsed' enzyme. This is produced by pulsing O₂ into fully reduced enzyme in the absence of ferrocytochrome c. Brunori et al (1979) demonstrated that the 'pulsed' oxidase accepts four electrons in the conversion to the fully reduced form, and the lag in intramolecular electron transfer is partially or fully relieved. The spectral consequence of pulsing the enzyme is a red shift of the Soret peak. Pulsed enzyme shows a spectral and kinetic resemblance to another transient form, the 'oxygenated' species (Wikström et al 1981). When pulsing the enzyme, a major part of the initial product can be the 'peroxy' form which may contain bound oxygen and two more electrons than the fully-oxidized form. This form then decays to the later 'pulsed' form. (Moody et al 1991).

The cause of the spectral differences between the resting and pulsed oxidase is unclear. SDS-PAGE electrophoresis does not show significant difference in subunit composition between the two species (Crimson 1991). The spectral difference must result from changes in tertiary structure in the vicinity of the redox centers. The similarity of the spectra of cytochrome oxidase and the initial pulsed form led to the proposal that the initial pulsed ('peroxy') enzyme has a low-spin cytochrome a₃ (Wrigglesworth et al 1988). The late-pulsed form may represent an intermediate cytochrome a₃ species in the

relaxation of the initial pulsed enzyme to the resting state. Raman spectroscopy (Babcock et al 1981) has revealed a low spin ferric haem a_3 , but MCD data suggested a high spin state (Babcock et al 1976). This discrepancy may be due to the heterogeneity of the initial pulsed enzyme, evidenced by the decay in minutes from the initial 'peroxy' form to the late form which is stable for several hours. Even the latter form is not homogeneous. Moody et al (1991) claimed that in their 'fast' enzyme preparation, there are at least two subpopulations, while Crinson (1991) also reported that the relationship between the cytochrome a reduction and the enzyme turnover is biphasic, indicating the existence of a low-turnover and a high-turnover forms of the enzyme. Pulsing the enzyme increases the proportion in the high-turnover form. A sulphur atom from a nearby amino acid, a partially reduced oxygen atom, and a water molecule may be the bridging ligands between haem a_3 and Cu_B in the resting, initial pulsed ('peroxy'), and late-pulsed enzymes respectively (Crinson 1991).

It has been generally accepted that the oxidized ('resting') enzyme contains two magnetically isolated spin $S=1/2$ centers, which correspond to the low spin ferric haem a and cupric Cu_A respectively (Wikström et al 1981). It also contains a spin-coupled $S=2$ centre, which can be best interpreted as arising from high-spin ferric haem a_3 ($S=5/2$) antiferromagnetically coupled to cupric Cu_B ($S=1/2$), yielding a binuclear center of spin $S=2$ (Tweedle et al 1978).

Cytochrome *a* is a hexacoordinated haem in which both axial positions are occupied by histidines, so it does not react with exogenous ligands. On the other hand, cytochrome *a₃* is a pentacoordinated haem with only one histidine as its axial ligand, so it can react with various exogenous ligands(Saraste 1990).

Oxidized enzyme in the 'resting' state as isolated is conspicuously unreactive with cyanide, which reacts readily with cytochrome *a₃* under turnover conditions or in partially reduced enzyme(Nicholls and Chance 1974, Erecinska and Wilson 1978). That has led to the suggestion that the sixth axial position of haem *a₃* in resting enzyme is occupied by an endogenous ligand, such as a μ -oxo bridge(Reed and Landrum 1979), or a sulfur atom from a nearby amino acid(Crinson 1991). Reductants will break this ligation and thus lead to higher reactivity with exogenous ligands including cyanide.

The fact that haem *a₃* but not haem *a* binds ligands in both the ferrous and ferric forms has been extensively used to evaluate the individual spectra of the two haems(Wikström et al 1981). Among these ligands, cyanide is the most studied species. Cyanide is a very effective inhibitor of cytochrome *c* oxidase. A stoichiometric amount of cyanide is sufficient to inhibit the enzyme completely(Nicholls and Hildebrandt 1978a). Initially Nicholls and Hildebrandt (1978b) concluded that the binding of a single HCN molecule prevented the reduction of both *a₃* and Cu_B. But later this conclusion was revised(Nicholls and Chanady 1982).

Excess reductant permits the introduction of three reducing equivalents into the cyanocytochrome *aa₃*, i.e. cytochrome *a*, Cu_A and Cu_B can all be reduced in the presence of cyanide.

MCD spectroscopy (Babcock et al 1976) reveals a low spin ferricytochrome *a₃*-HCN complex, but no low spin EPR signal corresponding to this complex is generated in the 'resting' enzyme. However, a low spin cyanide complex signal is detected in the presence of reducing equivalents (Shaw et al 1978).

This is explained by magnetic susceptibility studies (Tweedle et al 1978). When cyanide is added to the oxidized enzyme, a binuclear complex, presumably ferric haem *a₃*-HCN(*S*=1/2)-cupric Cu_B(*S*=1/2), is formed, with coupling between low spin-iron and copper. EPR cannot detect this complex, but MCD can still detect it.

The cyanide induced high to low spin change can also be monitored spectrophotometrically (Nicholls et al 1976), as evidenced by a red shift of the Soret peak upon adding cyanide. The binding of cyanide with oxidized enzyme is very slow, but the values of the rate constants vary considerably.

The problem of heterogeneity in the isolated enzyme has long been a source of discussion (Hartzell et al 1988). Moody et al (1991) claimed that in their enzyme preparation, there is a 'slow' subpopulation in which the haem *a₃* is in the high spin form, and two 'fast' subpopulations in which some haem *a₃* is in the low spin form. The pH used in the preparation has quite a significant influence. Moody et al (1991) argued that the 'fast' and 'slow' forms of oxidase are equivalent to the late 'pulsed' and 'resting'

forms of oxidase. If this is correct, the rate constants obtained by Van Buuren et al (1972), Brittain and Greenwood(1976) and Jones et al (1984) were characteristic of mixed species of the enzyme. Since these authors did not discuss in detail the problem of heterogeneity and the contributions of 'fast' form to their 'resting' preparations, and 'peroxy' form to their 'oxygenated' or 'pulsed' preparations, Mitchell et al (1992) may be correct in suggesting that the earlier enzyme preparations were mixtures of the 'slow'(resting), the 'fast'('pulsed') and the 'peroxy' forms.

Nicholls et al (1976) showed that although the rate of cyanide binding to fully reduced enzyme was more rapid than to fully oxidized species, the rate of onset of inhibition under turnover conditions was at least an order of magnitude greater still. Jones et al(1984) proposed that a transient 2 or 3-electron-reduced form of the enzyme during turnover was responsible for the observed extremely rapid binding. Mitchell et al (1992) examined the rates of binding to the fully oxidized(O), two-electron-reduced peroxy(P) and the three-electron-reduced oxyferryl(F) forms of the enzyme, and concluded that none of these states is responsible for the extremely rapid cyanide binding during turnover. On the other hand, they detected a very small fraction of one-electron-reduced (E state) oxidase within the 'fast' oxidized enzyme they prepared according to the method of Moody et al (1991). This small 'E' fraction has a rate constant for cyanide binding in excess of $10^4 \text{ M}^{-1}\text{s}^{-1}$. It is concluded by these authors to be the species responsible for the rapid binding of cyanide during turnover. The E state, according to them, is not

oxidizable by oxygen, but can be slowly oxidized by ferricyanide. The difference spectrum following incubation with ferricyanide suggested that the electron in the E state is free to equilibrate between the redox centers.

24

The binding of ferricytochrome *c* (or poly-L-lysine) was reported to induce a global protein conformational change that increases the HCN binding rate (Musatov and Konstantinov 1988). But Mitchell et al (1992) found that the cytochrome *c* stimulation of cyanide binding is most significant at intermediate ionic strengths, though the binding of cytochrome *c* to cytochrome oxidase is known to be electrostatic in nature. So the latter propose that the mediation of electron transfer from one-electron-reduced, cyanide-ligated enzyme to the free ferric oxidase by cytochrome *c* or poly-L-lysine, rather than a global protein conformational change, is responsible for the stimulation.

The final word has not been said yet as to which species is responsible for the extremely rapid inhibition by cyanide during turnover. Dioxygen activation and reduction in cytochrome *c* oxidase is a complicated process which can involve as many as 11 transient states of the enzyme (Babcock and Wikström 1992). Intracentre electron transfer means that several species can share the same redox status. Even if we suppose all the species that have been tested are truly involved in this oxidoreduction cycle, there are still too many species left untested. Some transient species might be so thermodynamically unstable that their lifetime is very short, making them difficult to study. For

example, Shaw et al(1978) detected by EPR a high spin ferric haem a_3 which is highly reactive with ligands such sulphide, cyanide and azide when generated by anaerobic oxidation of the reduced enzyme with ferricyanide or porphyrexide. The lifetime of this form is no longer than a few seconds.

I conclude that the higher reactivity with ligands of the enzyme in turnover conditions does not imply that either the 'pulsed' or the 'oxygenated' form is of catalytic significance.

Azide reacts comparatively quickly with the oxidized enzyme in contrast to cyanide(Nicholls and Chance 1974). But its spectral effect upon the enzyme is complex(Nicholls et al 1976). At a low concentration ($< 1\text{mM}$), the spectrum shows a slight blue shift. At higher levels ($> 20\text{mM}$), the Soret peak is shifted towards the red. Since azide is the one ligand which gives rise to both high-and low-spin complexes with other haem proteins(Nicholls 1976), it might be that at low concentration, azide causes a low to high spin shift of haem a_3 , while at high concentration, it has the opposite effect. Neither effect is as marked as those produced by cyanide and formate(formate shifts the Soret peak to the blue (Nicholls 1976)), and in neither case is any EPR-detectable low spin or high-spin haem species formed (Wilson and Leigh 1972). In partially reduced states of the enzyme, EPR identifies a signal indicative of a low spin ferric haem a_3 to which azide is bound. Failure to detect an EPR signal in the 'resting' enzyme-azide complex may be due to a similar cause to that with cyanide. A ferric a_3 -azide($S=1/2$)- cupric $\text{Cu}_B(S=1/2)$ species may be formed with weak ferromagnetic or

antiferromagnetic coupling between low-spin iron and copper.

26

Nicholls and Hildebrandt(1978a) pointed out that while the reduction of cytochrome *a* in the presence of azide under aerobic steady state conditions is almost instantaneous, the high to low spin shift of cytochrome *a₃* , which is characterized by a red shift of the high spin ferric peak in the Soret region, is relatively slow. This transition correlates with a 605nm(ferrous) α peak shift towards the blue of a few nanometers during the steady state. The α peak of fully reduced enzyme in the presence of azide remains at 605nm. The α peak shift does not occur with cyanide, even though , like azide , it gives a low spin(red-shifted) Soret peak. After studying similar effects caused by sulphide and alkyl sulphides, Nicholls and Hildebrandt(1978a) concluded that the α peak shift requires both (i) a low-spin cytochrome *a₃* (ii) a somewhat lipophilic ligand to haem *a₃* . This phenomenon is an important indication of the presence of haem / haem interaction in the enzyme.

Sulphide reacts readily with oxidized cytochrome oxidase , yielding an optical change similar to that induced by cyanide (Nicholls et al 1976), indicative a high to low spin transition of ferric *a₃*, but the red shift of the Soret peak is more marked with increased absorption at 445nm . A signal typical of low spin ferric haem-sulphide compounds is detected by EPR in the oxidized enzyme-sulphide complex(Wilson et al 1976).

Some phenomena , such as the high reactivity with oxidized enzyme , the increase of absorption at 445nm, and the detection of low spin EPR signals in the absence of other reducing agents,

can be readily explained by the partial reduction of the enzyme by sulphide .

27

Formate induces a blue shift of the Soret peak(Nicholls 1976), indicating a high spin ferric haem a_3 -formate complex. This was confirmed by an EPR study(Babcock et al 1976). In contrast to resting enzyme , cyanide- liganded or azide-liganded enzyme, formate apparently keeps haem a_3 in a high spin state whether haem a is reduced or not(Nicholls 1976). Competitive binding was found between the formate and azide pair (Nicholls 1975), and the formate and cyanide pair (Nicholls 1976).

Moody et al (1991) report that incubation of their 'fast' oxidase with formate produces a form of the enzyme with spectral and kinetic properties almost identical to those of 'slow' oxidase .These include the Soret peak position, the slow binding with cyanide and the lag in intramolecular electron transfer. These authors suggested that formate may mimic a binuclear center ligand which is present in the 'slow' form of cytochrome oxidase. Schoonover and Palmer(1991) also reported that the 'g=12' signal , which is characteristic of high-spin haem a_3 in 'slow' oxidase, reappears after adding formate to 'fast' oxidase. Although formate gives no spectroscopic sign of haem-haem interaction , like cyanide it does show kinetic evidence of such interactions(Nicholls 1976). Its affinity for the ferric high-spin a_3 declines as haem a becomes more reduced, while the affinity of cyanide for the ferric low-spin a_3 increases as haem a becomes more reduced. So the redox state of haem a can influence the affinity of formate and cyanide for ferric haem a_3 .

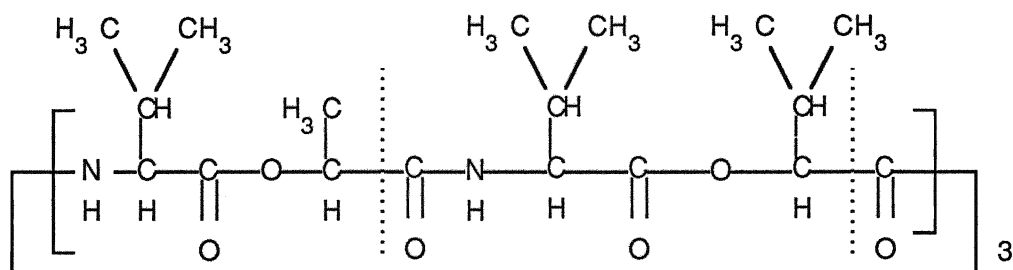
IV. Ionophores

Ionophores are lipid-soluble molecules that greatly decrease the electrical resistance of lipid bilayer membrane (Cramer and Knaff 1991). They can be classified as (i) mobile carriers such as nigericin, FCCP and valinomycin whose activity is frozen out at temperatures below the membrane lipid phase transition due to their mobile nature (ii) channels such as gramicidin whose activity is relatively insensitive to temperature in membranes with a phase transition.

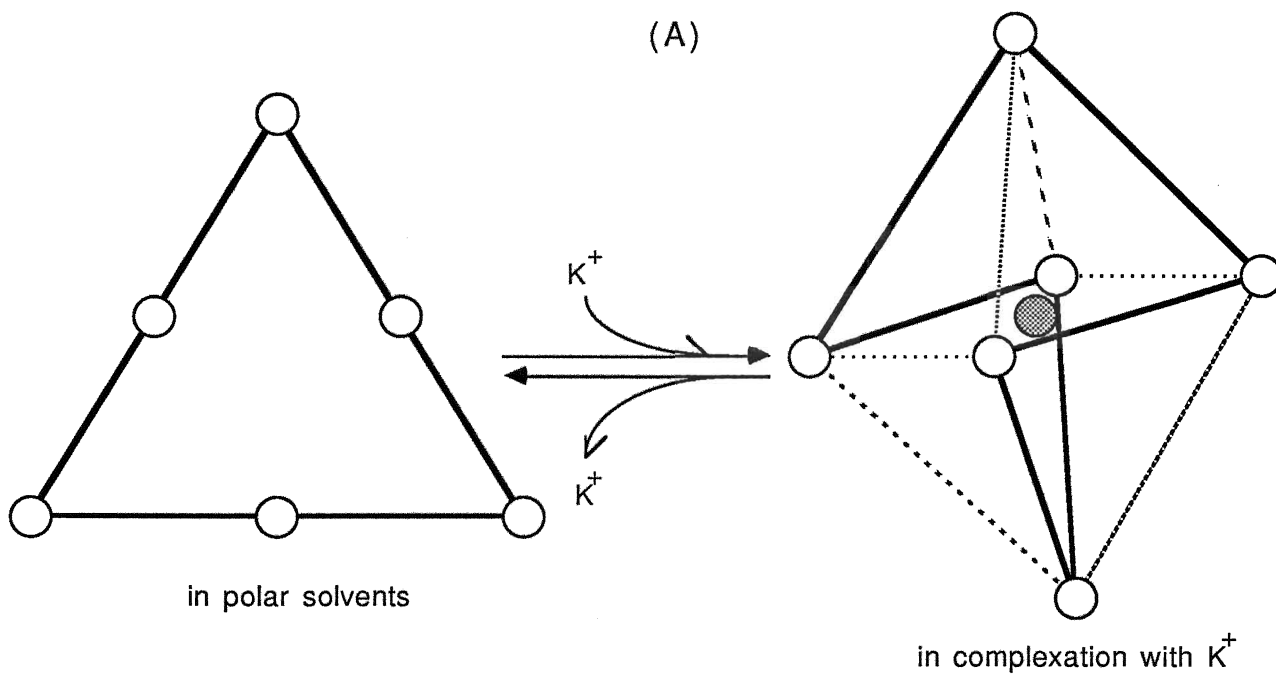
Valinomycin (see Fig. 3 for its molecular structure) is one of a group of antibiotics produced by *Streptomyces*. It contains three repeating units of (L-lactate)-(L-valine)-(D-hydroxyisovalerate)-(D-valine). The dehydrated K^+ ion is coordinated precisely and specifically (the cation specificity is $Rb^+ > K^+ \gg Na^+ > Li^+$) to carbonyl groups in the hydrophilic interior of the macrocycle, whose exterior is nonpolar and thereby soluble in the membrane bilayer. Because of its K^+ carrying ability, valinomycin dissipates the membrane potential $\Delta\psi$ in the presence of K^+ . It has been extensively used in mitochondrial and reconstituted systems to investigate the effect of a membrane potential $\Delta\psi$ upon the activity of the respiratory chain.

Mitchell(1966b) proposed that cytochrome oxidase generates an electrochemical proton gradient $\Delta\mu_{H^+}$ by catalysing

Fig. 3



(A)



(B)



-  carbonyl oxygen atom
-  potassium ion

Fig. 3. (a) **Structural formula of valinomycin**

29

Adopted from Fig. 3.32B (Cramer and Knaff 1991).

(b) conformational change of valinomycin upon binding of potassium ion

The six carbonyl oxygen atoms in valinomycin are in one plane when valinomycin is dispersed in polar solvents(Ovchinnikov 1974) in the absence of K^+ . In the presence of K^+ , the six carbonyl oxygen atoms coordinate with a K^+ and undergo conformational change, resulting a octahedral shape.

e^- transfer from ferrous cytochrome *c* on the C side of the membrane and H^+ transfer from the M side to the haem a_3/Cu_B center, where electrons and protons were consumed in the reduction of dioxygen to water. This is thermodynamically equivalent to translocation of one H^+ from the M side to the C side per transferred e^- , even though no H^+ ions are released on the latter side(Wikström et al 1981).

Later it was found that cytochrome *c* oxidase catalyses true H^+ translocation with uptake of $2H^+/e^-$ on the M side, release of $1 H^+/e^-$ on the C side of the membrane and consumption of $1 H^+$ in the reduction of O_2 (Wikström 1977, Proteau et al 1983). The H^+ pumping activity, i.e. the acidification of the medium after a ferrous cytochrome *c* pulse, cannot be seen in the absence of valinomycin. The reason seems to be that as a K^+ carrier, valinomycin markedly increases the K^+ permeability over the H^+ permeability to the membrane. But recently Steverding and Kadenbach(1989) reported that valinomycin not only acts as a ionophore, but also binds cytochrome oxidase tightly with a stoichiometry of 1:1. This binding has both spectral and kinetic consequences. The difference spectrum shows that valinomycin induces a red shift of the Soret peak of the oxidized enzyme, an effect which is superficially similar to that achieved by adding cyanide to the enzyme or pulsing the enzyme. The same spectral change was also observed using isolated cytochrome oxidase from *Paracoccus denitrificans*, which contains only subunits I and II(a third subunit was probably lost during purification). Since subunits I and II from *Paracoccus denitrificans* are

analogous to subunits I and II from beef heart enzyme, the authors suggested that valinomycin binds to one of the two catalytic subunits of cytochrome oxidase.

Steeverding and Kadenbach(1989) also found that the stoichiometry of H^+ pumped / e^- transferred reached a maximum in cytochrome oxidase vesicles when the stoichiometry of valinomycin : cytochrome oxidase reached 1 . In the absence of valinomycin, only an alkalinization of the medium was observed, due to rapid proton uptake. They concluded that the translocation of K^+ ions occurs via the enzyme-bound ionophore. It was also suggested that the H^+ pumping activity of the enzyme might result from a change of catalytic properties of the reconstituted cytochrome oxidase after binding of valinomycin.

This view was later supported by a comparative study of valinomycin and nonactin(Steeverding and Kadenbach 1990). Nonactin, another K^+ carrying ionophore , stimulated the passive influx of H^+ into the vesicles which didnot contain cytochrome oxidase at a greater rate than valinomycin did when HCl was added to the medium containing vesicles , suggesting that it might be a more powerful K^+ carrier than valinomycin. The spectral shift and stimulation of the respiration rate of the reconstituted cytochrome oxidase induced by nonactin were nevertheless lower than those induced by valinomycin. This apparent contradiction was also explained by assuming that besides being a K^+ carrier, valinomycin binds the enzyme directly and modifies its catalytic activity.

Another comparative study was done using valinomycin and

the channel-forming ionophore gramicidin(Prochaska and Wilson 1991). At low concentrations, gramicidin achieved an almost identical H^+/e^- stoichiometry to that of valinomycin when ferrous cytochrome *c* was added to oxidase-containing proteoliposomes; at a high concentration, however, only an alkalization was observed. Since the ion selectivity of gramicidin channels is $H^+ > K^+$ (Cramer and Knaff 1991) there is some doubt as to which ion was translocated to dissipate the $\Delta\psi$ during these experiments. But Prochaska and Wilson (1991) argued that as there are 10^6 more K^+ ions than protons, K^+ ions were dissipating the $\Delta\psi$ at low gramicidin concentrations while at higher concentrations, H^+ ions were also translocated.

Since no spectral shift was found with gramicidin even at a high concentration, and the concentration required to stimulate proton translocation is 40-70 fold less than with valinomycin, Prochaska and Wilson (1991) suggested that gramicidin does not bind the enzyme, or at least not in the same fashion. As it achieves an almost equal H^+/e^- ratio to that induced by valinomycin, this suggests that cytochrome oxidase is truly a redox-associated proton pump with the previously determined H^+/e^- ratio of one.

A similar valinomycin-induced red shift in the oxidized difference spectrum is also observed in phospholipid vesicles containing subunit III-deficient cytochrome oxidase(Prochaska and Wilson 1991), further supporting the idea that valinomycin binds with either subunit I or II as suggested by Steverding and Kadenbach(1989).

Local anesthetics such as lidocaine, tetracaine and dibucaine are used for anesthesia as well as in the treatment of cardiac arrhythmias (MacDonald and Wann 1978). They depress nerve action and cardiac signal conduction probably by blocking ion (Na^+ , K^+ and Ca^{2+}) channels in the membrane. Their effects are not limited to nerves, since they also affect a variety of other systems, including the respiratory chain in mitochondria (Chazotte and Vanderkooi 1981). Among these anesthetics, dibucaine is one of the most potent, whether in depressing nerve actions (Singer 1980) or inhibiting the respiratory chain (Chazotte and Vanderkooi 1981).

Altogether, four different kinds of local anesthetic effects have been suggested in the literature:

- (1) interaction with lipid bilayers (Eftink et al 1985);
- (2) interaction with lipid molecules intimately associated with the protein (Chazotte and Vanderkooi 1981);
- (3) direct interaction with the protein without mediation of lipid (Chazotte et al 1982);
- (4) action as an uncoupler (Grouselle et al 1990).

Chazotte and Vanderkooi (1981) found that local anesthetics inhibit all segments of the respiratory chain in mitochondria, with NADH dehydrogenase (Complex I) being the most sensitive, and cytochrome c oxidase (Complex IV) the least sensitive region. They also found that the 50% inhibitory

concentrations are inversely proportional to water solubility, suggesting that hydrophobic interactions may be of importance in determining the strength of interaction of the various agents with the enzyme . Concentrations of agents required for inhibition are too low to cause a general perturbation of the lipid bilayer, and inhibition by different anesthetics occurs in different concentration ranges. This implies a degree of specificity which cannot be accounted for in terms of lipid bilayer perturbation. These authors concluded that local anesthetics either interact directly with the protein or with the lipid molecules intimately associated with the protein. It was also found that the inhibitory potency increases with the temperature.

The dibucaine - cytochrome *c* oxidase interaction was also studied by thermal analysis(Vanderkooi and Chazotte 1982). It was found that inhibition by dibucaine increases with increase of temperature. The authors suggested that dibucaine inhibits the enzyme activity by causing a reversible perturbation of protein conformation whose magnitude is much smaller than that which accompanies thermal denaturation.

Apart from the inhibitory effect,, local anesthetics have also been reported to uncouple oxidative phosphorylation in isolated mitochondria (Dabadie et al 1987). Using a fluorescent dye, Grouselle et al (1990) demonstrated that local anesthetics , such as dibucaine, can reach mitochondria when applied to a cell culture medium . This process depends on their lipid-solubility and can be enhanced by the presence of a lipophilic anion such as

TPB⁻. Local anesthetics have the same effects on mitochondria inside the cells as on isolated mitochondria, i. e. they can decrease, and probably even collapse, the mitochondrial transmembrane potential. These effects of local anesthetics are reversible.

35

Singer(1980) studied the effects of four cationic local anesthetics on isolated cytochrome *c* oxidase . He found that benzocaine, the one uncharged anesthetic, had no detectable effect on enzyme function , while other three species cause a mixed type of inhibition, with the relative order of potency being dibucaine>tetracaine>procaine. He suggested an electrostatic interaction , but also pointed out that since procaine, dibucaine and tetracaine have similar pK values, inhibitory potency cannot be explained by such an electrostatic interaction alone.

Noticing that the inhibitory constants (K_i values) are very similar to the anesthetic concentrations required to double the width of the endothermic transition of dipalmitoylphosphatidylcholine liposomes, Singer(1980) proposed that both electrostatic and hydrophobic interactions occur, with the charged portion of the anesthetic molecule competing with the cytochrome *c* for binding while hydrophobic interactions between the anesthetic and oxidase-associated phospholipids form non-productive substrate-enzyme complexes.

Singer(1982) found that at pH 7.4 dibucaine behaved as an uncompetitive inhibitor of the isolated enzyme, while at pH 6.0 the inhibition pattern became mixed in type. Positively charged

dibucaine may act predominantly by competing with cytochrome *c* while the uncharged species interacts with the oxidase boundary lipid to form a non-productive complex.

36

The effect of dibucaine on cytochrome oxidase proteoliposomes was similar to that with isolated enzyme, but less marked. This 'protective' influence of the bulk bilayer might represent a dilution effect, i.e. binding of some of the local anesthetic by the bilayers.

In a follow up study, Singer(1983) showed that local anesthetics such as dibucaine and tetracaine had a much greater inhibitory effect on the stimulated (ionophore-treated) than on the unstimulated proteoliposome enzyme. The inhibition pattern of stimulated oxidase proteoliposomes is non-competitive with respect to cytochrome *c* concentration. Pretreating proteoliposomes with local anesthetics completely prevented the stimulating effects of ionophores, such as valinomycin+ FCCP. Singer(1983) suggested that this was due to the interaction between local anesthetics and the phospholipid component of the enzyme, which results in reduced internal electron transfer and dissociation of the oxidase from the regulatory role of the pH gradient.

Casanovas et al (1983) investigated the effects of eight species of local anesthetics on isolated cytochrome *c* oxidase. The inhibition varied from competitive through mixed to a non-competitive type. The patterns depended on anesthetic concentrations. These authors concluded that reagents presenting a strong anesthetic activity and existing in an ionized state bind

electrostatically to the enzyme at the cytochrome *c* binding site, or to a site nearby . They also observed a linear correlation between enzyme affinity and the octanol-water partition coefficient of the anesthetics . So hydrophobic interactions are also involved , and the interaction between enzyme and weakly ionized molecules may be mainly hydrophobic in nature. These conclusions are however weakened by the existence of quite a few exceptions.

A different model was offered by the same group(Casanovas et al 1985)in a study using the same local anesthetics . Here it was proposed that the binding site of local anesthetics is the phospholipids attached to cytochrome *c* oxidase . Strongly ionized molecules can bind to a peripheral site of the lipid phase surrounding the protein and therefore modulate the enzyme activity, resulting in mixed or non-competitive type of inhibition. This inhibition is relatively weak and may be electrostatic in nature. Weakly ionized and lipophilic molecules can compete with cytochrome *c* for binding at the active site located closer to the lipid hydrophobic phase. This inhibition is relatively strong and may involve both electrostatic and hydrophobic interactions.

Stringer and Harmon(1990) found that upon adding the artificial electron donors ascorbate and TMPD to intact mitochondria in the presence of dibucaine , the 604nm peak was nearly fully formed, but the 445nm peak only developed half of the height of that in the absence of dibucaine. Since 80-90% of the absorbance of reduced oxidase at 604nm is due to ferrous

cytochrome *a*, and the rest to *a*₃, while both cytochromes absorb equally at 445nm (Yonetani 1960), it was concluded that dibucaine inhibited electron transfer between the two cytochromes, allowing reduction of cytochrome *a* but not of *a*₃. The midpotentials of cytochromes *c*, *a* and *a*₃ are not affected by dibucaine. Dibucaine does not alter the absorbance maxima of cytochrome *a* and *a*₃. On the other hand, the reduction of CuA was hampered by dibucaine. So Stringer and Harmon (1990) propose that the attacking site of dibucaine was located neither on cytochrome *a* nor on cytochrome *a*₃, but on CuA.

Neither valinomycin nor dibucaine is a conventional oxidase ligand. Both are large molecules with multiple effects and no exact binding sites have been determined. In this thesis, the following questions are addressed: (i) what is the relationship between the dual role of valinomycin as enzyme ligand and as ionophore? (ii) do the results obtained by Steverding and Kadenbach (1990) demonstrate a relation between ligand binding and charge separation in the oxidase? (iii) what are the relationships between the roles of dibucaine as enzyme inhibitor and as membrane-perturbing agent? and (iv) do the results of Stringer and Harmon (1990) demonstrate a unique relation between dibucaine binding and electron transfer in the oxidase? The work described uses oxygen electrode, spectrophotometric, and fluorimetric techniques to study effects of valinomycin and dibucaine upon the enzyme in order to understand better the relationships between their roles as protein ligands and enzyme inhibitors and as membrane perturbants and ionophores.

MATERIALS AND METHODS

39

LIST OF REAGENTS:

Reagent	Supplier
Acetic acid (1N solution)	Fisher Scientific
Ammonium sulphate	BDH
Antimycin A(from <i>Streptomyces kitazawaensis</i> , crystalline)	Sigma
Ascorbate (L-ascorbic acid, sodium salt)	Sigma
Asolectin (Type IV-S, phosphatidylcholine)	Sigma
Catalase (EC 1.11.1.6) from Bovine liver	Sigma
Cholate (Cholic acid, sodium salt)	Sigma
Cytochrome <i>c</i> (Horse heart , Type VI)	Sigma
Dibucaine hydrochloride	Sigma
EDTA (Ethylenediamine tetraacetic acid, disodium salt)	Sigma
FCCP(<i>p</i> -trifluoromethoxycarbonylcyanide phenylhydrazone)	Dr .P .Heytler (Dupont Chem.)
D-Glucose	BDH
Glucose oxidase(EC 1.1.3.4.)from <i>Aspergillus niger</i> Type X	Sigma
HEPES(4-(2-hydroxyethyl)piperazineethanesulphonic acid)	Res.Organ.
Hydrochloric acid	Fisher Scientific
Lauryl (n-dodecyl-b-D) maltoside	Sigma
Nigericin	Calbiochem.
Potassium cyanide	BDH
Potassium dihydrogen orthophosphate	BDH

Potassium ferricyanide	Fisher Scientific	40
<i>di</i> -Potassium hydrogen orthophosphate	BDH	
Potassium hydroxide(1 N solution)	Fisher Scientific	
Potassium sulphate	BDH	
Sephadex G-25(Bead size 50-150 μ M)	Sigma	
Sodium borate	J.T.Baker	
Sodium dithionite	BDH	
Sodium formate	BDH	
Sodium hydroxide	Fisher Scientific	
Sodium nitrite	BDH	
Sodium phosphate .Monobasic	Sigma	
Sodium phosphate. Dibasic	Sigma	
Succinic acid (disodium salt)	Sigma	
TMPD(N,N,N,' N,'-tetramethyl-p-phenylenediamine. Dihydrochloride salt)	Sigma	
Tween-80	Sigma	
Valinomycin	Sigma	

* All reagents were of Analar™ grade or equivalent.

Purification of beef heart cytochrome c oxidase and submitochondrial particles

The enzyme preparation used throughout these studies was beef heart mitochondrial cytochrome c oxidase. The enzyme was purified according to the method of Kuboyama et al (1972). After connective and fat tissue has been removed , the beef heart is thoroughly minced and then washed several times in 5 mM sodium

phosphate, pH 7.4 . Submitochondrial particles are prepared from the washed mince according to the method described by Brodie and Nicholls (1970). The enzyme was isolated from these particles by differential detergent solubilization, initially in cholate and finally in Tween-80, and repeated ammonium sulphate fractionation. Tween-80 was used instead of the Emasol used by Kuboyama et al(1972) . The final enzyme preparation was stored in 100mM sodium phosphate, pH7.4 , 0.25% Tween-80 at -70°C.

The haem *a* /protein ratio of submitochondrial particles is 1.1 μ moles haem *a* /gram of protein. The haem *a* /protein ratios of the purified enzyme preparations used were 8.5-9.0 μ moles haem *a* /gram of protein. The concentration of protein was determined using the Biuret method (Gornall et al 1949). The concentration of cytochrome oxidase(two haems: *a* and *a₃*)was determined using an extinction coefficient of 27mM⁻¹cm⁻¹ for reduced minus oxidized enzyme at 605-630nm(Nicholls 1978) .

The concentration of the stock purified enzyme was between 400 and 700 μ M. The maximal turnover numbers were 470-580 μ M e⁻ μ Maa₃⁻¹sec⁻¹ in 50mM potassium phosphate, pH 7.4 at 30°C.

Preparation of pulsed cytochrome oxidase.

Pulsed cytochrome oxidase was prepared according to the method described by Crinson and Nicholls (1992). Pulsed cytochrome oxidase is 'resting' oxidase which has been fully reduced and then exposed to oxygen. Sephadex G-25 beads were swollen by overnight stirring in excess 50mM potassium

phosphate, pH 7.4 (30ml / g Sephadex G-25). The swollen beads were then poured into a glass column to form a 10cm × 1.5cm Sephadex G-25 gel filtration column. Purified oxidase in 50mM potassium phosphate , pH 7.4, 0.015% lauryl maltoside was reduced by the addition of 1.0mg/ml sodium dithionite and left on ice for 30 min to ensure complete reduction of the oxidase. Catalase (2000units/ml; one enzyme unit will decompose 1 μ mole H₂O₂ per min at pH 7.0 at 25 °C) was added to the mixture to ensure that any hydrogen peroxide was rapidly removed . The fully reduced enzyme was then loaded onto the column, which had been equilibrated with 50mM potassium phosphate , pH 7.4, 0.015% lauryl maltoside. This same air-saturated buffer medium was used to wash the enzyme through the column , the eluted enzyme being in the pulsed form as determined spectroscopically. The initial product has a Soret peak at 426nm and is unstable, as evidenced by the gradual blue shift of the Soret peak to 422nm, but this 422nm species is stable for at least 3 hours.

Preparation of cyanide-liganded and formate-liganded cytochrome oxidase .

Cyanide-liganded and formate-liganded cytochrome oxidase were formed by incubating 0.12 mM oxidase with 40 mM HCOONa or 2mM KCN respectively in 50 mM potassium phosphate , pH 7.4 containing 0.015% lauryl maltoside. The mixtures were incubated at 4°C for 48 hours and then diluted to the desired concentrations in 50 mM potassium phosphate, pH 7.4 , 0.015% lauryl maltoside for use in the assays.

Preparation of vesicles containing cytochrome oxidase

43

Sonicated vesicles containing cytochrome oxidase were prepared according to the method of Proteau et al (1983). 250 mg L- α -phosphatidyl choline(L- α -lecithin from soybean, Sigma P-3644) were dispersed in 5.0 ml 50 mM potassium phosphate, pH7.4 using a whirlimixer. To this was added 5 μ M enzyme.

This mixture was sonicated using a Heat Systems Sonicator : 3/4 inch probe, 30 % duty cycle, power 3, for 9 minutes. The sample was kept on ice and under a stream of nitrogen during sonication . The sonicated mixture was centrifuged at 13,000 rpm for 10 minutes , using the SS-34 rotor in the Sorvall RC-5 or the 870 rotor in the IEC B-20A centrifuge(temp. range 2-7°C). The clear supernatant from this spin was taken as the sonicated vesicles. Using the method described by Nicholls et al (1980), it was determined that total cytochrome oxidase concentration in the vesicles was between 3.6 μ M and 4.1 μ M , and 49% to 50% of the cytochrome *c* reaction sites were on the outside of the vesicle membrane. The respiratory control ratio was between 5 and 6.5.

Polarography

Turnover studies were carried out by measuring the oxygen consumption polarographically with a Clark type oxygen electrode(Yellow Springs Instruments) connected to a polarizing box (Brock University electronics shop). The signal was measured on either a Radiometer Rec 61 Servograph or a Cole-Parmer Versagraph chart recorder. The reaction vessel was a 4.3 ml

chamber which was magnetically stirred and thermostatically controlled by a water jacket. When the electrode was placed in the reaction vessel, air was excluded from the chamber, leaving only a small opening for injection of substrates using a Hamilton syringe.

44

Spectrophotometry

I. Spectra of cytochrome c oxidase derivatives

(a) titrations with valinomycin and dibucaine

Desired concentrations of cytochrome oxidase were added to a 1cm-lightpath, 1ml-volume quartz cuvette. Aliquots of valinomycin or dibucaine were added and spectral changes were monitored. Spectra were obtained using a Beckman DU-7 spectrophotometer and stored for later analysis, using a linked Apple II+ or Apple IIGS computer via a domestic data acquisition programme (Chanady et al 1985). Appearance of low spin cytochrome a_3 was followed using the 433-413nm wavelength pair. For valinomycin, the apparent dissociation constant, $K_d(\text{app})$, and the extinction coefficient $\Delta E_{\text{mM}433-413\text{nm}}$ were obtained by fitting the data to a user-defined 'Binding' function in the Multifit™ v.2.00 (Day Computing, Inc., Milton, Cambridge, UK) package on a Macintosh Classic 68000 device. The derivation of this 'Binding' function is as follows:

$$K_d(\text{app}) = [e][L]/[eL] \quad \text{Eq. 2}$$

Where $[e]$ is the free enzyme concentration, $[L]$ is the free ligand concentration, $[eL]$ is the enzyme-ligand complex concentration.

Since $[e]_t = [e] + [eL]$, $[L]_t = [L] + [eL]$ (where $[e]_t$ is the total

enzyme concentration, $[L]_t$ is the total ligand concentration), Eq. 2 45
can be rewritten as

$$K_d(\text{app}) = [e]_t - [eL] \cdot ([L]_t - [eL]) / [eL] \quad \text{Eq. 3}$$

$$E_{mM} = \Delta A / [eL] \quad \text{Eq. 4}$$

Where ΔA is the spectral change induced by the ligand, E_{mM} is extinction coefficient of this spectral change.

Substituting $[eL]$ with $\Delta A / E_{mM}$ according to Eq. 4, Eq. 3 can be again rearranged as :

$$\Delta A = E_{mM} \cdot \{ ([e]_t + [L]_t + K_d) - \text{SQRT}(\text{SQR}([e]_t + [L]_t + K_d) - 4 \cdot [e]_t \cdot [L]_t) \} / 2$$

-----Eq. 5

Where SQRT is the square root of the operand . SQR is the square of the operand. Eq. 5 is the 'Binding' function.

For dibucaine, $K_d(\text{app})$ and $E_{mM433-413\text{nm}}$ were obtained both by fitting data to Eq. 5 and by using a double reciprocal plot , and the results were compared. It is not possible to determine $K_d(\text{app})$ and $E_{mM433-413\text{nm}}$ for valinomycin by a simple double reciprocal plot since the valinomycin concentration used was comparable to the enzyme concentration used.

(b) Dual wavelength spectrophotometric study of the kinetics of valinomycin and dibucaine binding with cytochrome oxidase

The kinetics of valinomycin binding with the resting enzyme were followed by monitoring the spectral change at the 433-413nm wavelength pair using an Aminco DW2 UV/Vis spectrophotometer, in dual wavelength mode, linked to a Compaq 286 computer with an Olis™ data acquisition package. Different

concentrations of valinomycin were added to 4 μ M enzyme in a 1cm-lightpath , 3ml-volume quartz cuvette to start the reaction. The apparent rate constants k_{app} for the binding were obtained by fitting the trace to a appropriate function in the Olis™ fitting programme.

The kinetics of dibucaine binding with the resting enzyme were studied by adding 1.5mM dibucaine to 5 μ M enzyme, then monitoring the spectral change at the 433-413nm wavelength pair using an Aminco DW2 UV/Vis spectrophotometer(in dual wavelength mode), linked to a Compaq 286 computer with an Olis™ data acquisition package. A 1cm-lightpath, 1ml-volume quartz cuvette was used. Dibucaine binding with the enzyme in turnover conditions was studied by monitoring the steady state of cytochrome *c* reduction. Active enzyme concentrations during the shifting cytochrome *c* steady states which accompany dibucaine binding were analysed by the method of Nicholls et al (1974), treating the active enzyme species as having a concentration proportional to the function $[c^{2+}]_o[c^{3+}]_t/[c^{3+}]_o[c^{2+}]_t$, where $[c^{2+}]_o/[c^{3+}]_o$ is the ratio of reduced to oxidized cytochrome *c* immediately before dibucaine(the enzyme inhibitor) addition, and $[c^{2+}]_t/[c^{3+}]_t$ is the corresponding ratio at any subsequent time.

II. Spectra of cytochrome *c* oxidase during turnover

(a) Steady state spectral scan.

The spectra of cytochrome *c* oxidase during turnover were studied by a Beckman DU-7 spectrophotometer and stored for

later analysis, using a linked Apple II+ or Apple IIGS computer via a domestic data acquisition programme(Chanady et al 1985) . Experiments were performed in a 1cm-lightpath , 1ml-volume quartz cuvette. Reduction was initiated by adding suitable concentrations of either ascorbate plus cytochrome *c* or ascorbate plus TMPD to an aerobic solution containing cytochrome oxidase . The reduction of cytochrome *a* , cytochrome *a* + *a*₃ , and cytochrome *c* were followed by monitoring the absorbance increase at the 605nm band , 445nm band, and 550nm band respectively. The reduction of Cu_A was studied by following the absorbance decrease at the 830nm band. After anaerobiosis, dithionite was added to secure the full reduction of the oxidase. The experimental temperature was 30°C.

(b) Dual wavelength spectrophotometry

Steady-state studies of the enzyme in turnover were performed in an Aminco DW2 UV/Vis spectrophotometer, in dual wavelength mode, linked to a Compaq 286 computer with an Olis™ data acquisition package. Experiments were performed in a 1cm-lightpath , 1ml-volume quartz cuvette. Reduction was initiated by adding suitable concentrations of either ascorbate plus cytochrome *c* or ascorbate plus TMPD to an aerobic solution containing cytochrome oxidase . The reduction levels of cytochrome *a* , cytochrome *a* + *a*₃ , and cytochrome *c* were followed using the wavelength pairs 605-630nm , 445-470nm and 550-540nm respectively. After anaerobiosis, dithionite was added to secure the full reduction of the oxidase. The

experimental temperature was 30°C.

48

Fluorescence and phosphorescence spectrophotometry

I. Fluorescence and phosphorescence spectra

Fluorescence and phosphorescence spectra of resting cytochrome oxidase and valinomycin-liganded oxidase were obtained using a Perkin Elmer LS-50 luminescence spectrometer and stored, using a McCOMP 386 computer with the FLDM data acquisition programme, for later analysis. A solution containing 0.2 μM resting enzyme, 50mM potassium phosphate, pH 8.0 and 0.015% lauryl maltoside was added to a 1cm-lightpath, 3ml-volume fluorescence cuvette. Where indicated, the "oxygen trap" was composed of 80nM glucose oxidase, 20nM catalase and 0.05% glucose. To minimize the quenching of phosphorescence by oxygen, the buffer had been bubbled with pure argon for 20 minutes before taking phosphorescence spectra and a layer of mineral oil was put on the surface of the deoxygenated solution to prevent it from contacting the atmosphere again. The spectra of the valinomycin-liganded species were taken 40 minutes after 9 μM valinomycin was added to the solution. The experimental temperature was 14°C. The filter position was set at 'clear'. For fluorescence spectra, the emission and excitation wavelengths were 330nm and 290nm, and both the excitation and emission slits were set at 5.0 nm; for phosphorescence spectra, the emission and excitation wavelengths were 445nm and 275nm, the gate time was 5.0ms, and the delay time is 0.2ms. Both

excitation and emission slits were set at 15 nm to increase the signal, and the average of 10 scans was taken to produce the final result.

49

II. Nitrite quenching of phosphorescence of cytochrome oxidase \pm valinomycin.

Phosphorescence spectra were obtained as above. A solution containing 7 μ M cytochrome oxidase or 7 μ M cytochrome oxidase plus 10 μ M valinomycin, 50mM potassium phosphate, pH8.0 and 0.015% lauryl maltoside was added to a 1cm-lightpath, 3ml-volume fluorescence cuvette . The buffer had been bubbled with pure argon for 20 minutes to remove the oxygen before being added to the cuvette, and a "oxygen trap" composed of 80nM glucose oxidase , 20nM catalase and 0.05% glucose was also included. As described above, mineral oil was put on the top of the deoxygenated solution, and during subsequent measurements, aliquots of sodium nitrite were added using a Hamilton syringe. The phosphorescence emission spectra were measured using either 260nm or 295nm as the excitation wavelength . The excitation spectra were recorded using 460nm as the emission wavelength . The gate time was 3.0 ms , and the delay time was 0.4ms. Both the excitation slit and emission slit were set at 15.0nm . The experimental temperature was 4°C.

Part I : Valinomycin-cytochrome oxidase interaction

A. Spectroscopic effects of valinomycin

In order to understand the spectroscopic effect of valinomycin, control experiments were first carried out with conventional ligands. These derivatives were prepared as described in **Methods and Materials**.

Fig. 4A shows the Soret spectra of the resting enzyme, and the formate-liganded, 'pulsed' and cyanide-liganded cytochrome oxidase. The absorption maxima are located at 419nm, 416nm, 424nm and 427nm respectively. Fig. 4B presents the corresponding difference spectra. Both 'pulsed' and cyanide-liganded enzyme have a peak at 433nm and a trough at 413nm, while the formate-liganded enzyme has a peak at 413nm and a trough around 433nm, essentially the reverse of the 'pulsed' enzyme spectrum. Addition of valinomycin to the resting enzyme has a similar effect to that of cyanide. That is, it shifts the Soret peak of the oxidase spectrum to the red, although the amplitude of the valinomycin effect is less marked (Fig. 5).

The time course of the development of the valinomycin spectrum is shown in Fig. 6. The difference spectra also have a peak around 433nm and a trough at 413nm, as with the cyanide-liganded species. The development of this valinomycin-induced spectral shift takes around 30 min. It can therefore be studied by following the absorbance change at the wavelengths of the peak and trough positions, i.e., 433nm and 413nm, where the effect is at a maximum.

Fig. 4(A)

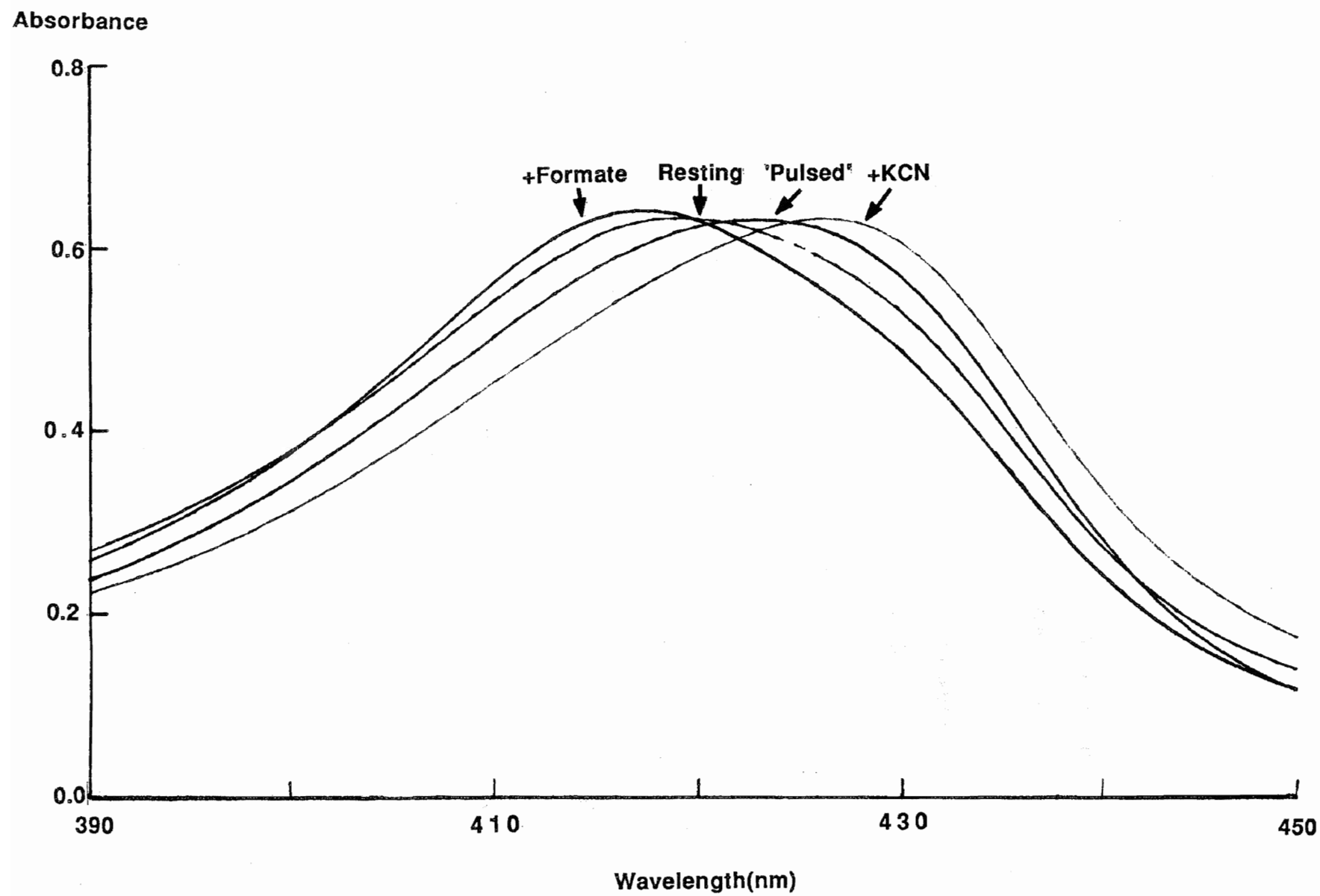


Fig. 4A. **Absolute spectra of high and low spin forms of cytochrome oxidase** 51

The experiments were carried out in 50mM potassium phosphate , pH 7.4 , 0.015% lauryl maltoside at 30°C, using the Du-7 Beckman spectrophotometer. The enzyme concentration was 4 μ M. The pulsed enzyme spectrum was taken 45 minutes after the preparation . Formate and cyanide concentrations were 40mM and 2mM respectively where indicated. The details of formation of 'pulsed ', formate-liganded and cyanide-liganded enzyme are described in **Methods** .

Fig. 4(B)

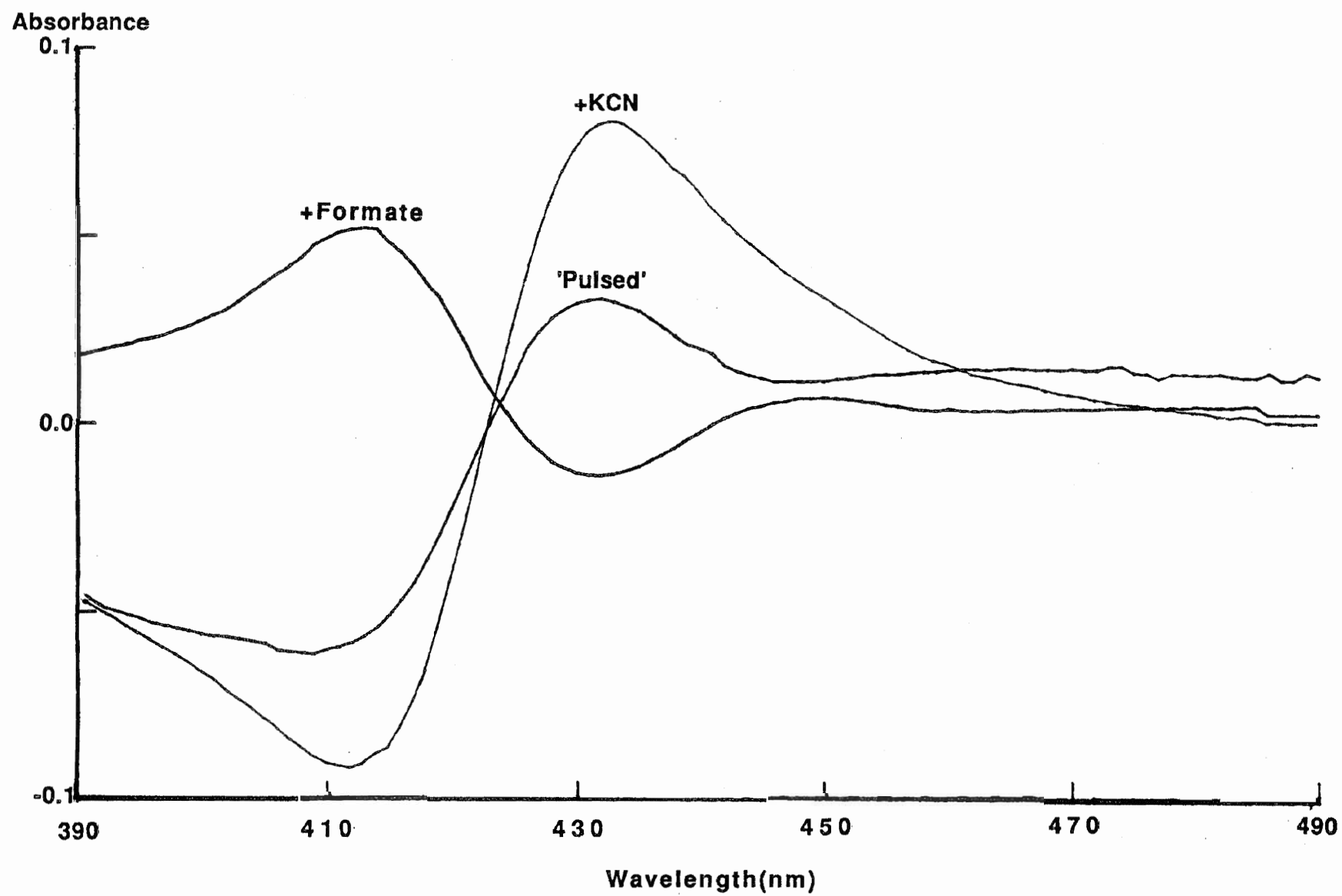


Fig. 4B. Difference spectra of high and low spin forms of cytochrome oxidase 52

The difference spectra were obtained from the absolute spectra in Fig. 4A by subtracting the resting enzyme spectrum from the spectra of other species. Experimental conditions are as in Fig. 4A.

Fig. 5

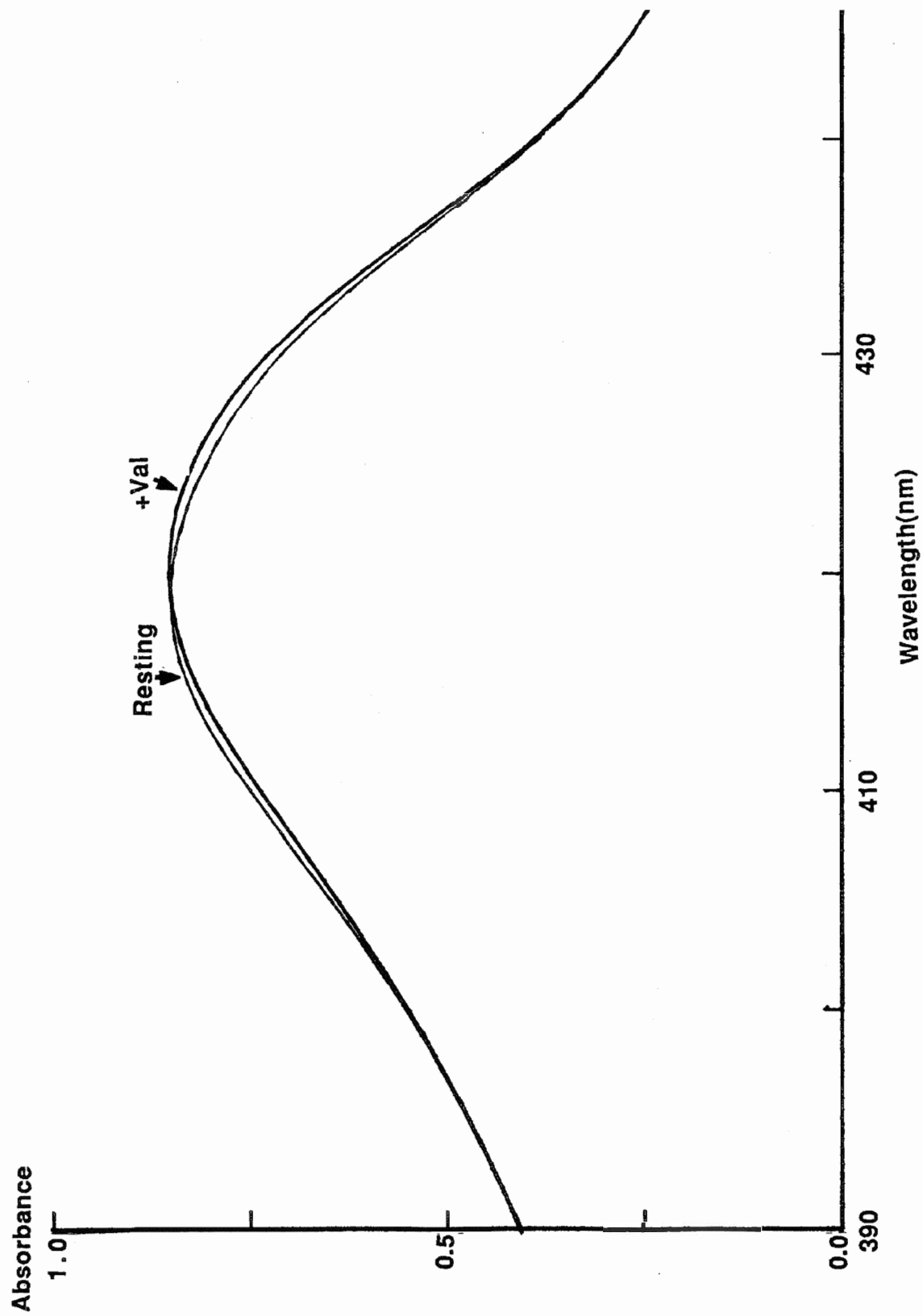


Fig. 5 Spectra of the resting and valinomycin-liganded enzyme.

53

Experiments were conducted in 50mM potassium phosphate , pH7.4, 0.015% lauryl maltoside at 30°C using the DU-7 Beckman spectrophotometer. The enzyme concentration was 4 μ M. 100 μ M ferricyanide was added to the cuvette to keep the enzyme in its oxidized form. The spectrum of the valinomycin-liganded species was taken 30 mins after 4 μ M valinomycin had been added to the cuvette.

Fig. 6

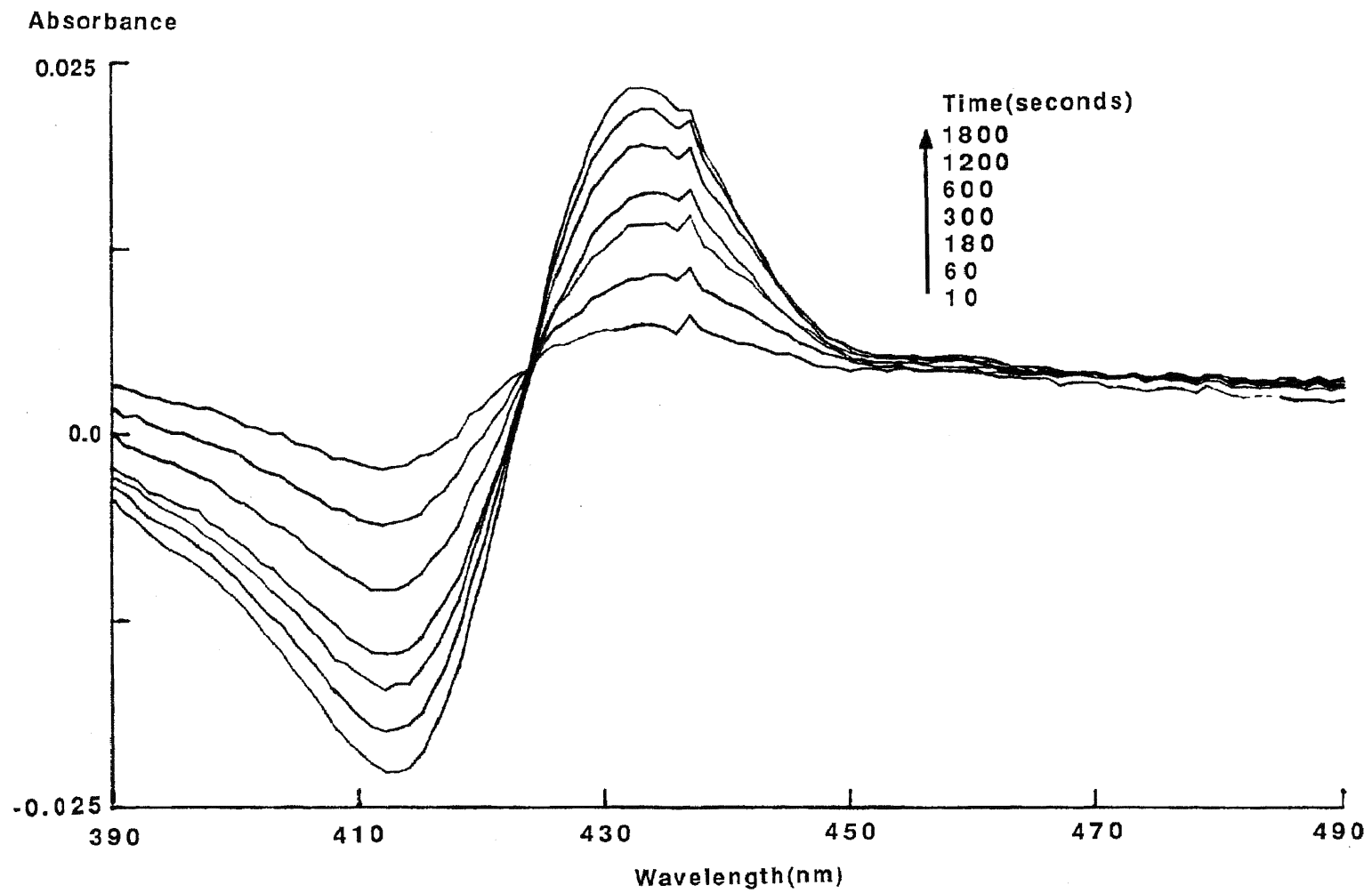


Fig.6 Progressive appearance of valinomycin-oxidase complex : Difference spectra(valinomycin-liganded minus resting enzyme).

54

Experiments were conducted in 50mM potassium phosphate ,pH7.4, 0.015% lauryl maltoside at 30°C using the DU-7 Beckman spectrophotometer. The enzyme concentration was 4 μ M. Spectra were taken at 10sec, 1min, 3min, 5min, 10min, 20min and 30min after 4 μ M valinomycin had been added to 4 μ M resting enzyme. The spectrum of resting enzyme was subtracted from each valinomycin spectrum.

A sample of enzyme was incubated with varying amounts of valinomycin and the spectral change recorded after 15min. Fig. 7 plots the corresponding absorbance change as a function of valinomycin concentration.

In Fig.7A, the results are shown for the reaction in 10mM HEPES, while in Fig.7B the corresponding results in the presence of 100mM K_2SO_4 are seen. The effect of ionic strength upon the valinomycin-induced spectral shift is rather limited. The difference extinction coefficient ($\Delta E_{mM433-413nm}$) has the same value of probably $22mM^{-1}cm^{-1}$ at both high and low ionic strengths. The data were fitted to an appropriate "Binding" equation in Multifit™(please see **Methods**), and the results are plotted as the solid lines in the two figures. The dissociation constant, K_d , for high ionic strength is $2.5\mu M$, and that for low ionic strength is $3.1\mu M$. If these parameters are used, the resulting curves fit the data quite nicely.

The rate of valinomycin binding was followed in the DW-2 dual wavelength spectrophotometer. Fig. 8A shows the spectral changes as a function of valinomycin concentration. The initial rate V_0 of the absorbance change at 433-413nm wavelength pair, calculated as ΔA per minute, varies linearly with valinomycin concentration. On the other hand, the apparent rate constant k , with the dimension sec^{-1} , is independent of valinomycin concentration and reflects the half time for formation of the appropriate fraction of bound enzyme in each case(Fig. 8B).

The linear relation between initial rate and valinomycin

Fig. 7

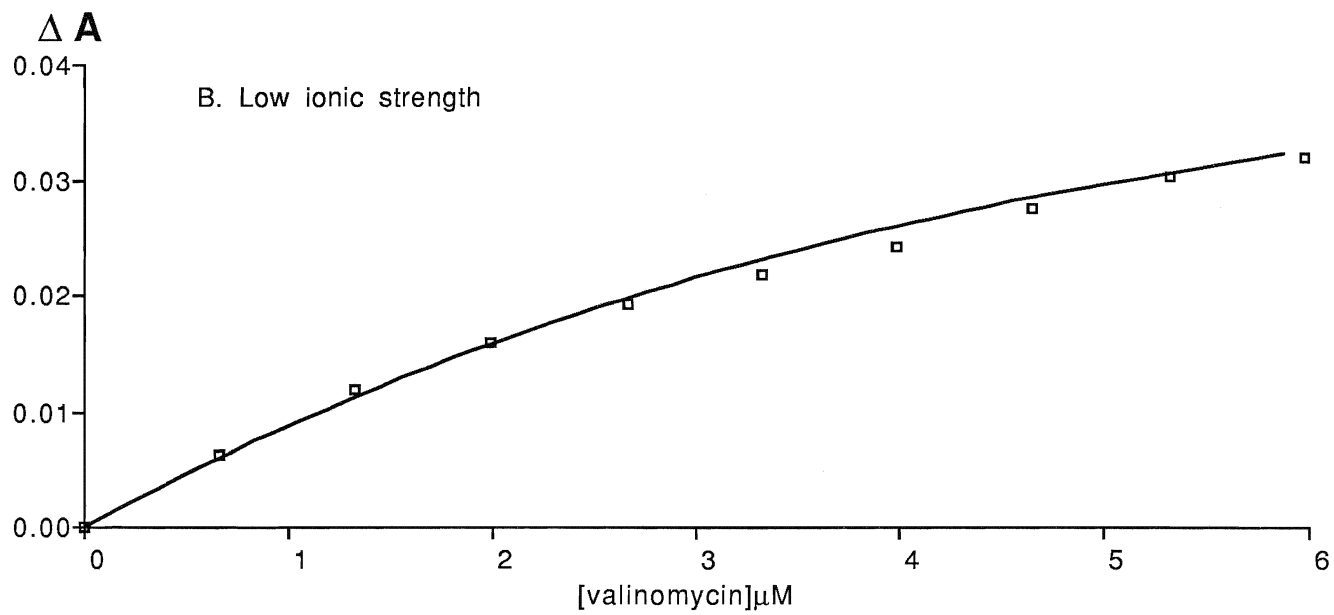
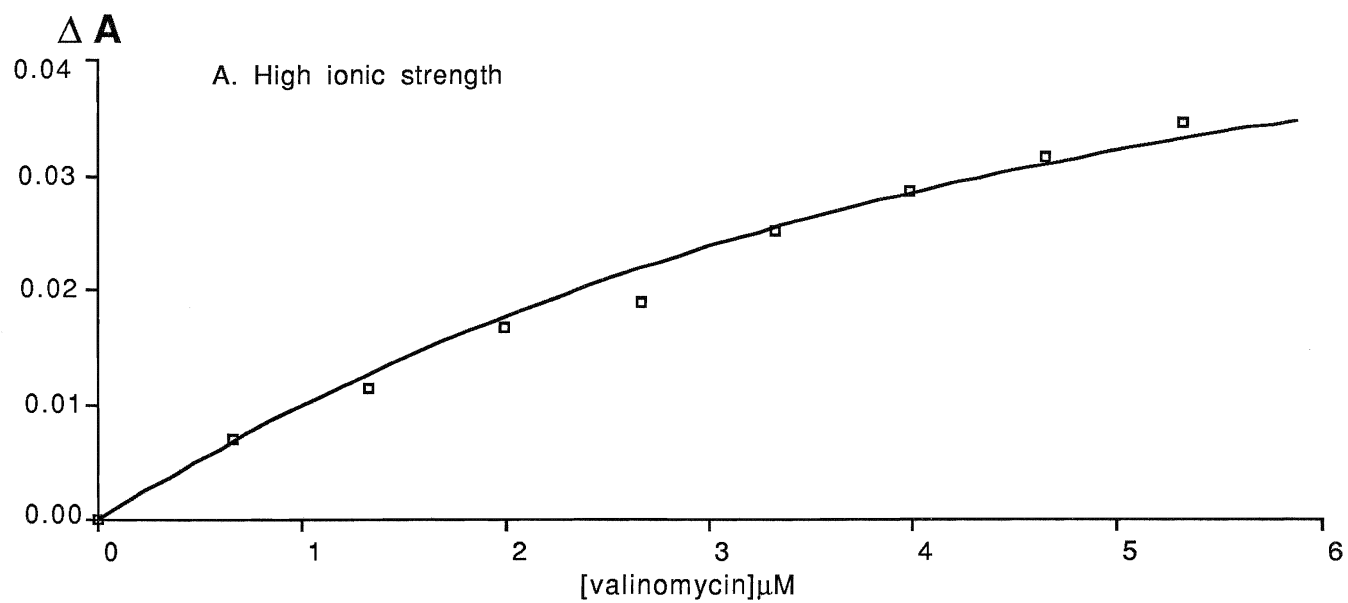


Fig. 7 Effect of valinomycin concentration upon the spectral shift of cytochrome oxidase at high & low ionic strengths.

56

The experiments were performed in 10mM potassium HEPES, or 10mM potassium HEPES + 100mM K₂SO₄ buffer, pH7.4 , 0.015% lauryl maltoside at 30°C using the DU-7 Beckman spectrophotometer . The oxidase concentration was 2.5 μ M . Aliquots of valinomycin were added and spectral changes recorded after 15 mins incubation.

The solid lines were obtained by fitting the data with a "Binding" function(This function is defined as Eq. 5 in **Methods**). The **Multifit**[™] fitting programme for the Macintosh was used. The extinction coefficients for high and low ionic strengths are $22.9 \pm 4 \text{ mM}^{-1}\text{cm}^{-1}$ and $21.5 \pm 2 \text{ mM}^{-1}\text{cm}^{-1}$ respectively. The dissociation constant K_d for high ionic strength is $2.8 \pm 1.0\mu\text{M}$, while that for low ionic strength is $3.1 \pm 0.7\mu\text{M}$.

A. titration plot at high ionic strength(10mM potassium HEPES + 100mM K₂SO₄.)

B. titration plot at low ionic strength(10mM potassium HEPES alone)

Fig. 8(A)

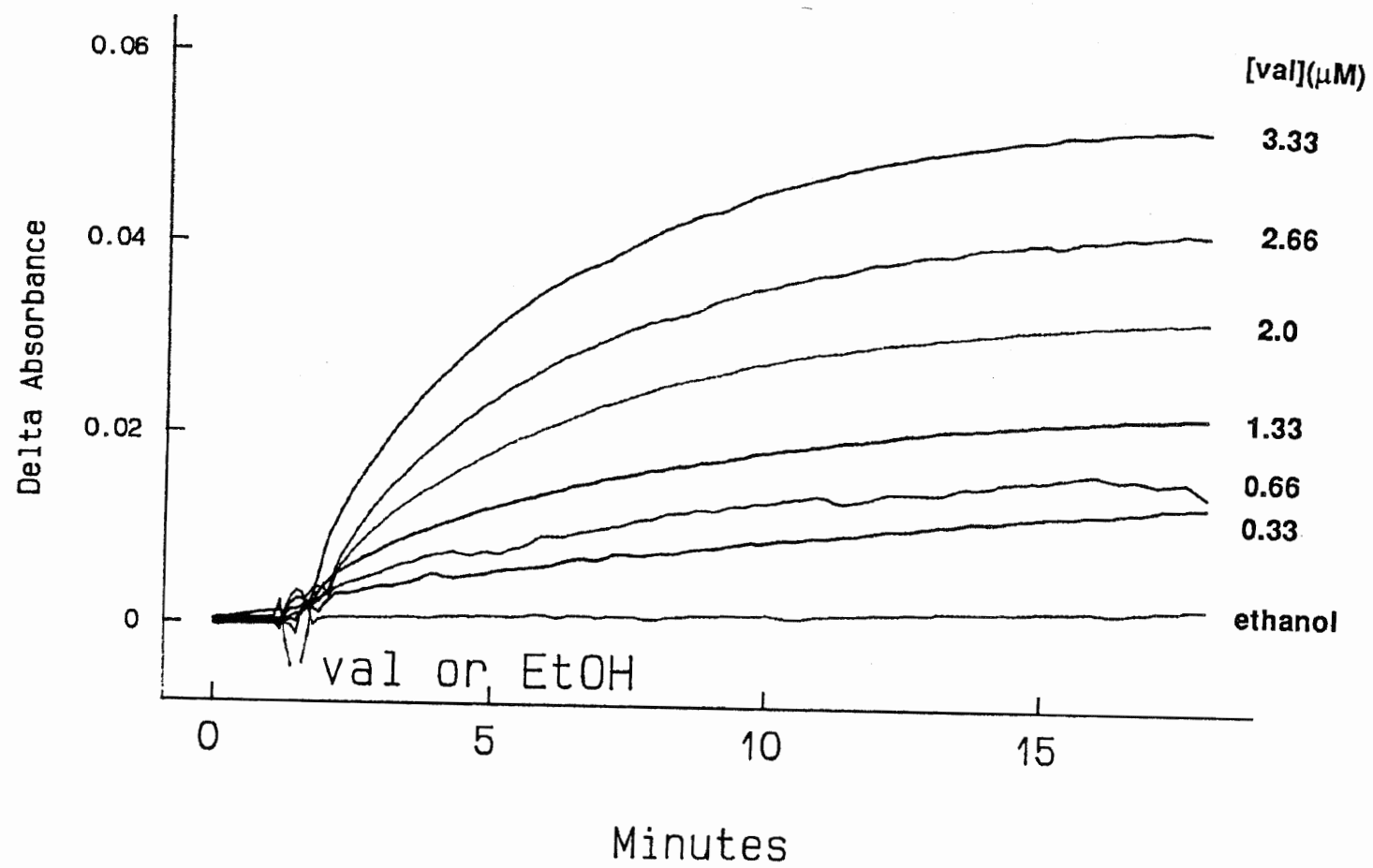


Fig. 8A. Kinetics of valinomycin binding to resting cytochrome oxidase : Time courses of valinomycin binding followed at 433-413nm.

57

The experiments were carried out in 50 mM potassium phosphate , pH7.4 , 0.015% lauryl maltoside at 30°C in a DW-2 Olis™ dual wavelength spectrophotometer. 0 - 3.33 μ M valinomycin were added to 4.0 μ M enzyme in a 1cm-lightpath, 3ml-volume quartz cuvette to start the reaction as indicated on the trace. Ethanol concentration was kept constant at 0.4 %. The results of a single experiment are shown . Fitted kinetic values are given in Fig. 8B.

Fig. 8(B)

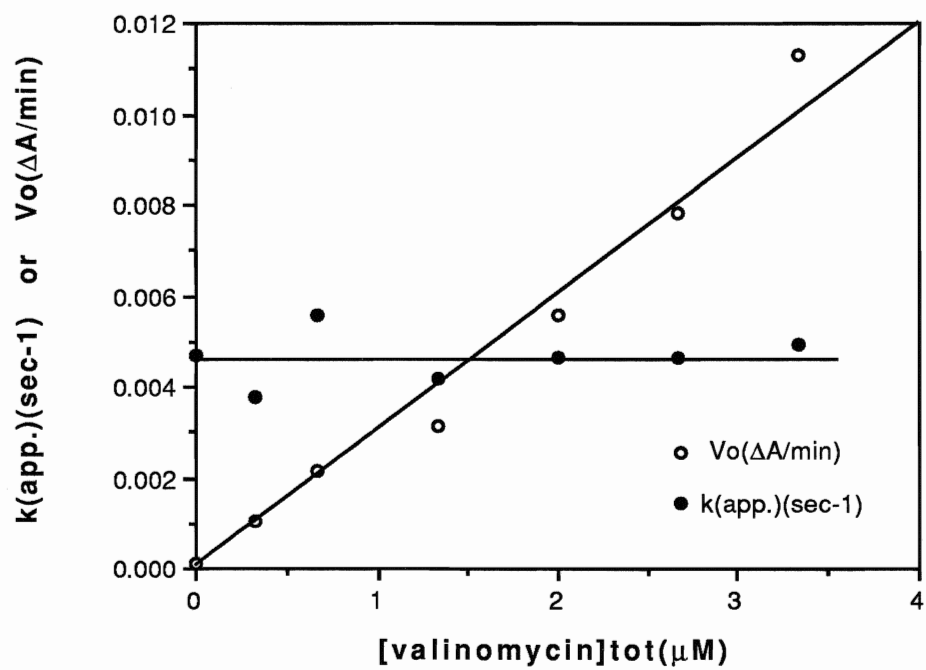
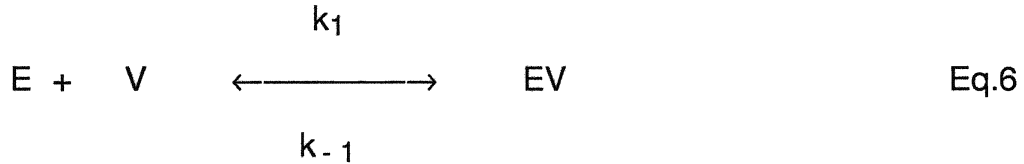


Fig. 8B Kinetics of valinomycin binding to resting cytochrome oxidase : Analysis of valinomycin binding kinetics.

58

Apparent rate constants k_{app} for binding were obtained as the reciprocals of apparent half times $t_{1/2}$. The initial rate V_0 was obtained by fitting the curves in Fig. 8(A) with the "straight line" function from the Olis™ fitting programme within two minutes after adding valinomycin. Data are from the single experiment of Fig. 8A. Conditions as in the legend to Fig. 8A.

concentration indicates that the valinomycin-enzyme interaction is a 2nd order reaction, which can be described by the following equation(Mathews and van Holde 1990): 59



Where E : enzyme V: valinomycin EV: valinomycin-enzyme complex

The rate of the formation of the valinomycin-enzyme complex can be described by the following equation:

$$d([\text{EV}])/dt = k_1 * [\text{E}] * [\text{V}] - k_{-1} * [\text{EV}] \quad \text{Eq. 7}$$

When $t=0$, the concentration of EV is insignificant, so the contribution of the second item at the right of equation 7 can be neglected :

$$d([\text{EV}])/dt|_{t=0} = k_1 * [\text{E}] * [\text{V}] \quad \text{Eq.8}$$

The slope obtained from the relation between the initial rate V_0 and the valinomycin concentration in Fig. 8B is $3.2 \Delta A \text{ min}^{-1} \text{mM}^{-1}$. Using the extinction coefficient $E_m = 22 \text{mM}^{-1} \text{cm}^{-1}$ obtained from Fig. 7 and an enzyme concentration $[\text{E}] = 4 \mu\text{M}$, k_1 can be calculated according to Eq. 8 as $600 \text{ M}^{-1} \text{s}^{-1}$. As:

Table I

Parameters	Fig.8 (Kinetics)	Fig.7 (Equilibrium)
k_1	$600\text{M}^{-1}\text{s}^{-1}\#$	_____
k_{app}	$0.0046\text{s}^{-1}\#$	_____
k_{-1}	$0.0022\text{s}^{-1}\#$	0.0015- $0.0019\text{ s}^{-1}\#$
k_{-1}/k_1	$3.7\mu\text{M}$	_____
K_d	_____	$2.5\text{-}3.1\ \mu\text{M}\#$

* $k_{-1} = k_{\text{app}} - k_1[E]$

** $k_{-1} = k_1 K_d (k_1 \text{ from column 2})$

#Direct measurement

Table 1. **Rate constants for valinomycin-cytochrome oxidase interaction.** 61

Values listed in the second column are those used for the fittings in Fig. 8B . Values listed in the third column are those obtained from the fittings in Fig. 7 . Experimental conditions are listed in the legends to Figs. 8A and 7 respectively.

Fig. 9

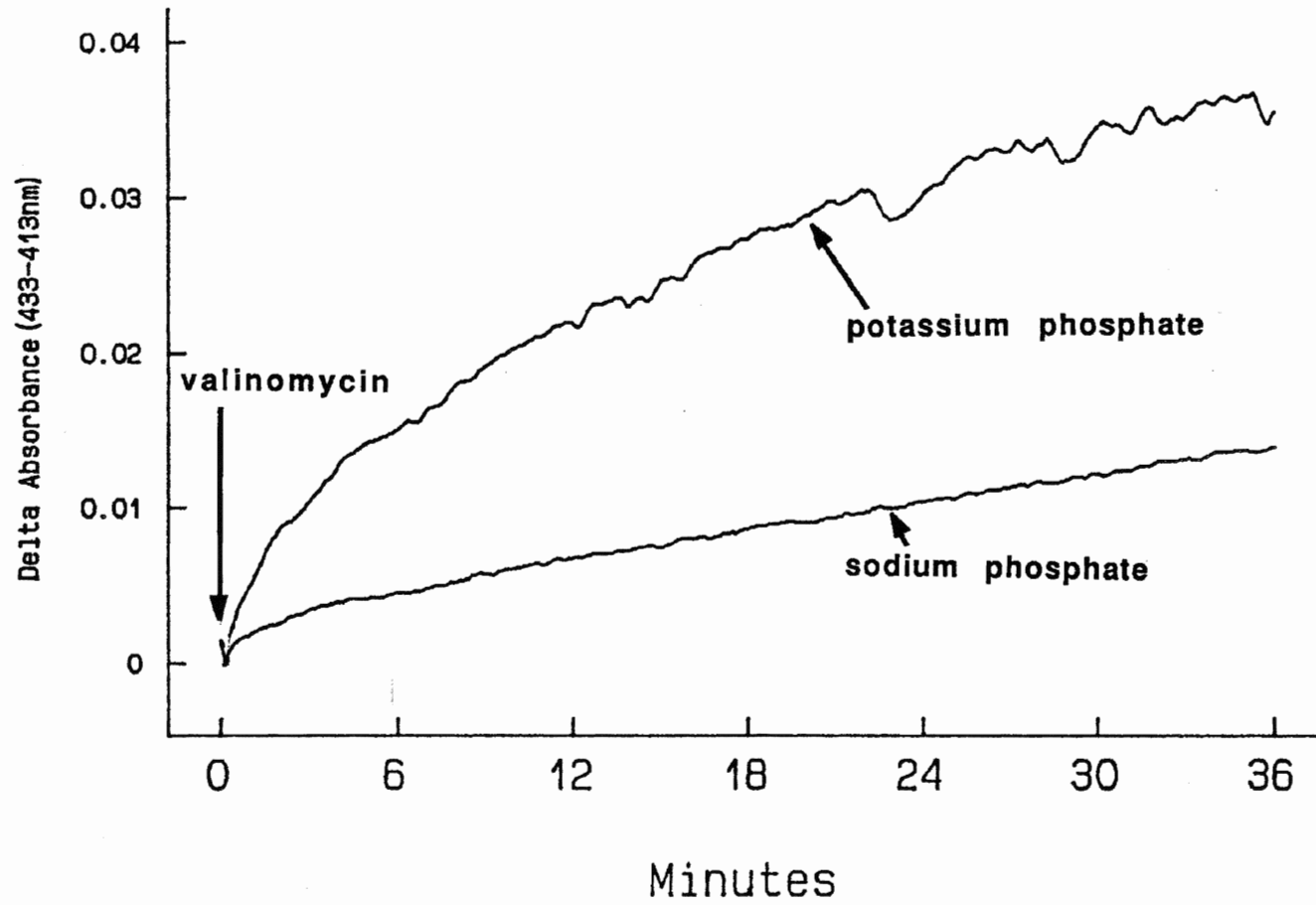


Fig. 9 Effect of cation composition upon the valinomycin-induced spectral shift of cytochrome oxidase

62

The experiments were carried out in a DW-2 Olis dual wavelength spectrophotometer at 30°C. The medium was 50 mM potassium or sodium phosphate , pH 7.4. It also contained 0.015% lauryl maltoside . The enzyme concentration was 2.5 μ M and 3.3 μ M valinomycin was added to a 1cm-lightpath, 3ml-volume quartz cuvette to start the reaction as indicated on the trace.

Table 2

Medium	$\Delta A_m(433-413nm)^*$	Initial rate ($\Delta A/min$)**
potassium phosphate	0.036	4.2E-3
sodium phosphate	0.014	7.9E-4
Ratio	2.5	5.0

* Maximal absorbance change(2.5 μ M enzyme)

** Rate of absorbance change(3.3 μ M valinomycin)

Table 2. Comparative study of valinomycin-cytochrome oxidase interaction in different media

63

The listed values are obtained from the single pair of experiments shown in Fig. 9, using the Olis™ double exponential fitting routine. The second column lists the final maximal absorbance changes at the indicated wavelengths. The third column lists the initial rates of absorbance change. All conditions are given in the legend to Fig. 9.

Fig. 10

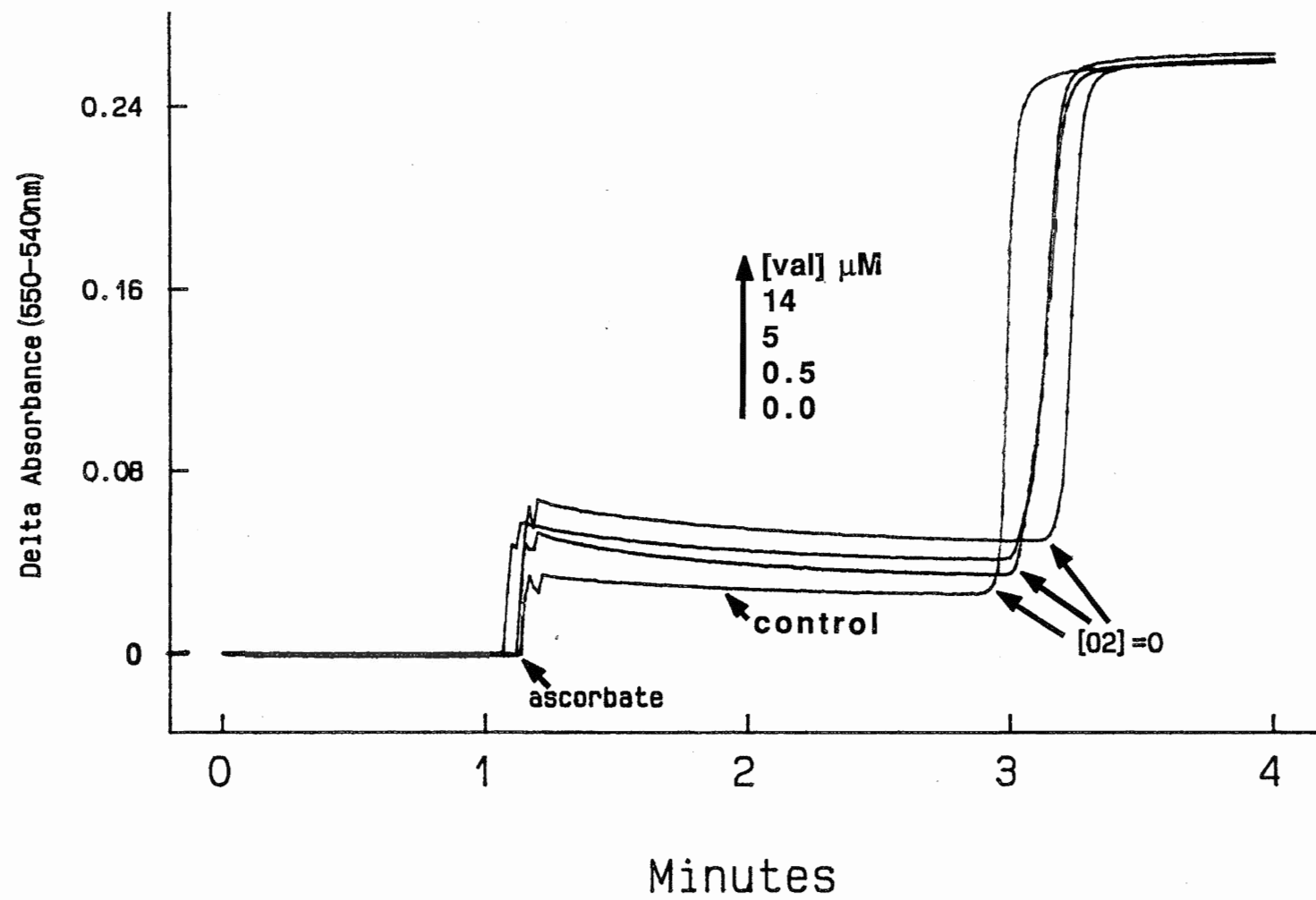


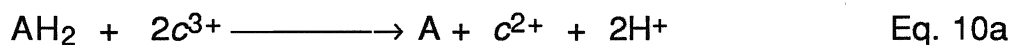
Fig. 10. Effect of valinomycin upon steady state enzyme activity.

64

The experiments were performed in 50mM potassium phosphate, pH 7.4 , 0.015% lauryl maltoside and 13 μ M cyt. *c* at 30°C. 1.5 μ M cyt. *aa₃* was incubated at the desired valinomycin concentration for 1.0 h before 10mM ascorbate was added to start the reaction. The reduction of cytochrome *c* was monitored at the 550-540nm wavelength pair, using the DW-2 dual wavelength spectrophotometer. A 1cm-lightpath, 1 ml-volume quartz cuvette was used to hold the reaction mixture. The figure shows the results of a single experiment. Replicates give similar results (steady state values differing by no more than $\pm 5\%$).

Cytochrome *c* is reduced by ascorbate according to Eq. 10 :

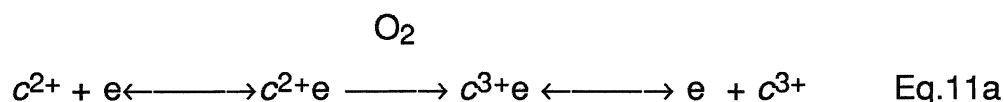
65



$$v = k_r[\text{c}^{3+}][\text{AH}_2] \quad \text{Eq. 10b}$$

where AH and A are reduced and oxidized forms of ascorbate respectively, *v* is the velocity, *k_r* is the rate constant for reduction.

Cytochrome *c* is reoxidized by cytochrome oxidase according to Eq.11(Minnaert 1961):



$$v = k_o[\text{c}^{2+}]\text{e}/(\text{K}_m + [\text{c}]_{\text{total}}) = 4[\text{O}_2]/t_{\text{anaerobic}} \quad \text{Eq. 11b}$$

Where *k_o* is the rate constant for oxidization of ferrous cytochrome *c* by the oxidase, *K_m* is the Michaelis constant for cytochrome *c* and *t_{anaerobic}* is the time taken for the solution to become oxygen-free .

In Fig. 11A, *k_r*, the rate constant of reduction of cytochrome *c* by ascorbate was calculated from Eq. 10b and plotted against valinomycin concentration. Valinomycin has little effect on *k_r*, indicating that the inhibition does not occur at this step. The average value of *k_r* under these conditions was 80M⁻¹ s⁻¹. On the other hand, *k_o* , the rate constant for oxidization of ferrous cytochrome *c* by the oxidase, decreases substantially with an increase in valinomycin concentration (Fig. 11B). But even at a high valinomycin concentration, there is still some

Fig.11

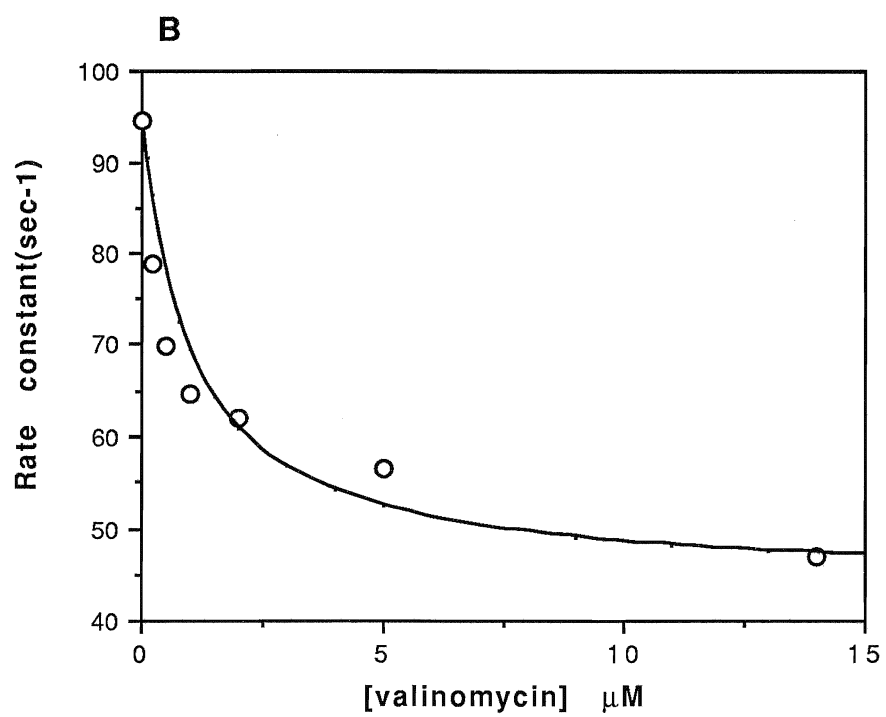
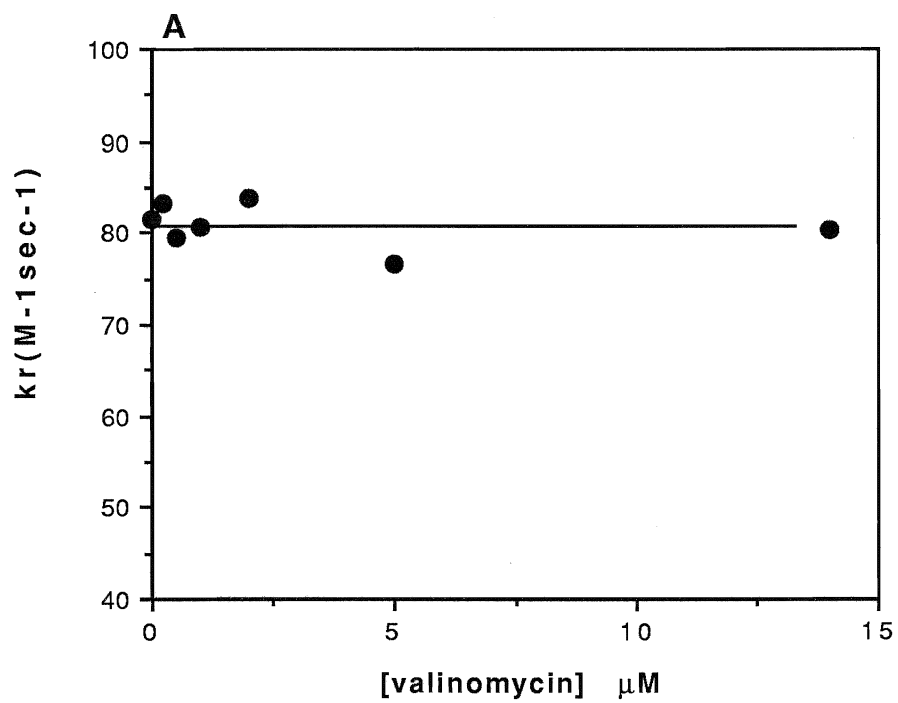


Fig. 11. Kinetic analysis of the effects of valinomycin upon the ascorbate-cytochrome *c*-cytochrome *aa₃*-O₂ steady state.

66

A. Reduction of cytochrome *c* by ascorbate.

The second order reduction rate constants were calculated from the steady state data of Fig. 10 according to the method described on p.65 of the **Results**. The straight line is drawn for a constant k_r value of $81\text{M}^{-1}\text{s}^{-1}$. Conditions are as in the legend of Fig.10. Error bars are not shown (see Fig. 10 legend).

B. Enzymatic activity (turnover).

The turnover number k_o is the oxidation rate constant calculated according to the method described on p.65 of the **Results** . The theoretical curve is drawn for a K_d of $1\mu\text{M}$ and a residual activity of 45%. Conditions are as in the legend of Fig. 10. Error bars are not shown (see Fig. 10 legend).

residual enzyme activity. The maximum percentage inhibition is approximately 55%, and the K_i , the valinomycin concentration causing half of the maximum inhibition, is estimated as $1.0\mu\text{M}$ (see fitted curve, Fig.11B) .

The valinomycin effect upon electron transfer in the absence of cytochrome *c* was investigated by following the steady state reduction of cytochrome *a* by ascorbate plus TMPD at 605-630nm (Fig. 12). A relatively low buffer concentration (10mM potassium phosphate) was used to promote the reaction velocity without adding too high a concentration of reductant. The steady state reduction of cytochrome *a* increases from 23% in the control condition to 28% in the presence of $10\mu\text{M}$ valinomycin. The anaerobiosis time also increases when valinomycin is present, indicating an inhibition of the intrinsic enzyme activity in the absence of cytochrome *c* .

Valinomycin is both an ionophore, and, as shown above, an inhibitor of cytochrome oxidase. It is therefore important to understand the relationship between these two functions of valinomycin. The respiration rate of cytochrome oxidase-containing proteoliposomes was studied over a wide range of valinomycin concentration (up to $8.5\mu\text{M}$) , using the O_2 electrode method(Fig. 13). When another ionophore , either FCCP or nigericin, is present, less than $0.1\mu\text{M}$ valinomycin is enough to stimulate fully the respiration of the proteoliposomes. As the valinomycin concentration is increased, a partial inhibition of the FCCP or nigericin-stimulated rate , giving a 20% decrease of the maximal respiration rate, is observed. K_i , the valinomycin

Fig. 12

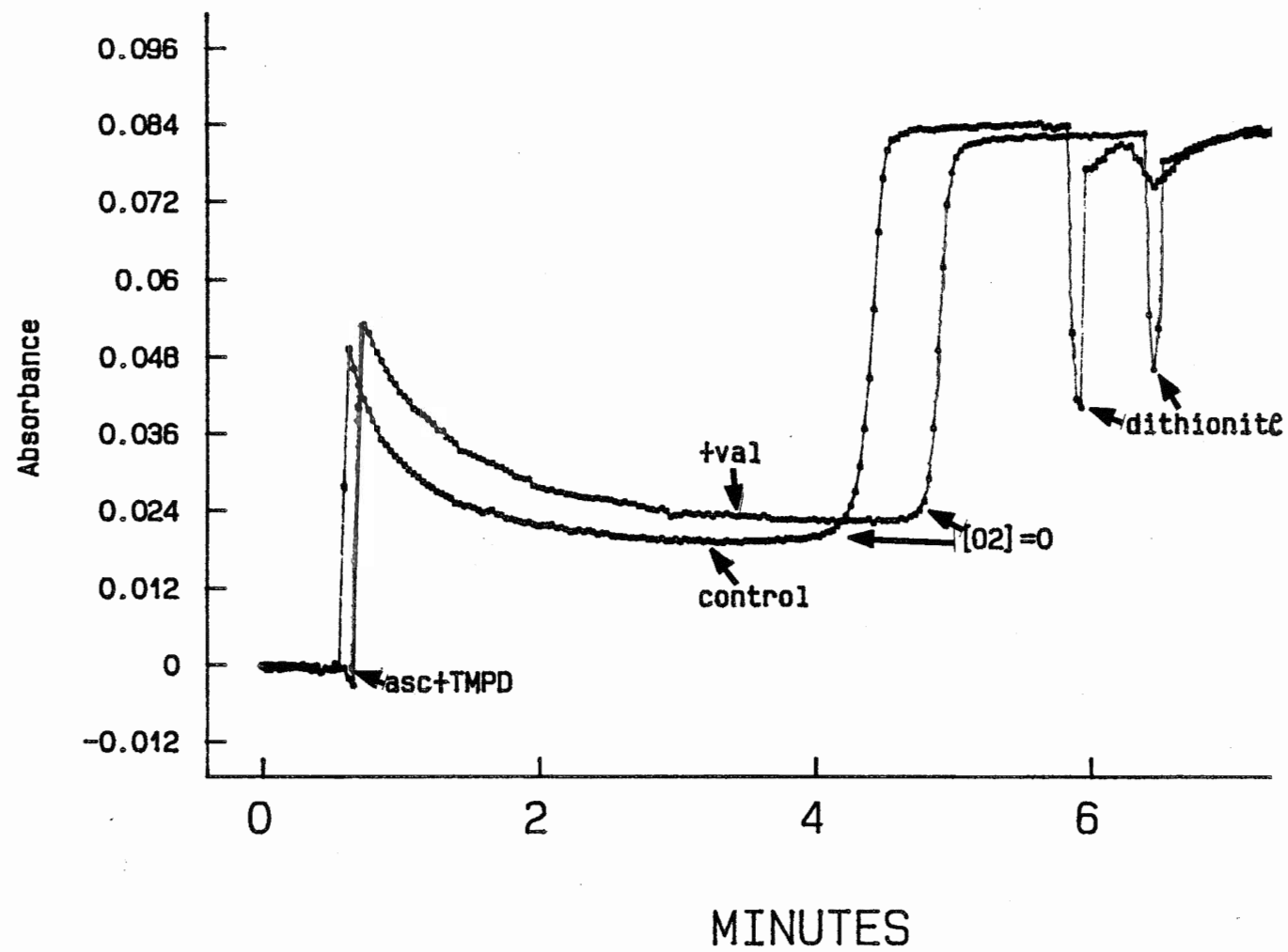


Fig. 12 Steady state reduction of cytochrome *a* induced by TMPD: action of valinomycin.

68

The experiments were conducted in 10mM potassium phosphate , pH 7.4, 0.015% lauryl maltoside at 30°C. 3.1 μ M cytochrome *aa₃* was incubated in 10 μ M valinomycin for 30 min before 10mM ascorbate plus 0.4mM TMPD were added to start the reaction. The reduction of cytochrome *a* was monitored at 605-630nm wavelength pair, using DW-2 dual wavelength spectrophotometer. A 1cm-lightpath,1ml-volume quartz cuvette was used to hold the reaction mixture.

Fig. 13

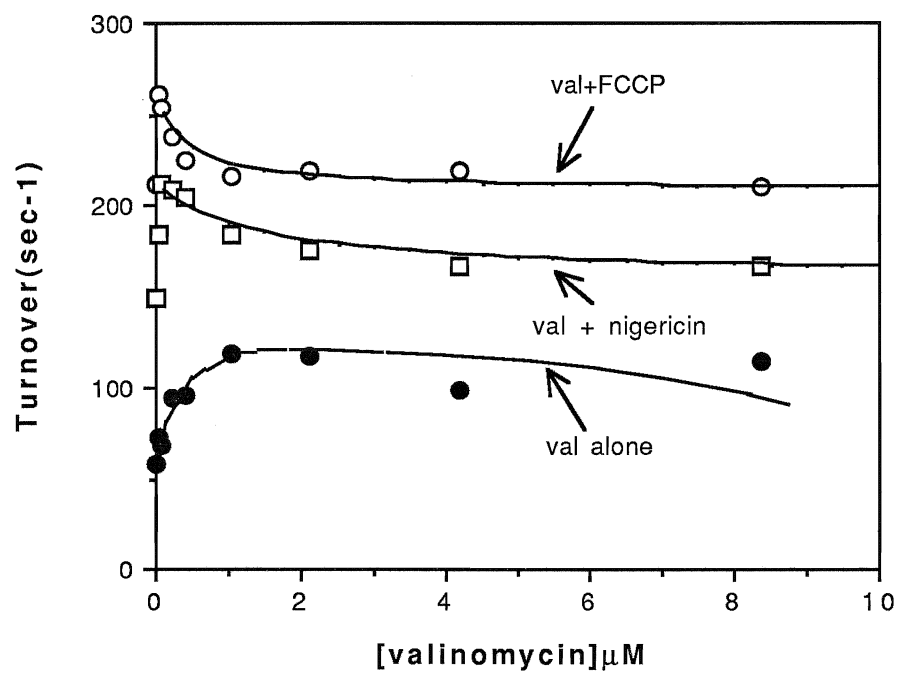


Fig. 13. **Respiration rates of cytochrome oxidase-containing proteoliposomes: influence of different valinomycin concentrations in presence and absence of FCCP and nigericin.**

69

Polarographic experiments were carried out with sonicated COV prepared as described in **Methods**, with lipid:protein ratio=25:1 and 49% cytochrome *aa₃* externally-facing. The reaction medium was 50mM potassium phosphate, pH 7.4, with 9 nM (total) *aa₃*, 10 μ M cytochrome *c*, 1.0 μ M FCCP and 0.16 μ M nigericin where indicated. The valinomycin concentrations range from 0.0 to 8.5 μ M. The experimental temperature was 30°C. The figure shows the results of a single set of experiments. Similar experiments give essentially similar results.

concentration required to cause a half maximal effect , is estimated as $1.0\mu\text{M}$.

70

When valinomycin alone is present , the respiration rate increases slightly with increasing concentrations of valinomycin up to approximately $2\mu\text{M}$. The K_d for this effect, the valinomycin concentration required to cause a half maximal increase, is about $0.2\mu\text{M}$. It may be noted that the maximal activity in the absence of either FCCP or nigericin is about 50% that in their presence and 40% of the maximal activity at the lowest concentrations of valinomycin.

C. Protein fluorescence and phosphorescence effects of valinomycin-cytochrome oxidase interaction

Protein fluorescence and phosphorescence have proven to be very useful as monitors of protein conformation(Lakowicz 1983, Papp and Vanderkooi 1989). Fig. 14A shows that the fluorescence excitation spectrum of cytochrome oxidase has a peak at 281nm , which is close to the normal protein absorption peak. After adding the "oxygen trap", a slight increase of intensity can be seen, but the peak position does not change. Valinomycin causes a slight quenching but does not change the peak position either. The position of the emission spectrum peak(Fig.14B) is located at 336nm when aa_3 alone is present, but it moves to 338nm when the " oxygen trap" is added. The "oxygen trap" also causes a broad intensity increase in the longer wavelength range above 338nm, which is probably due to strong fluorescent interference from flavin groups in glucose oxidase in the

Fig. 14(A)

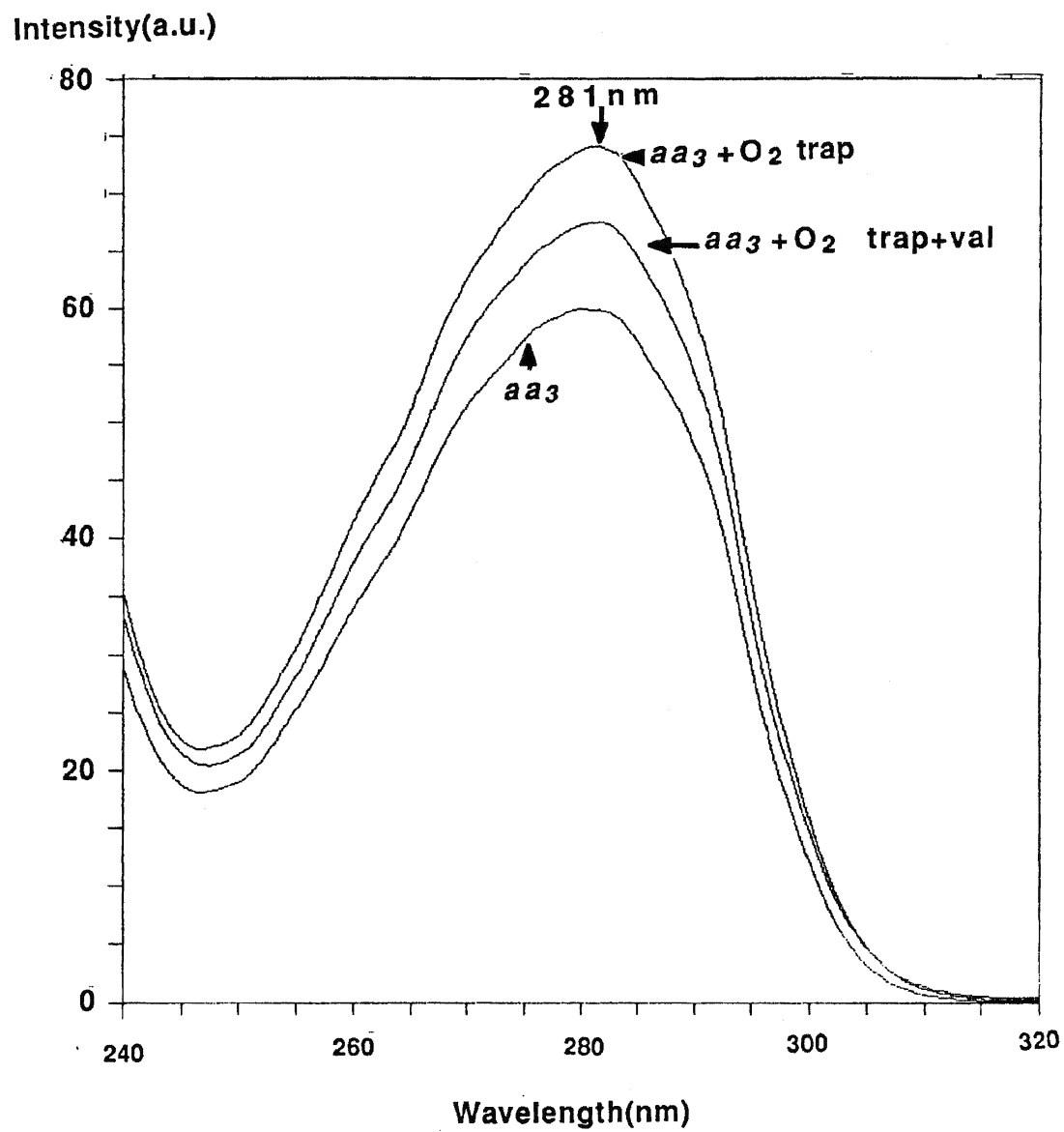


Fig.14A. Fluorescence excitation spectra of cytochrome oxidase \pm valinomycin

71

Fluorescence spectra were obtained using a Perkin Elmer LS-50 luminescence spectrometer and stored, using a McCOMP 386 computer with the FLDM data acquisition programme, for later analysis. 0.2 μ M *aa₃* was added to a 1cm-lightpath, 3ml-volume fluorescence cuvette containing 50mM potassium phosphate, pH 8.0 and 0.015% lauryl maltoside. Where indicated, the "oxygen trap" was composed of 80nM glucose oxidase, 20nM catalase and 0.05% glucose. The spectra of the valinomycin-liganded species were taken 60 min after 9 μ M valinomycin was added to the solution. The experimental temperature was 14°C. Both the excitation slit and the emission slit were 5.0nm. The filter position is 'clear'. The Y axis unit is arbitrary. The emission wavelength = 330nm.

Fig. 14(B)

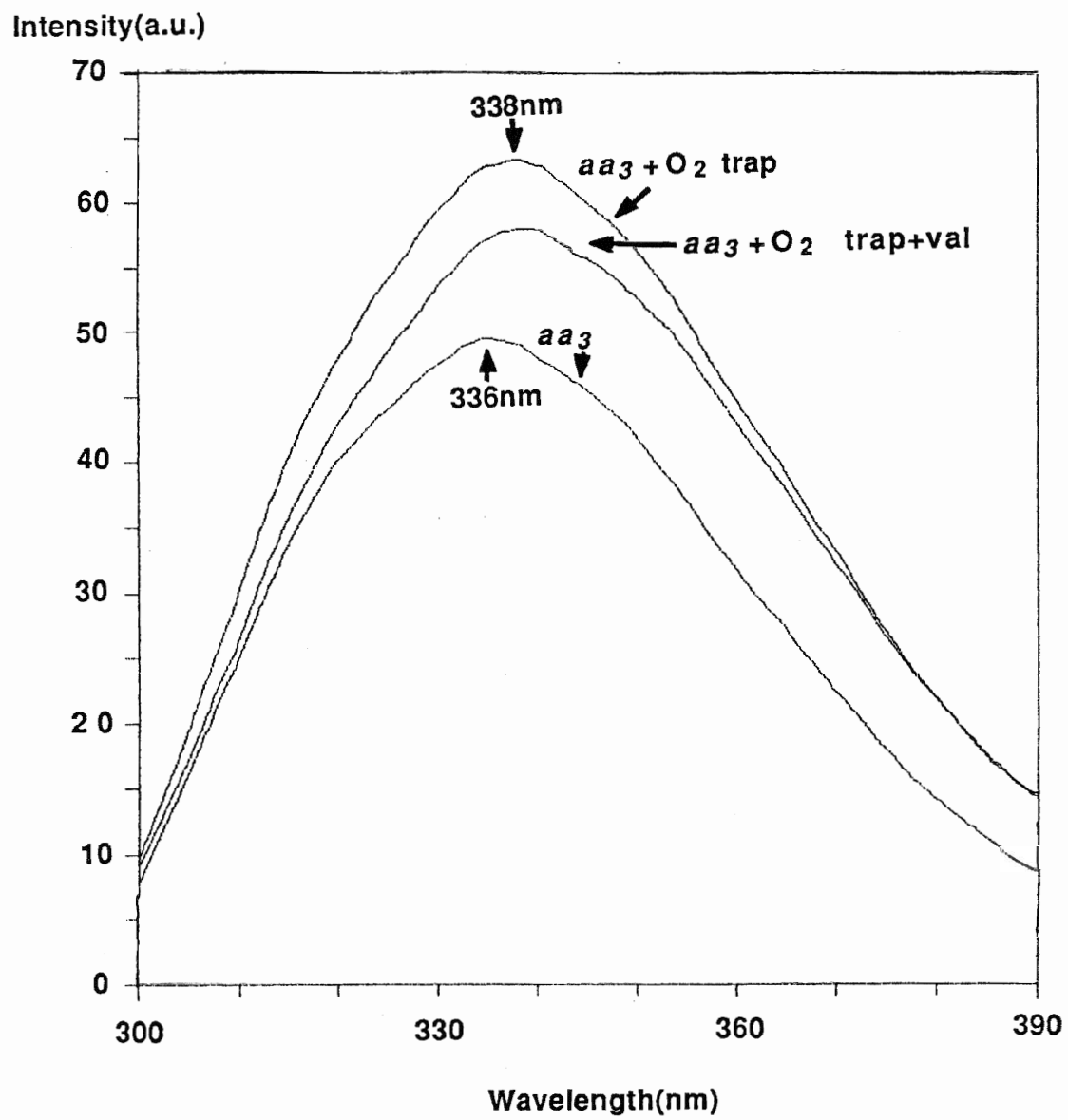


Fig.14B Fluorescence emission spectra of cytochrome oxidase \pm valinomycin 72

The excitation wavelength = 290nm. Other conditions were identical as those of Fig. 14A.

"oxygen trap". Valinomycin causes a slight quenching (8%) of the intensity at the 338nm peak, and has very little effect in the longer wavelength range.

Recently room temperature phosphorescence from cytochrome oxidase has been reported (Papp et al, 1991) and suggested to be a more selective probe of protein structure than fluorescence. Fig.15A shows that phosphorescence excitation spectra of *aa₃*, *aa₃* + "oxygen trap", and *aa₃* + "oxygen trap" + valinomycin all have a peak position at 275nm, so that if excited at 275nm, the emission spectra should give the maximal signal. The emission spectra (Fig.15B) show two peaks. The smaller peak around 340nm is most probably due to a contribution from fluorescence, since the fluorescence emission spectra also have a peak around this wavelength (see Fig. 14B). But the intensity has dropped from 65 (arbitrary unit) to 0.1, indicating that the lifetime of this signal is very short. On the other hand, the bigger peak around 447nm is the true phosphorescence peak, which has a longer lifetime. Adding the "oxygen trap" or valinomycin causes a slight increase of the intensity of both peaks, but the peak positions are not affected.

In order to understand better the valinomycin-induced conformational change of the enzyme, NaNO_2 quenching behaviour towards cytochrome oxidase in the absence and presence of valinomycin was also investigated (Fig. 16). Some experimental conditions were slightly changed to optimize the phosphorescence signal. The *aa₃* concentration was increased from 0.2 μM to 7 μM to increase the signal, and the experimental temperature was

Fig. 15(A)

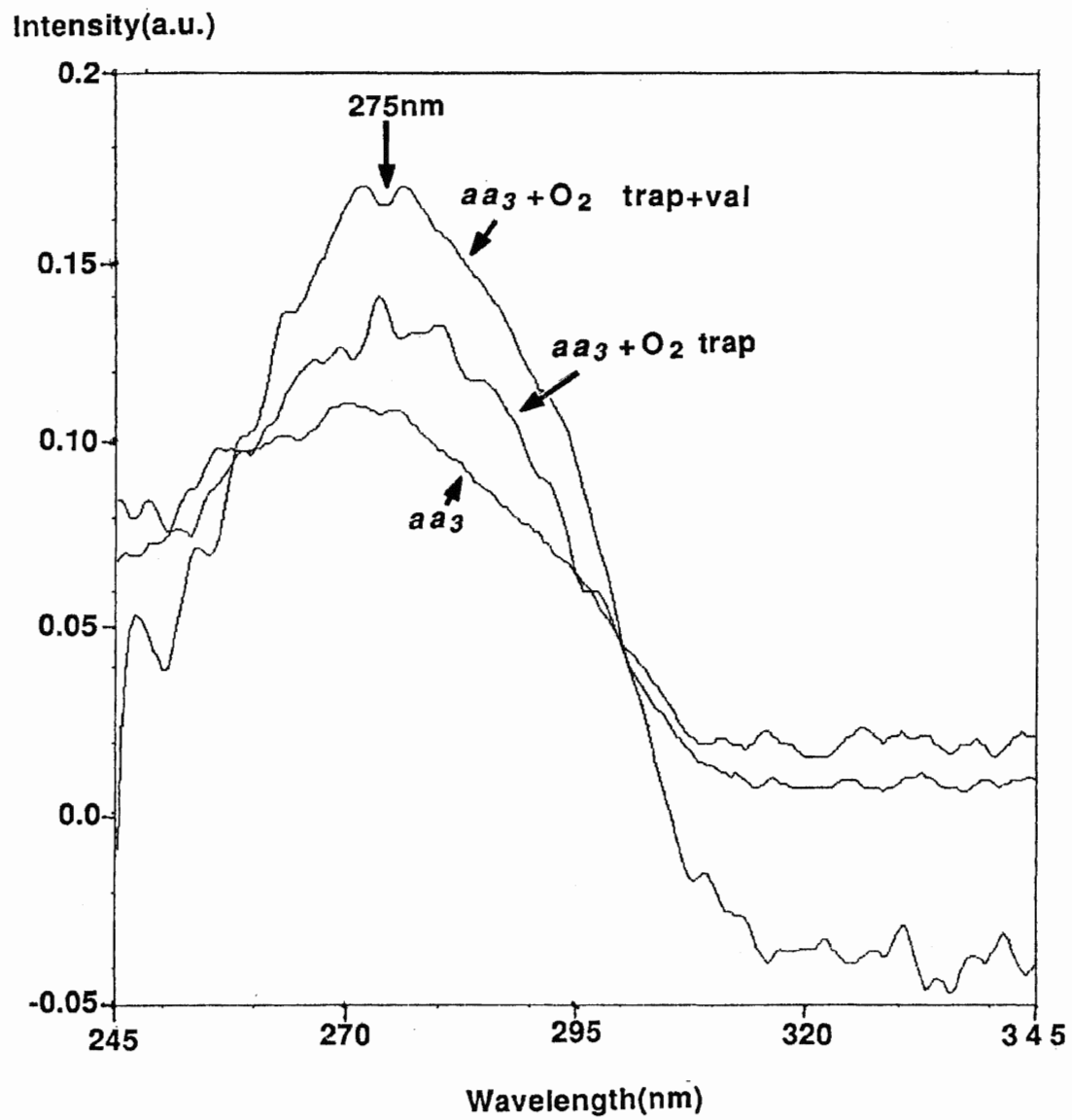


Fig.15A Phosphorescence excitation spectra of the deoxygenated cytochrome oxidase \pm valinomycin

74

Phosphorescence spectra were obtained using a Perkin Elmer LS-50 luminescence spectrometer and stored, using a McCOMP 386 computer with the FLDM data acquisition programme, for later analysis. 0.2 μ M *aa₃* was added to a 1cm-lightpath, 3ml-volume fluorescence cuvette containing 50mM potassium phosphate, pH 8.0 and 0.015% lauryl maltoside. The buffer had been bubbled with pure argon for 20 min to remove the oxygen before being added to the cuvette, then a layer of mineral oil was put on the top of the deoxygenated solution to prevent it from contacting the atmosphere. Where indicated, the "oxygen trap" was composed of 80nM glucose oxidase, 20nM catalase and 0.05% glucose. The spectra of valinomycin-liganded species were taken 30 min after 9 μ M valinomycin was added to the solution. The experimental temperature was 14°C. Both the excitation slit and emission slit were 15.0nm. The Y axis unit is arbitrary. Average of 10 scans were taken in each case. The Gate time = 5.0ms . Delay time = 0.2ms . The emission wavelength = 445nm.

Fig. 15(B)

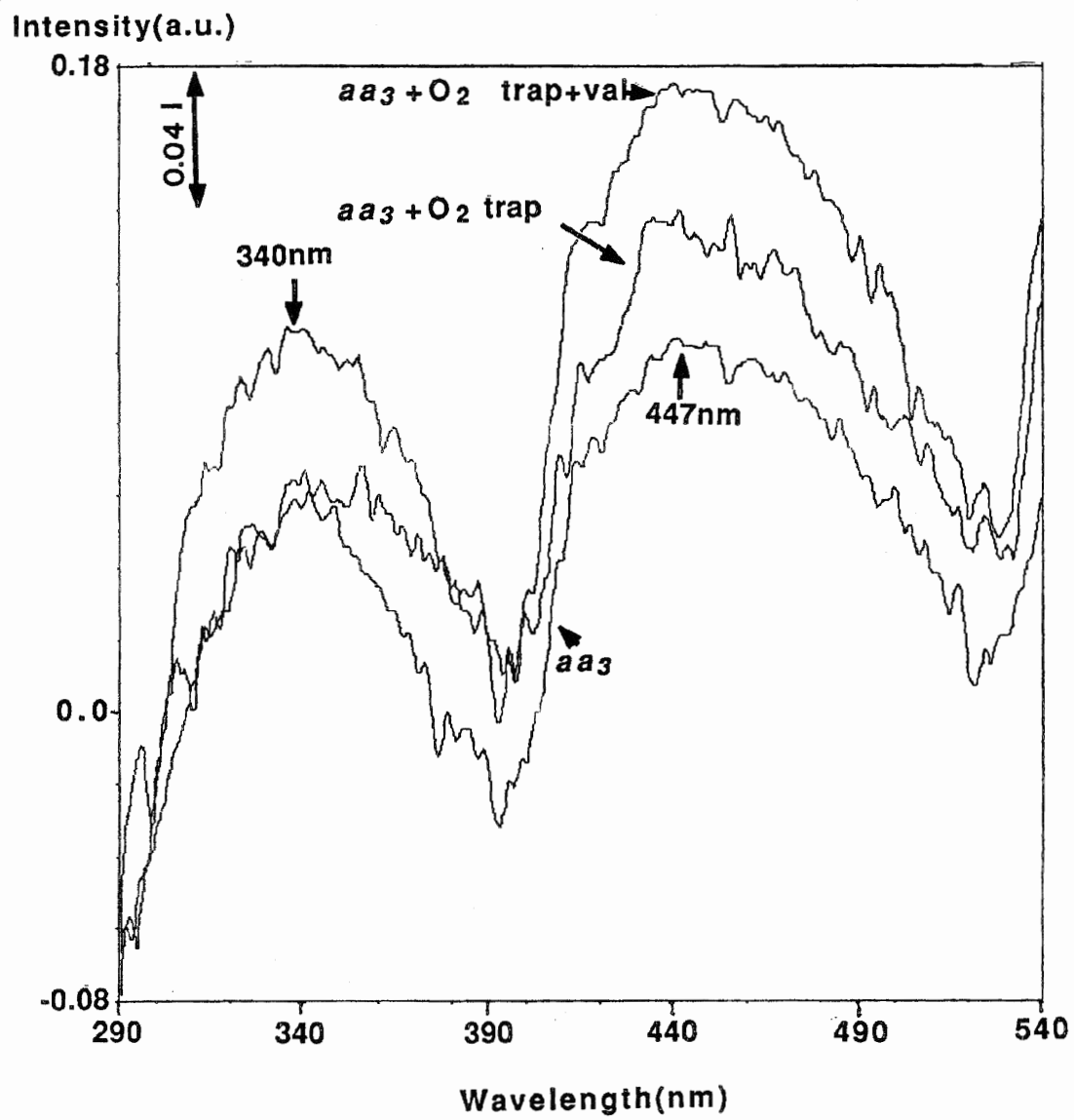


Fig.15B Phosphorescence emission spectra of the 75
deoxygenated cytochrome oxidase \pm valinomycin

The excitation wavelength = 275nm. Other conditions were identical with those of Fig. 15A.

Fig. 16

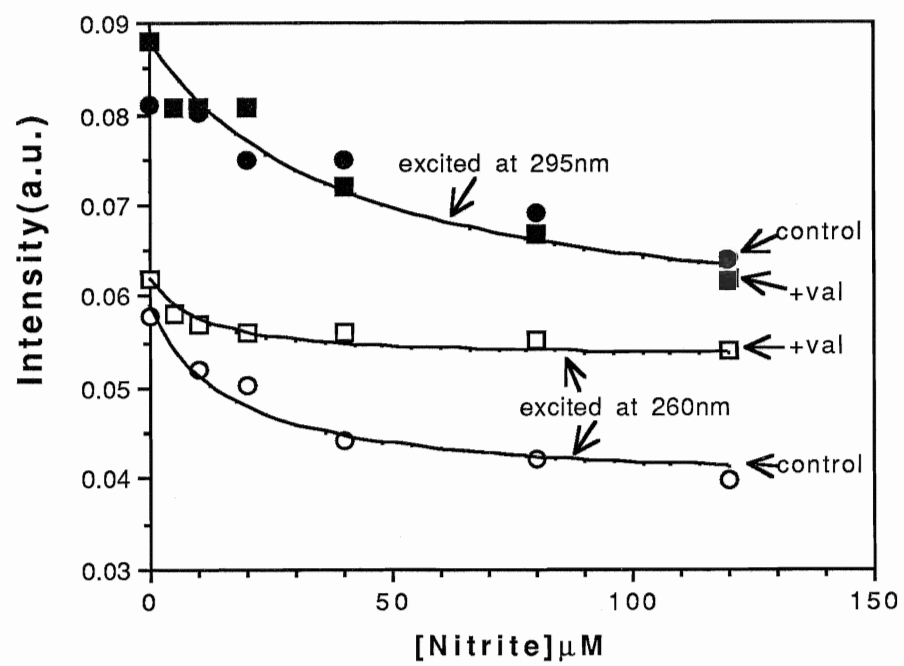


Fig. 16 NaNO_2 quenching of phosphorescence of cytochrome oxidase \pm valinomycin

76

Phosphorescence spectra were obtained using a Perkin Elmer LS-50 luminescence spectrometer and stored, using a McCOMP 386 computer with the FLDM data acquisition programme, for later analysis. 7 μM *aa₃* or 7 μM *aa₃* plus 10 μM valinomycin was added to a 1cm-lightpath, 3ml-volume fluorescence cuvette containing 50mM potassium phosphate, pH8.0 and 0.015% lauryl maltoside. The buffer had been bubbled with pure argon for 20 min to remove the oxygen before being added to the cuvette, and a "oxygen trap" composed of 80nM glucose oxidase, 20nM catalase and 0.05% glucose was also included. A layer of mineral oil was then put on the top of the deoxygenated solution to prevent it from contacting the atmosphere. During subsequent measurements, aliquots of NaNO_2 were added using a Hamilton syringe. The phosphorescence emission spectra were measured using either 260nm or 295nm as the excitation wavelength. The excitation spectra were recorded using 460nm as the emission wavelength. The gate time was 3.0 ms, and the delay time was 0.4ms. Both the excitation slit and emission slit were 15.0nm. The experimental temperature was 4°C. Background contribution has been subtracted from all the data. The Y axis unit is arbitrary.

decreased from 14°C to 4°C for the same reason; the decay of the protein phosphorescence is much faster at higher temperatures (Papp and Vanderkooi 1989). The delay time was increased from 0.2 ms to 0.4 ms to decrease the interference from the fluorescence signal.

Since the concentration of *aa₃* is rather high (7μM *aa₃* corresponds to about 1.4 mg/ml protein concentration), the phosphorescence excitation spectrum peak is no longer located at 275nm due to severe light reabsorption. So instead of using 275nm as the excitation wavelength, the two wavelengths 260nm and 295nm, which correspond to artificial maxima in the excitation spectrum, were used for excitation in emission spectral scans. Fig.16 shows that when 295nm was used as the excitation wavelength, the NaNO₂ quenching behaviour was not changed by the presence of valinomycin. The percentage of maximal quenching is 37%, while the quenching constant K_D , the reciprocal of the nitrite concentration required to have a half maximal effect, is estimated as 0.033μM⁻¹.

On the other hand, when 260nm was used as the excitation wavelength, the percentage of maximal quenching decreases from 34% to 14%, while the quenching constant K_D increases from 0.04 μM⁻¹ to 0.1 μM⁻¹ when valinomycin is present. The detailed results are summarized in Table 3.

Table 3

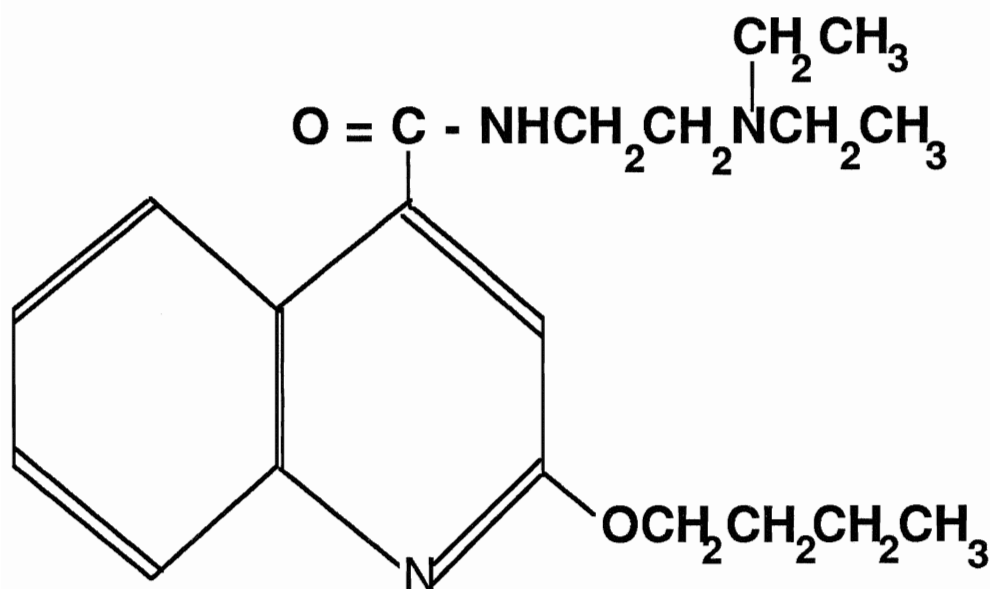
Excitation wavelength	Additions	$K_D(\mu\text{M}^{-1})$	Maximum % quenching
260nm	none (control)	0.04	34%
	plus valinomycin	0.1	14%
295nm	none (control)	0.033	37%
	plus valinomycin	0.033	37%

Table 3. Nitrite quenching of phosphorescence of cytochrome oxidase \pm valinomycin 78

The apparent quenching constants listed in column three are the reciprocals of the nitrite concentrations giving half maximal effects. The quenching percentages listed in column four are the maximal values reached at high nitrite concentrations. The actual values in both columns are those used in the fits shown in Fig. 16. The conditions are presented in the legend to Fig. 16.

A. Spectroscopic effects of dibucaine

Dibucaine contains a heterocyclic structure and two hydrophobic chains:



The absorption spectrum of dibucaine(Fig.17A) shows that it absorbs in the UV region(below 370nm) , but not in the visible region . The chromophore is presumably the heterocyclic ring which contains conjugated bonds. The absorption values at 290nm and at 330nm increase linearly with dibucaine concentration(Fig.17B) , indicating that the Beer-Lambert law is observed. The slope of the line, which represents the extinction coefficient E_{mM} , can be obtained by fitting the data to the 'Simple' function in the Cricket™ programme :

$$E_{m290nm} = 5.50mM^{-1}cm^{-1}$$

and

80

$$E_{m330nm} = 7.80mM^{-1}cm^{-1}$$

The above values are helpful in estimating concentrations of dilute dibucaine solutions.

It has been reported that K_i for the dibucaine-oxidase interaction is in millimolar range (Chazotte and Vanderkooi 1981; Singer 1980, 1982 and 1983; Stringer and Harmon 1990). At the effective millimolar concentration range, dibucaine absorption in the UV region (260nm-330nm) will be over 5.0A based on the extinction coefficients listed above. Since the excitation wavelengths for cytochrome c oxidase are located in this region (Papp et al 1991), it is impossible to conduct an enzyme fluorescence or phosphorescence study because of the severe interference from the dibucaine absorption.

On the other hand, because dibucaine does not absorb in the visible region (Fig.17A), where the spectra of the metal centres of cytochrome c oxidase are located, the dibucaine-induced spectral changes of the enzyme can be studied spectrophotometrically in a similar way to those of valinomycin.

Dibucaine induces a red shift of the enzyme's Soret peak like that with valinomycin (Fig. 18). The difference spectra show a progressive spectral change with time (Fig. 19). But unlike the valinomycin-induced spectral shift (Fig. 6), the kinetic behaviour of this spectral shift is more complicated. The isosbestic point of the difference spectra shifts with

Fig. 17(A)

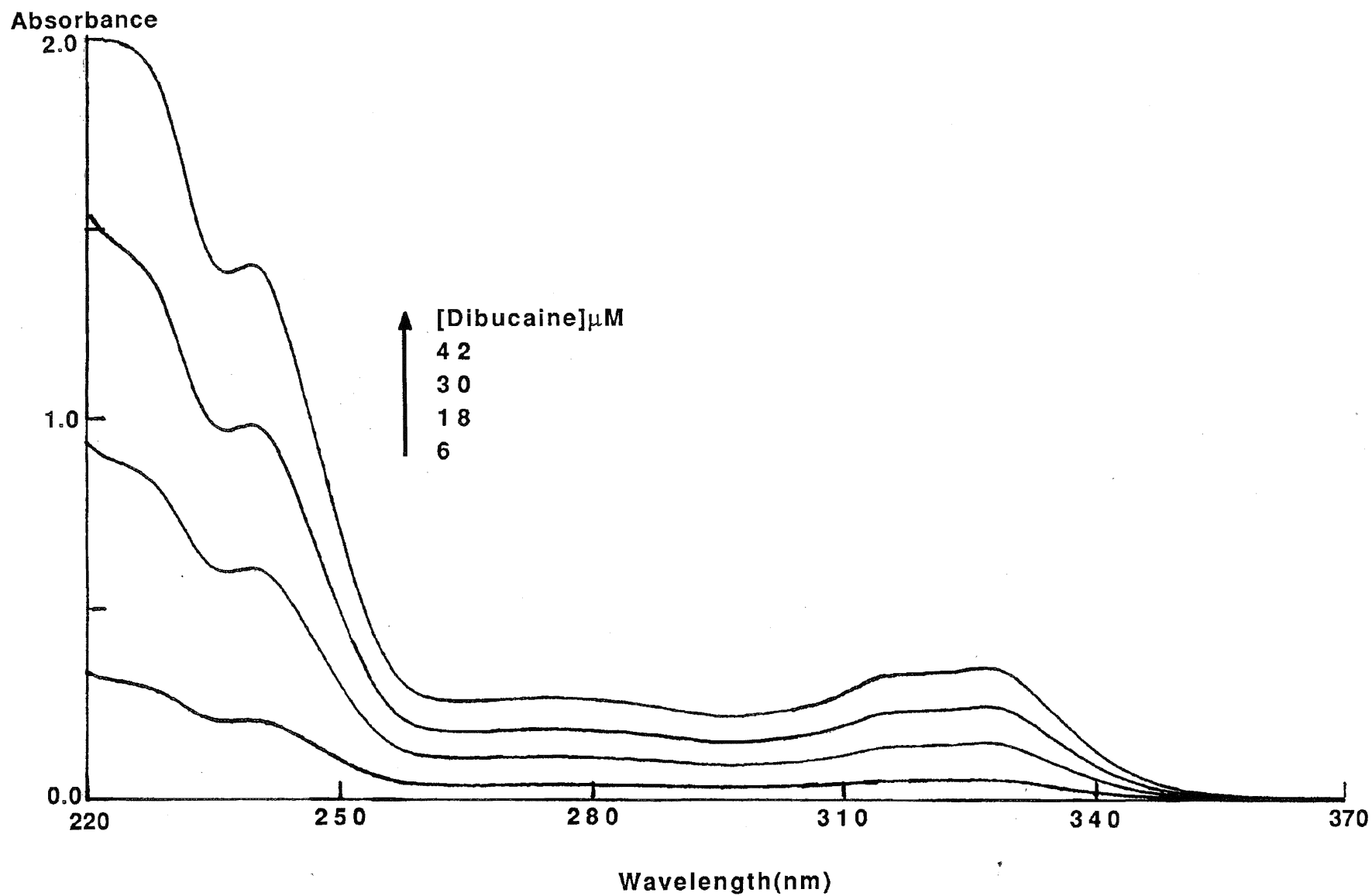


Fig. 17A. **Absorption spectra of dibucaine.**

81

Dibucaine concentrations between 6 and 42 μM , as indicated .
Measurements in 50mM potassium phosphate, pH 7.4 and 0.015%
lauryl maltoside at 30°C. DU-7 Beckman spectrophotometer:
1cm-lightpath, 1ml-volume cuvette .

Fig. 17(B)

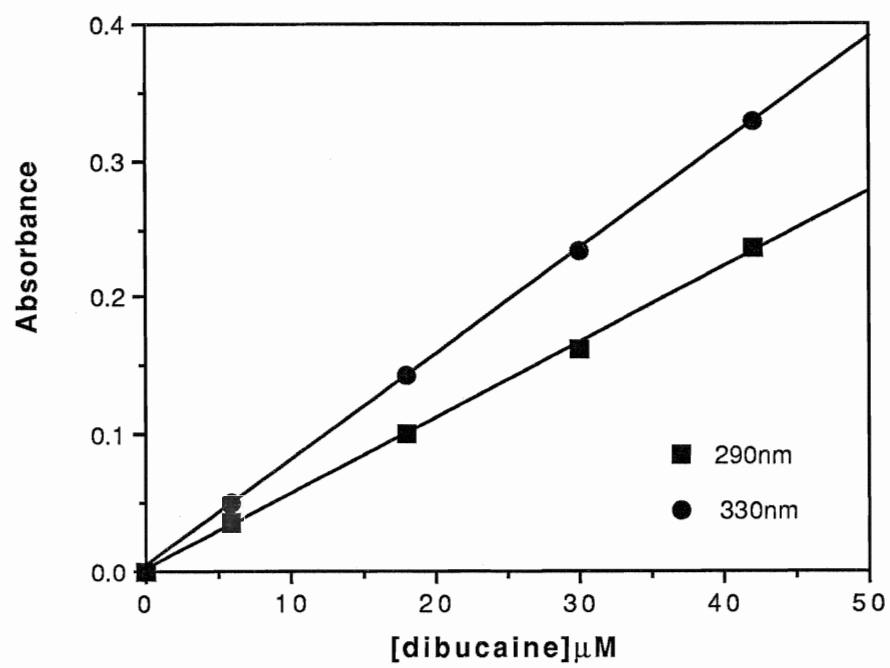


Fig. 17B Absorbance change as a function of dibucaine concentration :

82

Data from Fig. 17A. Buffer contribution to absorption is subtracted from all the data. Conditions as in the legend to Fig. 17A. Conditions are as in the legend to Fig. 17A.

Fig. 18

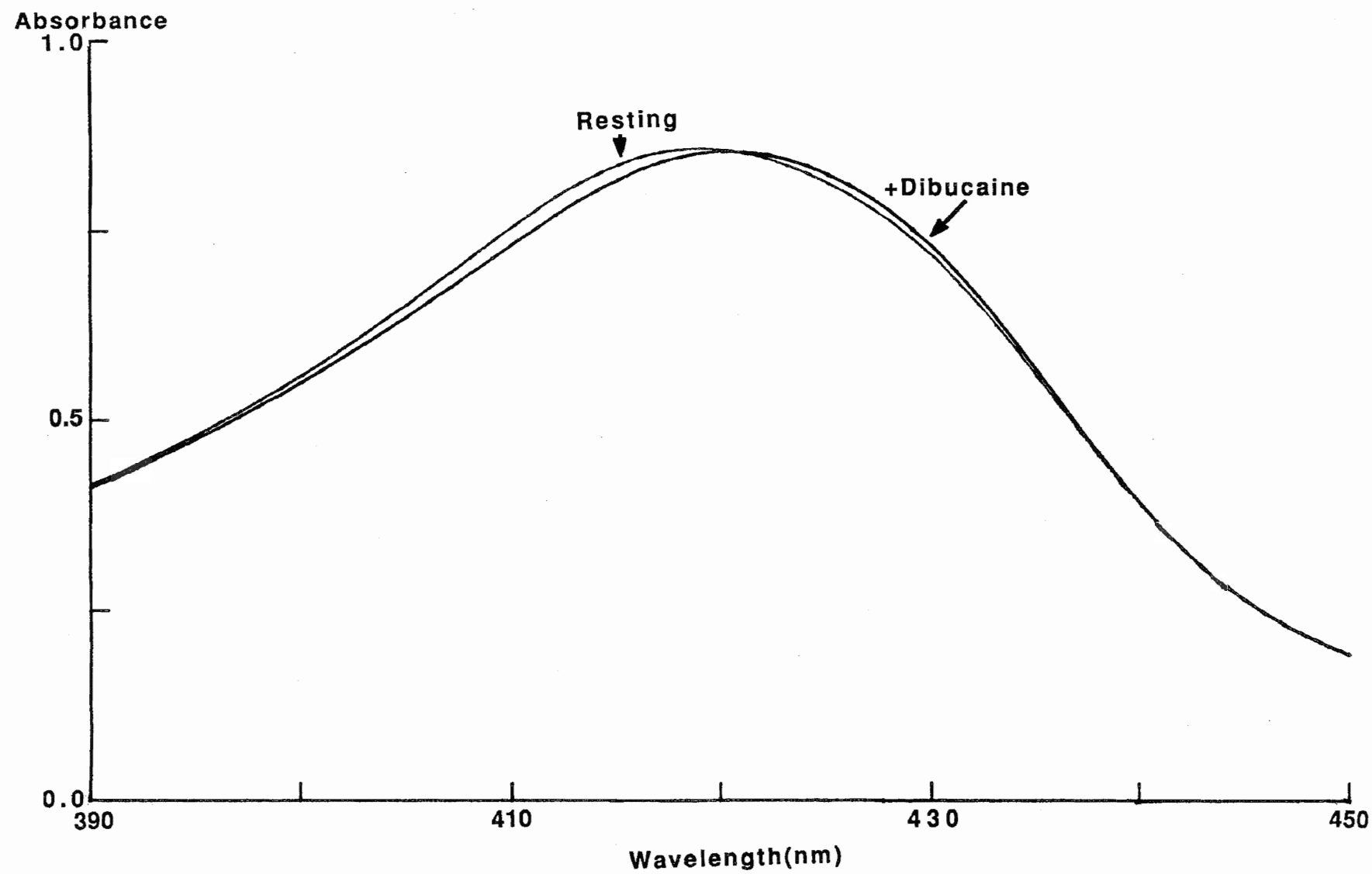


Fig. 18 **Absolute spectra of resting enzyme and dibucaine-liganded enzyme.**

83

Experiments in 50mM potassium phosphate, pH 7.4, 0.015% lauryl maltoside at 30°C, with 4 μ M resting enzyme. 100 μ M ferricyanide was added to keep the enzyme in the oxidized form. The spectrum of the dibucaine-liganded species was taken 30 min after 2mM dibucaine was added to the cuvette. DU-7 Beckman spectrophotometer; 1cm-lightpath, 1ml-volume cuvette .

Fig. 19

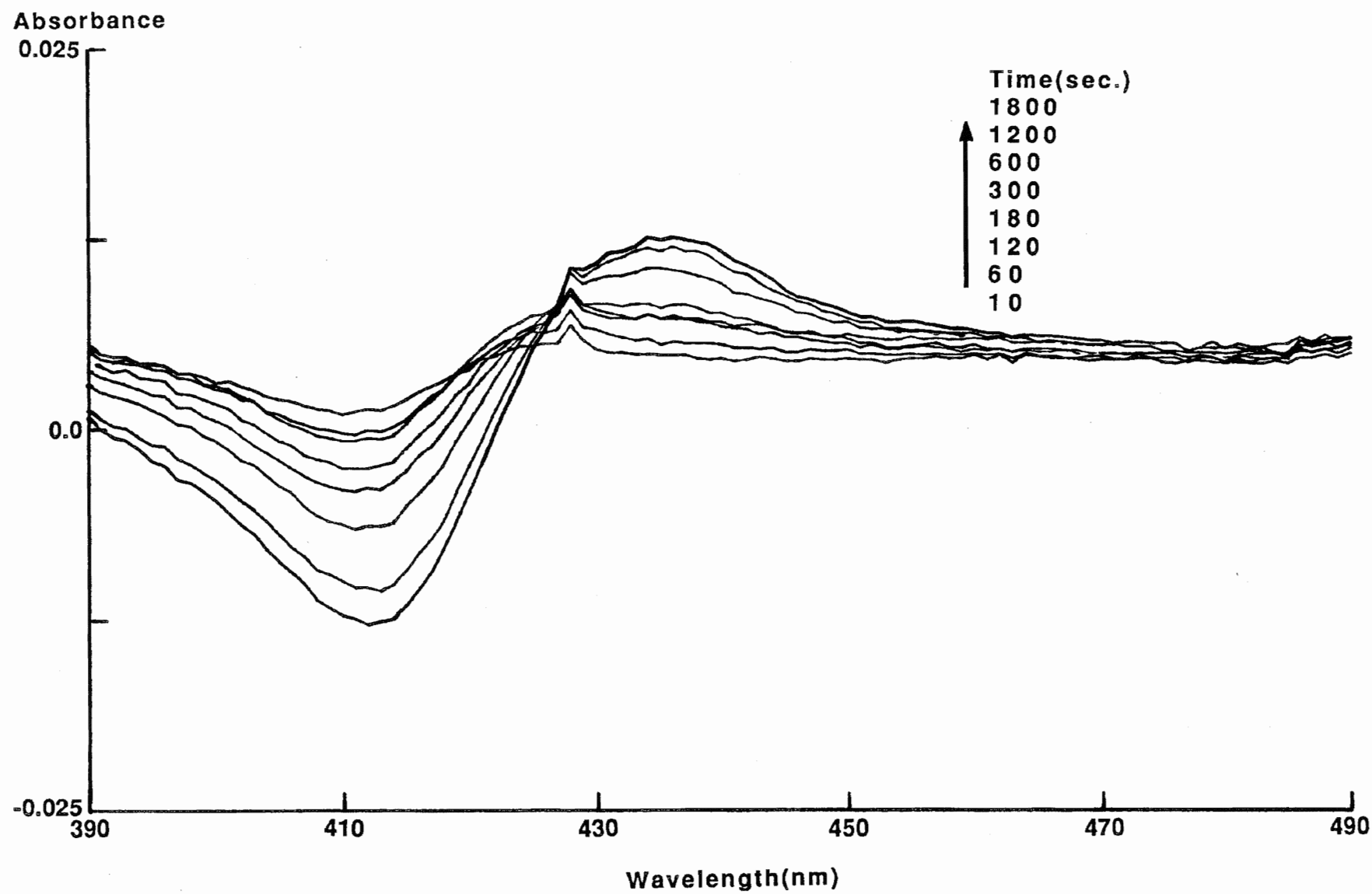


Fig.19 Difference spectra of dibucaine-liganded species minus resting enzyme. 84

Experiments in 50mM potassium phosphate,pH 7.4, 0.015% lauryl maltoside at 30°C with 4 μ M resting enzyme . Spectra were taken at 10sec, 1min, 2min, 3min,5min, 10min, 20min and 30min after addition of 1.5mM dibucaine . The spectrum of resting enzyme was subtracted from each spectrum. DU-7 Beckman spectrophotometer; a 1cm-lightpath, 1ml-volume quartz cuvette.

time , suggesting a multiphasic process . The peak was originally located at 430nm, and then it slowly shifted to 436nm. The trough stayed at 413nm. In this respect the dibucaine effect differs from the valinomycin effect, which appears to result in a single final species (Fig. 8A) . The rate of dibucaine binding was studied by monitoring the spectral change at the 433-413nm wavelength pair instead of 436nm-413nm (Fig. 20A), in order to be consistent with the parallel study with valinomycin(Fig. 8A) . When dibucaine was added to the enzyme, a biphasic trace was obtained. The data were fitted to a double exponential rise function in the Olis™ fitting programme. The values of the maximal spectral change ΔA and the rate constant k_{app} for the fast phase can be calculated as 0.01A and 0.019 sec^{-1} respectively , while ΔA and k_{app} for the slow phase are 0.07A and 0.00019 sec^{-1} . The corresponding logarithmic plot is shown in Fig. 20(B). Assuming that $k_{app} = -\text{slope}/\log(e) = -2.303 * \text{slope}$, the result is very close to that obtained by direct fitting.

Formate alone induced a opposite spectral shift to that with dibucaine with a total ΔA of 0.036. When formate was added after dibucaine addition , the dibucaine-induced red shift was partially reversed with a total ΔA of 0.055 . The data were fitted to a double exponential decay function in the Olis™ fitting routines . The corresponding logarithmic plots are shown in Fig. 20C. The rate constants for the formate effect changed very little in the presence of dibucaine, indicating that dibucaine does not hamper formate binding at the binuclear centre .

Fig. 20(A)

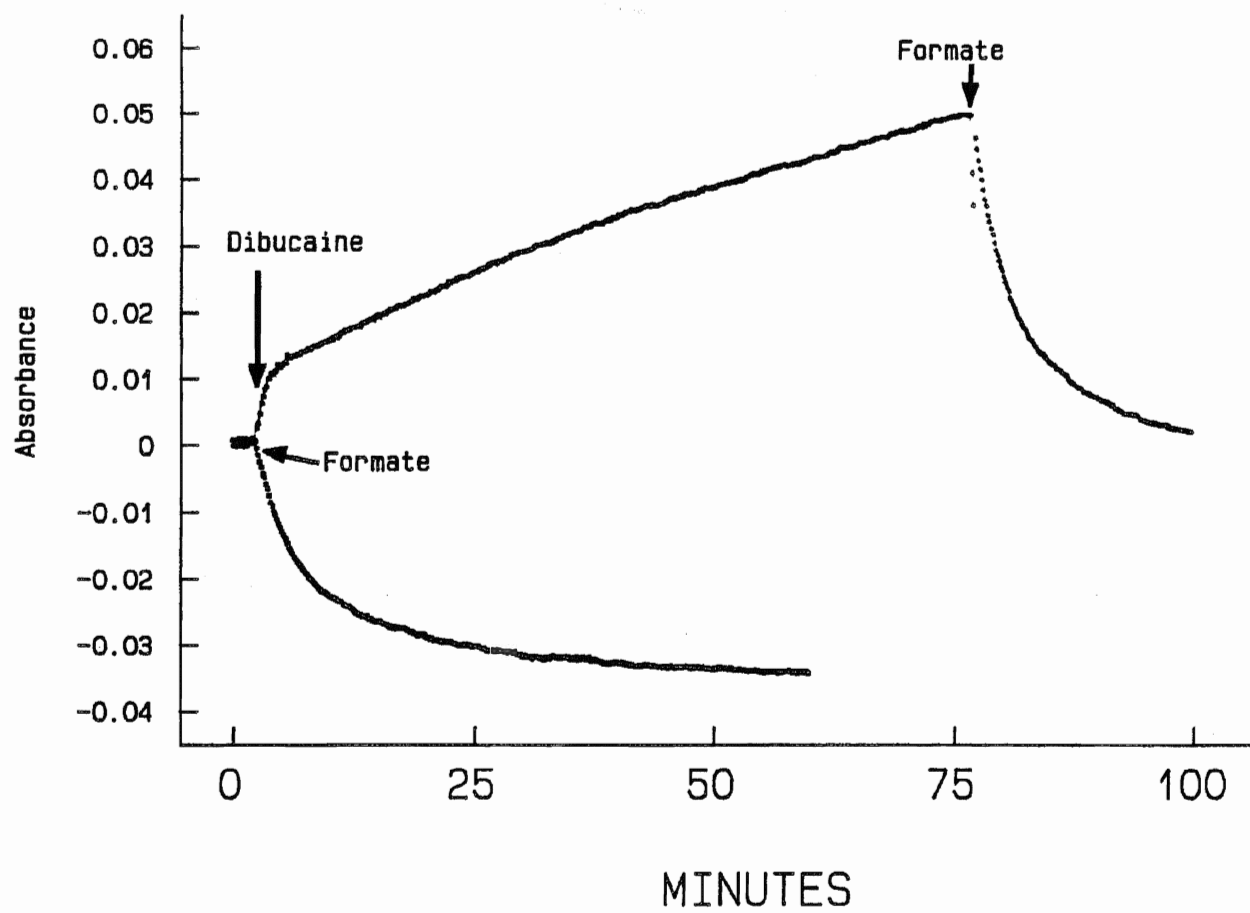


Fig. 20(A) Time course of dibucaine binding to resting cytochrome oxidase: comparison with formate binding. 86

Experiments in 50 mM potassium phosphate , pH7.4 , 0.015% lauryl maltoside at 30°C with 1.5 mM dibucaine or 3mM sodium formate added to 5.0 μ M resting enzyme to start the reaction. At the end of the dibucaine reaction , 3mM sodium formate was also added to compare the formate and dibucaine effects. Spectral changes monitored at 433-413nm . DW-2 Olis dual wavelength spectrophotometer ; 1cm-lightpath, 1ml-volume cuvette.

Fig. 20(B) **Analysis of dibucaine binding kinetics : logarithmic plots of the differential absorbance changes.** 87

Experimental data from the results in Fig. 20(A). The end point (maximal absorbance change) was estimated using the Olis™ fitting routine for a double exponential rise function (see **Methods**). Starting $\log(\Delta A_m - \Delta A)$ arbitrarily set to 0.00. The straight line shows the results of the fit to the chosen experimental points (closed symbols). 1.5mM dibucaine plus 5.0 μ M resting enzyme at 30°C pH 7.4.

Fig. 20(C) **Analysis of formate binding kinetics : logarithmic plots of the differential absorbance changes(\pm dibucaine).**

Experimental data from the results(inverted from absorbance decrease) in Fig. 20(A). The end points (maximal absorbance changes) were estimated using the Olis™ fitting routine for a double exponential rise function (see **Methods**). Starting $\log(\Delta A_m - \Delta A)$ arbitrarily set to 0.00. The straight line shows the results of the fit to the chosen experimental points (closed symbols: with dibucaine; open symbols: control). 3.0mM sodium formate plus 5.0 μ M resting enzyme at 30°C pH 7.4 \pm dibucaine. Other conditions as in the legend to Fig.20(A).

Fig.21A plots the spectral changes at 433-413nm in 50mM potassium phosphate buffer as a function of dibucaine concentration . The dissociation constant K_d and the maximal extinction coefficient ΔE_{mM} can be obtained from Eq. 12:

$$K_d = [E] \cdot [D] / [ED] \quad \text{Eq.12}$$

Since $\Delta A_{\max} = [E]_{\text{tot}} \cdot E_{mM}$, $\Delta A = [ED] \cdot E_{mM}$, and $[E]_{\text{tot}} = [E] + [ED]$, we have :

$$1/\Delta A = (K_d/\Delta A_{\max})/[D] + 1/\Delta A_{\max} \quad \text{Eq. 13}$$

According to Eq. 13, a double reciprocal plot, i.e. $1/\Delta A$ vs. $1/[D]$ will result in a straight line. The Y axis intercept is the reciprocal of ΔA_{\max} , which can be used to calculate ΔE_{mM} . The X axis intercept is the reciprocal of K_d . Fig. 21B shows that $1/\Delta A$ changes linearly with $1/[D]$. The apparent dissociation constants K_d and extinction coefficients ΔE_{mM} can also be obtained by fitting the data directly to an appropriate "Binding" equation in Multifit™(see **Methods** for details).

The effect of ionic strength was investigated by monitoring the spectral change at two different buffer concentrations(Fig. 22A). The apparent dissociation constants K_d and extinction coefficients ΔE_{mM} were obtained using the two methods described above. Fig. 22B is the double reciprocal plot of the data from Fig. 22A.

The results from Figs. 21 and 22 are summarized in Table 4. The parameters obtained by direct fitting and from the double reciprocal plot are in essential agreement. Although the ionic

Fig. 21

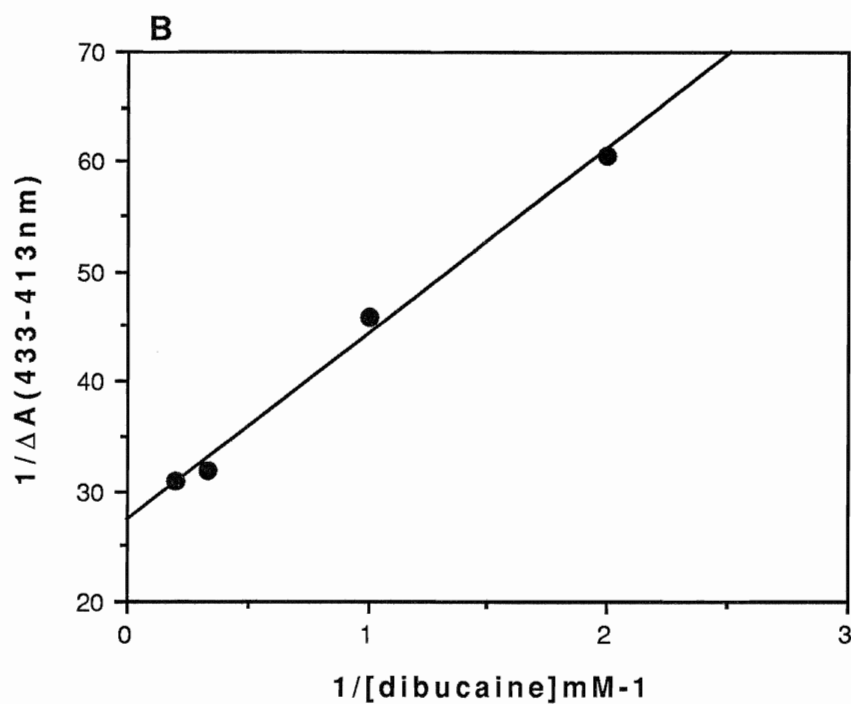
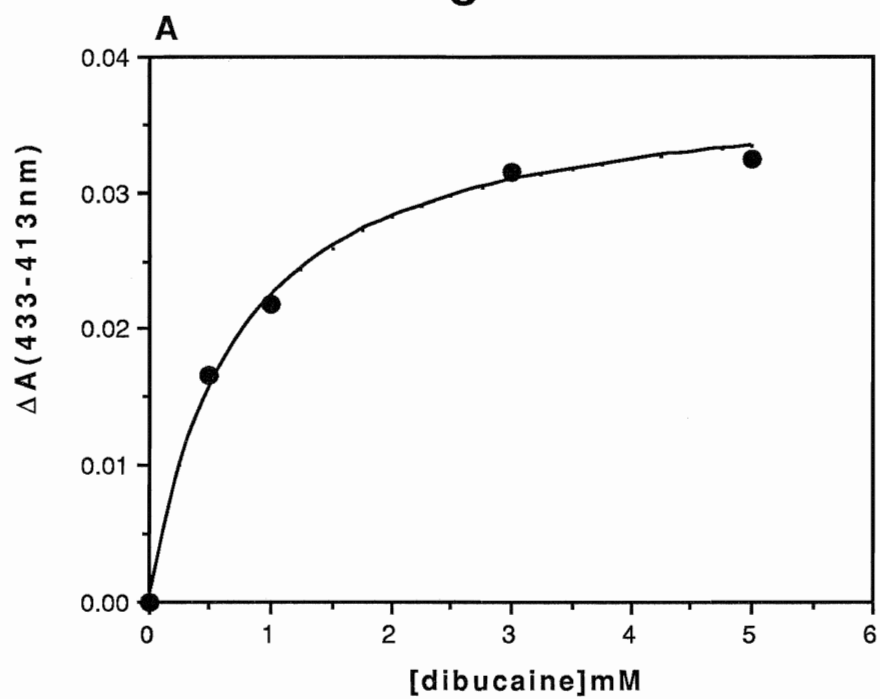


Fig. 21 Effect of the dibucaine concentration on the magnitude of the cytochrome oxidase spectral shift

89

Experiments in 50 mM potassium phosphate , pH7.4, 0.015% lauryl maltoside at 30°C . Separate aliquots of 3.9 μ M enzyme were incubated at the indicated dibucaine concentrations for 2 hours . DU-7 Beckman spectrophotometer; 1cm-lightpath, 1ml-volume cuvette .

A. titration curve(spectral change at 433-413nm)

B. double reciprocal plot(spectral change at 433-413nm)

Fig. 22

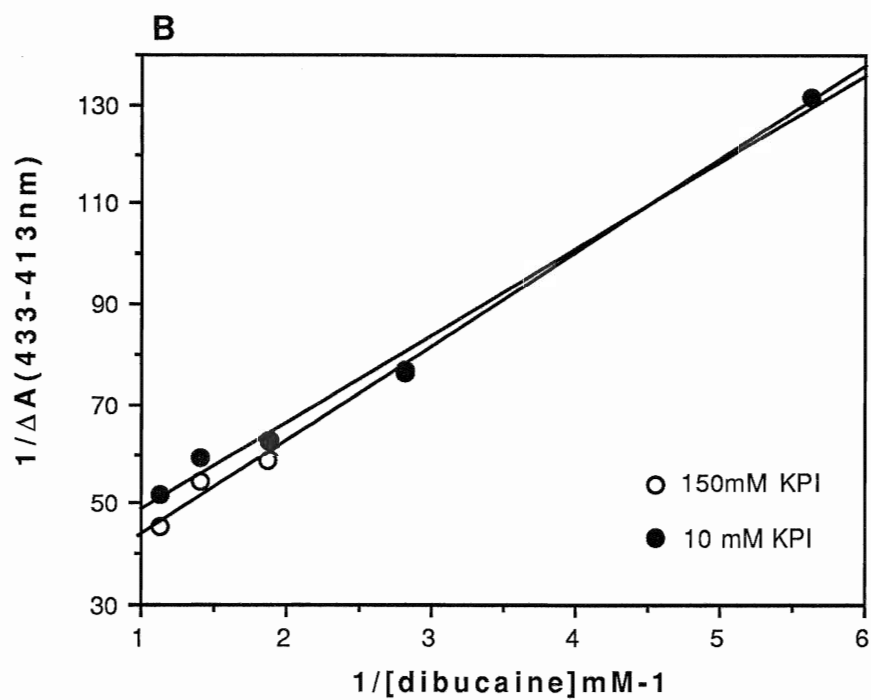
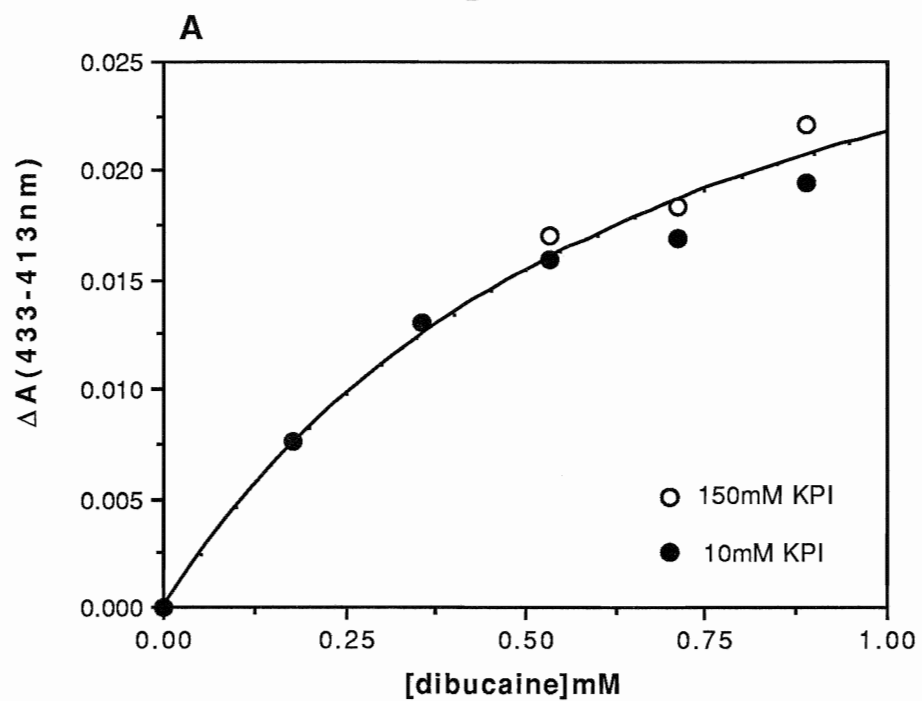


Fig. 22 Effect of ionic strength upon the dibucaine-induced enzyme spectral shift

90

Two sets of experiments were carried out in 10 mM or 150mM potassium phosphate , pH7.4, respectively, with 0.015% lauryl maltoside at 30°C . Separate aliquots of 3.9 μ M enzyme were incubated at the indicated dibucaine concentrations for 2 hours . DU-7 Beckman spectrophotometer; 1cm-lightpath, 1ml-volume cuvette .

A. Titration curve (spectral change at 433-413nm).

Open symbols : 150mM potassium phosphate.

Close symbols : 10mM potassium phosphate.

B. Double reciprocal plot (spectral change at 433-413nm).

Open symbols : 150mM potassium phosphate.

Close symbols : 10mM potassium phosphate.

Table 4

potassium phosphate (mM)	By direct fitting		By the double reciprocal plot	
	K_d (mM)	ΔE (433-413nm) $\text{mM}^{-1} \text{cm}^{-1}$	K_d (mM)	ΔE (433-413nm) $\text{mM}^{-1} \text{cm}^{-1}$
10 *	0.47 ± 0.07	7.51 ± 0.5 $\text{mM}^{-1} \text{cm}^{-1}$	0.56 ± 0.08	8.23 ± 0.7 $\text{mM}^{-1} \text{cm}^{-1}$
50 #	0.65 ± 0.06	9.55 ± 0.26 $\text{mM}^{-1} \text{cm}^{-1}$	0.62 ± 0.07	9.40 ± 0.4 $\text{mM}^{-1} \text{cm}^{-1}$
150 *	0.72 ± 0.1	10.02 ± 1.0 $\text{mM}^{-1} \text{cm}^{-1}$	0.76 ± 0.08	10.35 ± 0.8 $\text{mM}^{-1} \text{cm}^{-1}$

* Values are from Fig. 22.

Values are from Fig. 21.

Table 4. Dibucaine-induced spectral changes in the media of different ionic strengths. 91

The values in the second row are obtained from the data of Fig. 21. The values in the first and third rows are obtained from the data of Fig. 22. Columns two and three list the apparent dissociation constants (K_d values) and maximal absorbance changes obtained from the Multifit™ direct fitting routine. Columns four and five list the corresponding dissociation constants (K_d values) and maximal absorbance changes obtained from the double reciprocal plots shown in Figs 21B and 22B. All conditions are listed in the legends to Figs. 21 and 22.

strength varied from 10mM potassium phosphate to 150mM potassium phosphate , K_d and ΔE_{mM} changed only slightly, indicating that electrostatic forces are not the major factor which determines the dibucaine -oxidase interaction.

The apparently similar spectral effects of dibucaine, valinomycin and cyanide upon resting cytochrome oxidase(Figs. 4A, 5 and 18) prompted some parallel spectral studies under enzymatic turnover conditions. To avoid complications from the presence of cytochrome *c* , an artificial reducing system composed of ascorbate plus TMPD was used. Ascorbate was added in excess to keep the enzyme substrate TMPD completely in its colorless reduced form. 10 seconds after adding reducing equivalents to the resting enzyme , 69 % of the cytochrome *a* was reduced(Fig.23A), evidenced by a substantial absorption increase at both 445nm and 604nm . In the later steady state(8 min after adding reducing equivalents), cytochrome *a* became slightly reoxidized, indicating that the enzyme had become more active . The 445nm band of the reduced enzyme is due to both *a* and *a₃* in roughly equal proportions(Yonetani 1960), so cytochrome *a₃* remained mostly oxidized during the steady state since the 445nm band developed to only about half of its possible maximum . The 419nm band moved to 424nm during the steady state. This phenomenon was explained by Nicholls and Hildebrandt (1978a) as a high to low spin shift of the ferric *a₃* as a result of a enzyme conformational change during the steady state. When formate, a conventional ligand for high spin haem *a₃*, was added to the resting enzyme, a blue shift of the Soret peak from 419nm

Fig. 23(A)

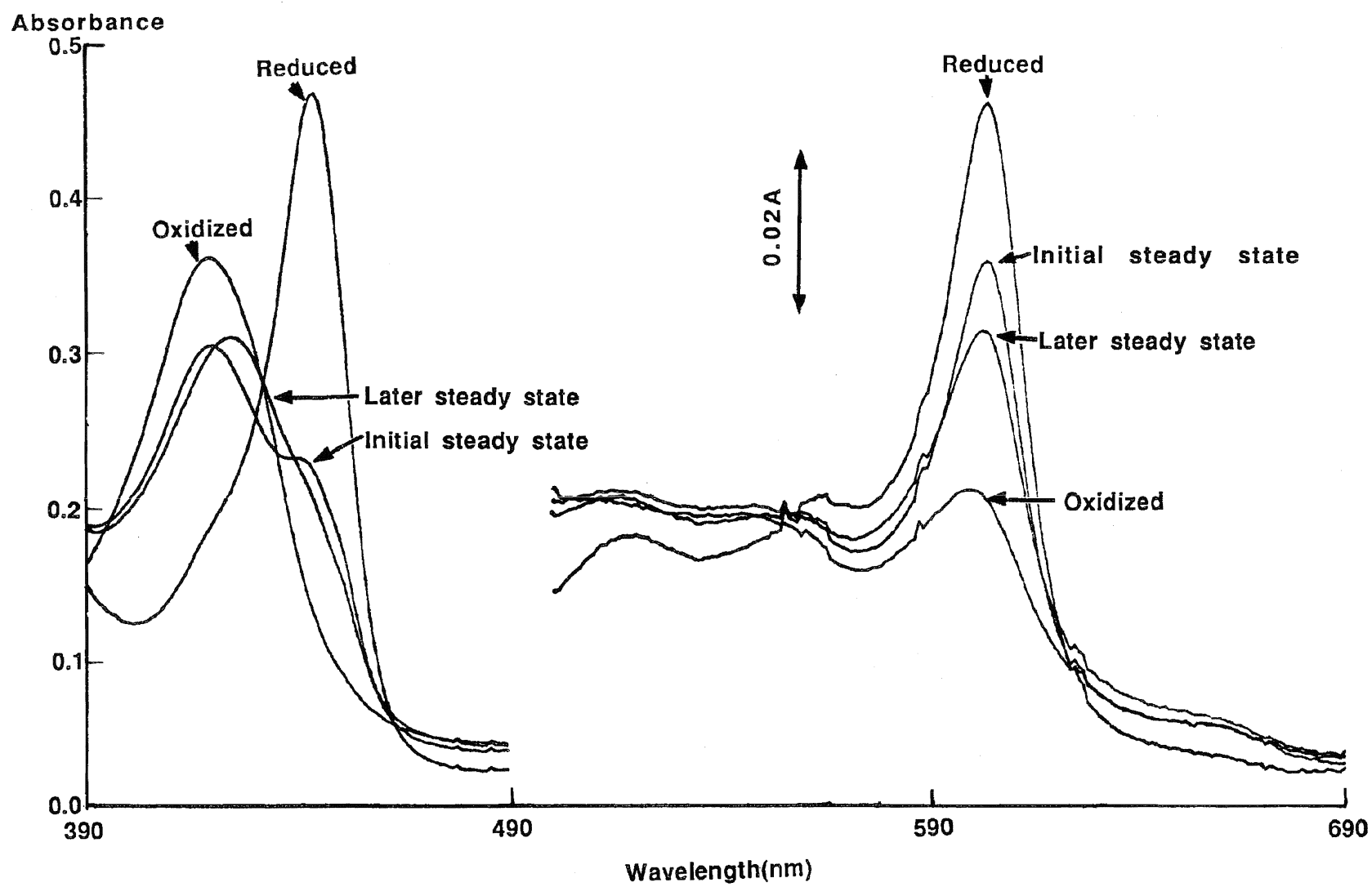


Fig. 23A The early and late steady state behaviour of cytochrome oxidase : control 93

The experiments were performed in 50 mM potassium phosphate, pH 7.4, 0.015% lauryl maltoside at 30°C with 14 mM ascorbate plus 0.27 mM TMPD added to 3 μ M oxidase in a 1cm-lightpath, 1ml-volume quartz cuvette. DU-7 Beckman spectrophotometer.

Fig. 23(B)

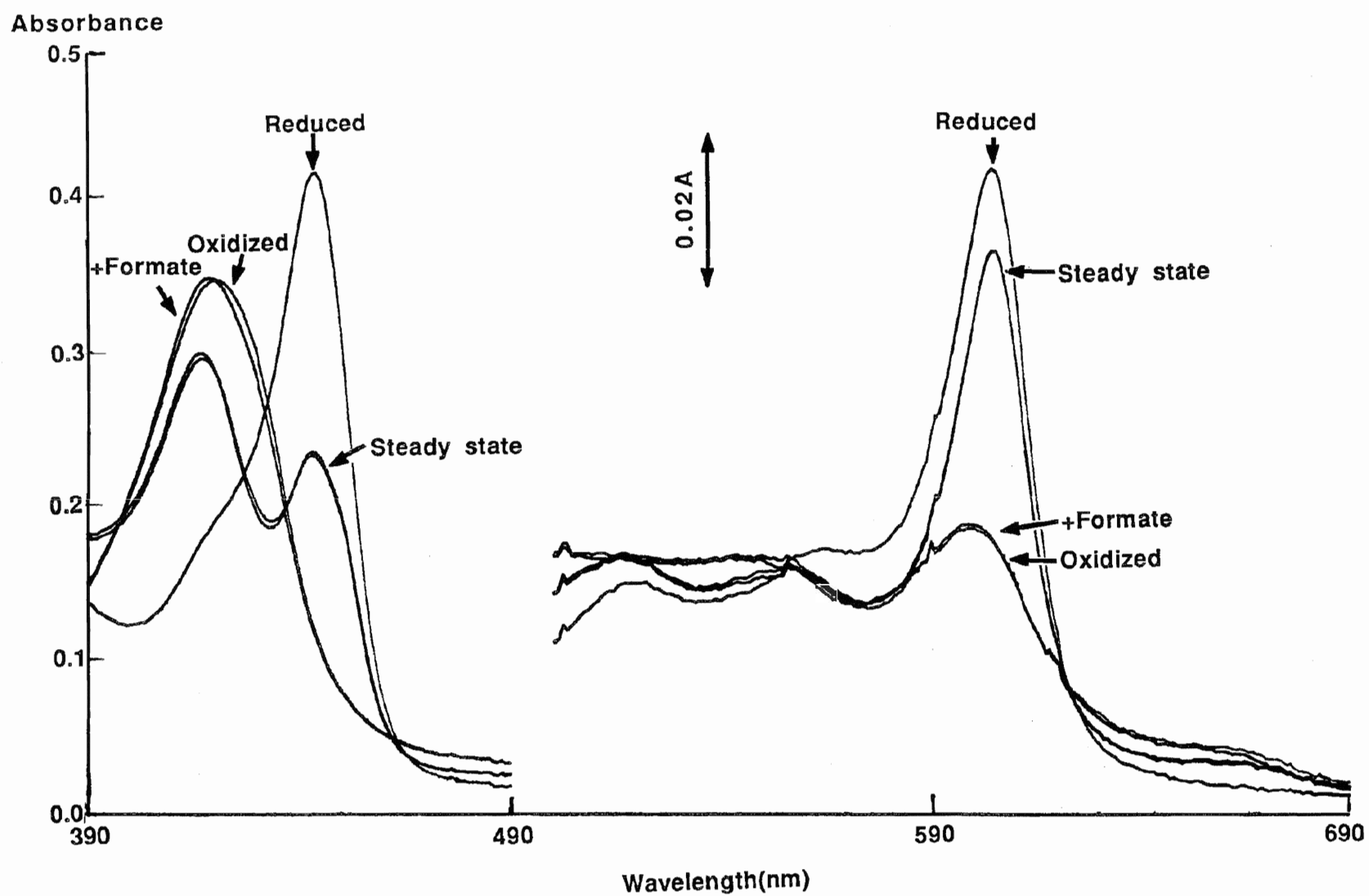


Fig. 23B. The early and late steady state behaviour of cytochrome oxidase : in the presence of formate 94

14 mM ascorbate plus 0.27 mM TMPD were added to 3 μ M oxidase in presence of 40mM formate, other conditions are identical as those of Fig. 23A.

Fig. 23(C)

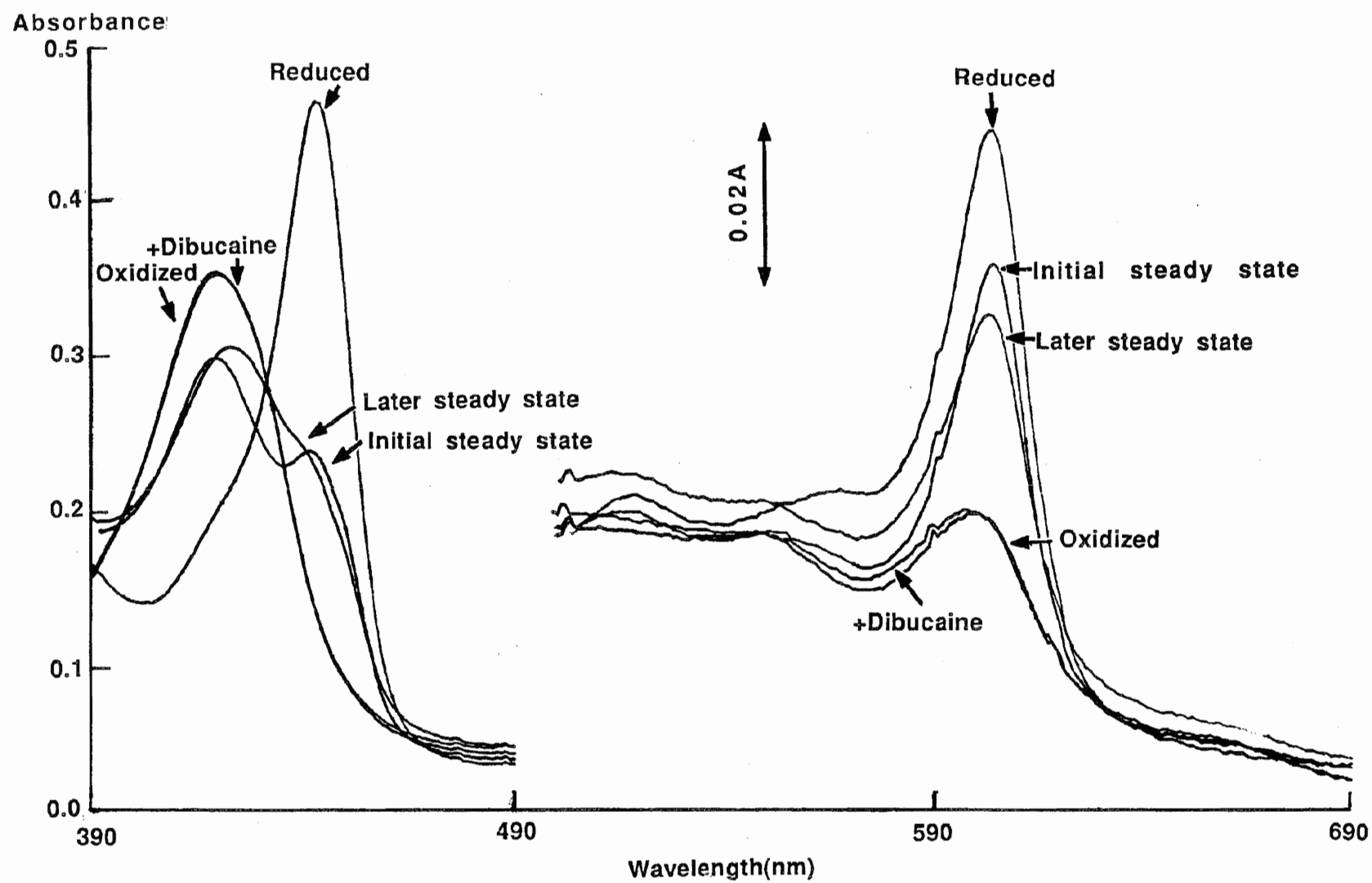


Fig. 23(D)

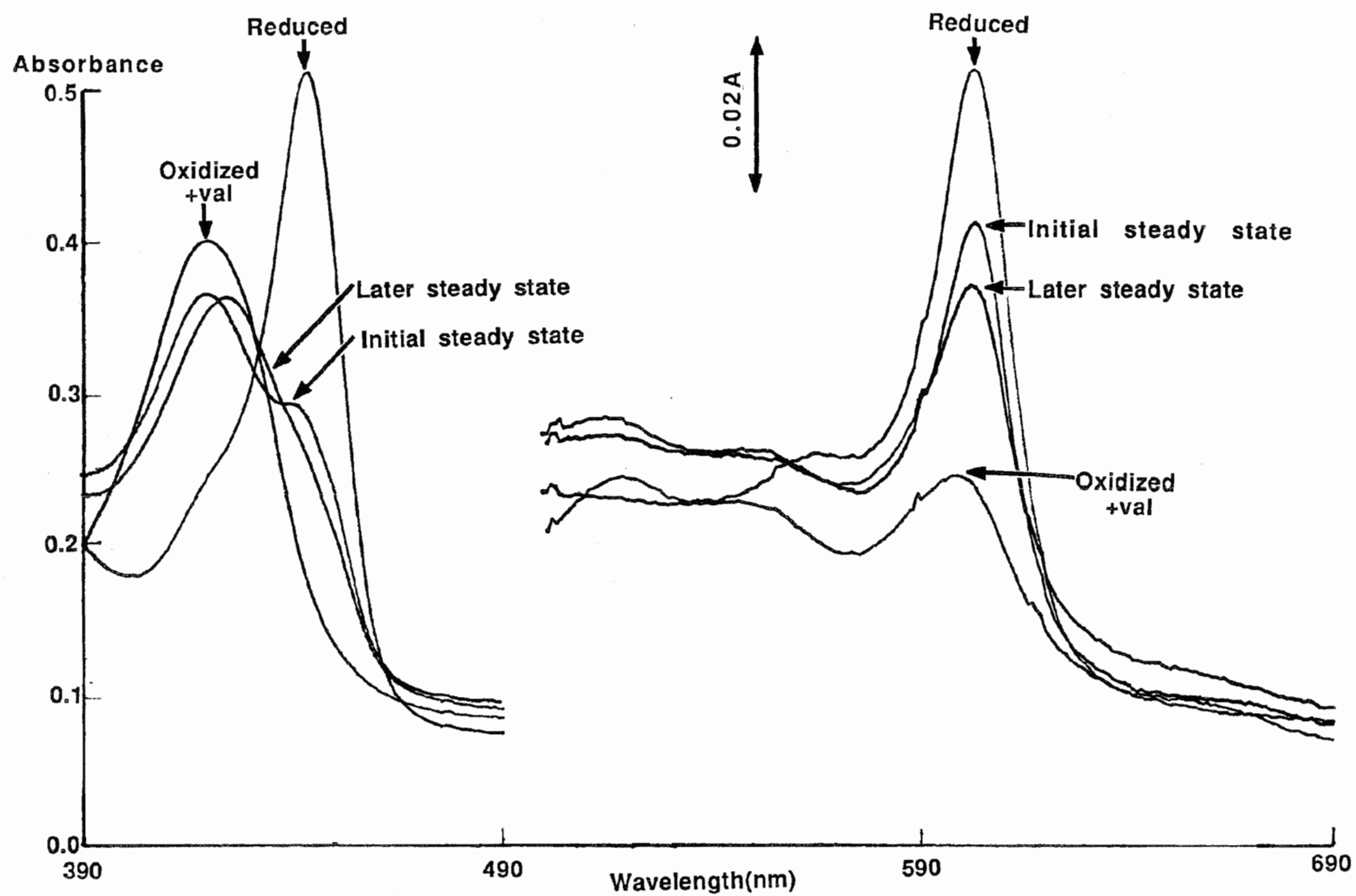


Fig. 23D The early and late steady state behaviour of cytochrome oxidase : in the presence of valinomycin 96

14 mM ascorbate plus 0.27 mM TMPD were added to 3 μ M oxidase in presence of 4 μ M valinomycin, other conditions are identical as those of Fig. 23A.

to 417nm was seen(Fig. 23B), indicating a low to high spin shift of ferric a_3 (Nicholls 1976) . Formate also kept cytochrome a_3 in the high spin form during the steady state, so that the 417nm band remained at the same wavelength . A higher 605nm band and a well-developed trough between the 417nm and 445nm bands indicate that cytochrome a was much more reduced(>90% , see Fig.24) during the formate-inhibited steady state compared with control conditions, due to the inhibition of electron transfer between cytochrome a and the binuclear center (Nicholls 1976). In the presence of dibucaine(Fig. 23C) , the initial steady state spectrum showed a higher 605nm band and a more marked split of the 419nm and 445nm bands than in control conditions, indicating inhibition of electron transfer. The later steady state spectrum is similar to that in control conditions, and features a decrease of absorption at both 605nm and 445nm as well as a red shift of the Soret peak from 419nm to 424nm . The valinomycin effect is similar to that of dibucaine (Fig. 23D); a slight increase in the steady state of cytochrome a was also seen, which is consistent with the previous observations when the cytochrome a steady state was monitored at the 605-630nm wavelength pair(Fig. 12).

From the above experiments as summarized in Fig. 24, it is clear that although both dibucaine and valinomycin have similar effects upon the resting enzyme spectrum to those of conventional low spin haem ligands such as cyanide and azide, the two former ligands exhibit quite different spectral behaviour during the steady state. Although they cause a slight increase in

Fig. 24

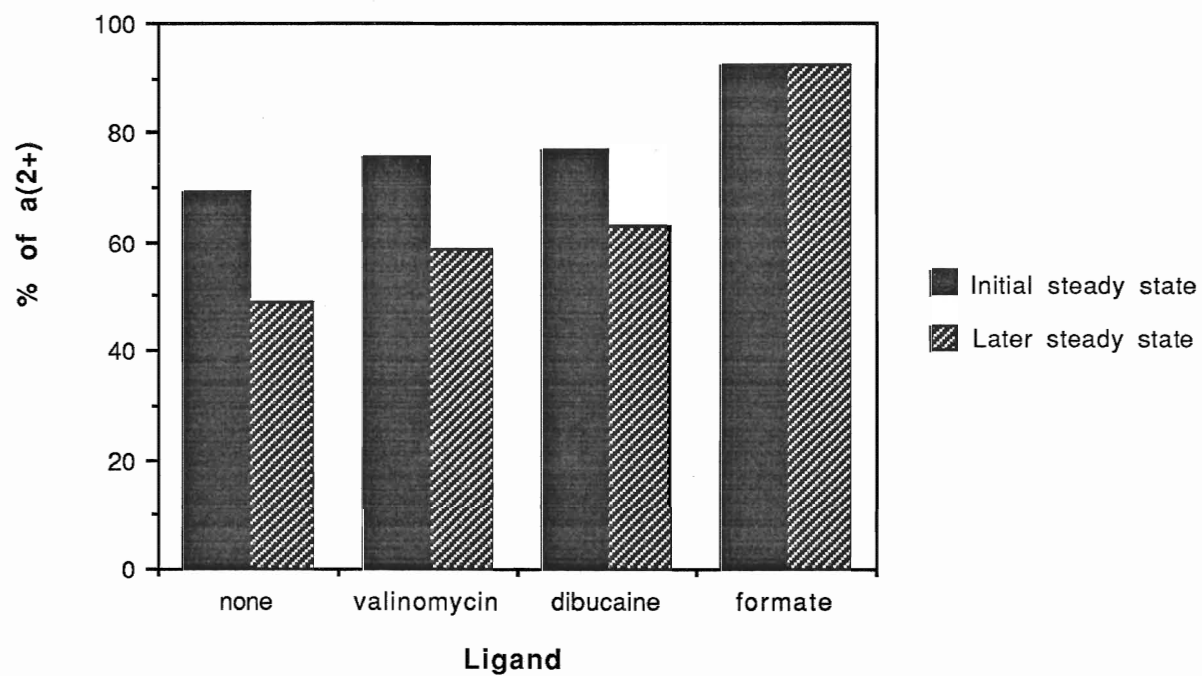


Fig. 24. Cytochrome *a* steady states in the presence of different ligands

98

Values are obtained from the sets of scanned spectra shown in Fig. 23, using the differences between the absorbances at 604nm and 630nm and calculating the percentage of reduced cytochrome *a* by assuming that 85% of the ΔA after anaerobiosis is due to reduced cytochrome *a* (Yonetani 1960). This summary figure shows the results of a single set of experiments. Similar experiments give similar results (steady state values differing by no more than $\pm 5\%$). All conditions are listed in the legends to Fig. 23A, B, C and D .

the steady state of reduced cytochrome *a*, dibucaine and valinomycin have no dramatic effects upon the steady state pattern . On the other hand, the 419nm peak disappears in the later steady state spectrum when cyanide or azide is present (Nicholls and Hildebrandt 1978a), and a small shoulder at 430nm develops .

99

B. Kinetic effects of dibucaine

The inhibition of cytochrome oxidase activity by dibucaine has been extensively studied by Singer(1980, 1982, 1983) using an oxygen electrode technique. The inhibition can also be studied by monitoring the cytochrome *c* redox steady state at 550-540nm spectrophotometrically (Fig. 25). Employing a similar method to that used to study inhibition by valinomycin , k_r (see Eq.4b) , the rate constant for reduction of cytochrome *c* by ascorbate, is plotted against dibucaine concentration (Fig. 26A). The value of k_r changes very little with increasing dibucaine concentration, suggesting that dibucaine does not inhibit electron transfer between ascorbate and cytochrome *c* . The progressive decrease in k_o (the rate constant for oxidization of ferrous cytochrome *c* by the enzyme) with increasing dibucaine concentration (Fig. 26B) confirms the previous observation (Singer 1980, Stringer and Harmon 1990) showing that dibucaine is an oxidase inhibitor . This inhibition is not an artifact caused by the artificial electron donor systems used in this and other studies . The maximum percentage inhibition is approximately 80%, and the K_i , the calculated dibucaine concentration causing

Fig. 25

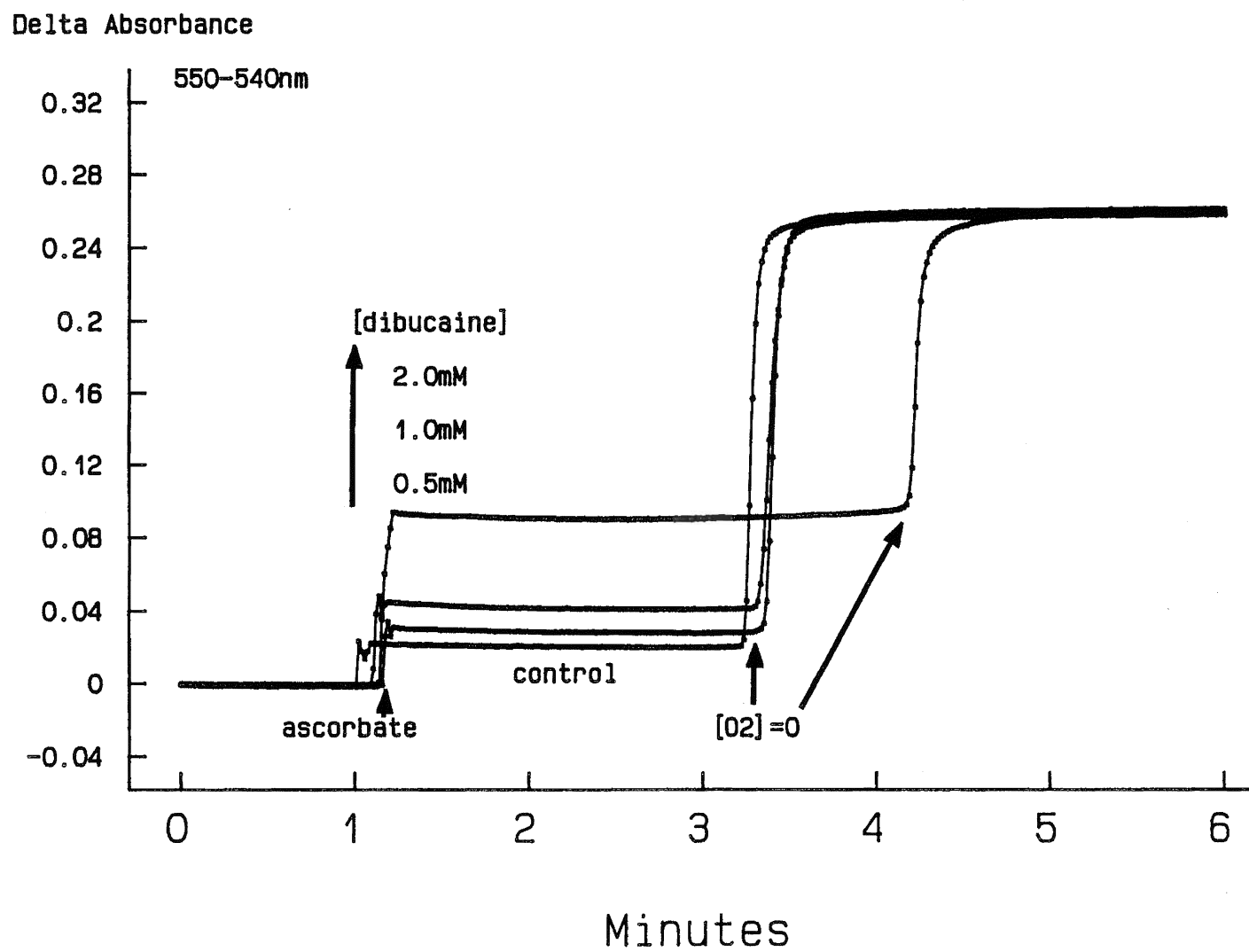


Fig. 25. Effect of dibucaine upon steady state enzyme activity. 100

The experiments were performed in 50 mM potassium phosphate, pH=7.4, 0.015% lauryl maltoside at 30°C . 12 μ M cytochrome c and 1 μ M oxidase were incubated at the desired dibucaine concentration(0-2.0mM) for 30 mins before adding 10mM ascorbate to start the reaction. 1cm-lightpath , 1ml volume quartz cuvette ; DW-2 dual wavelength spectrophotometer.

Fig.26

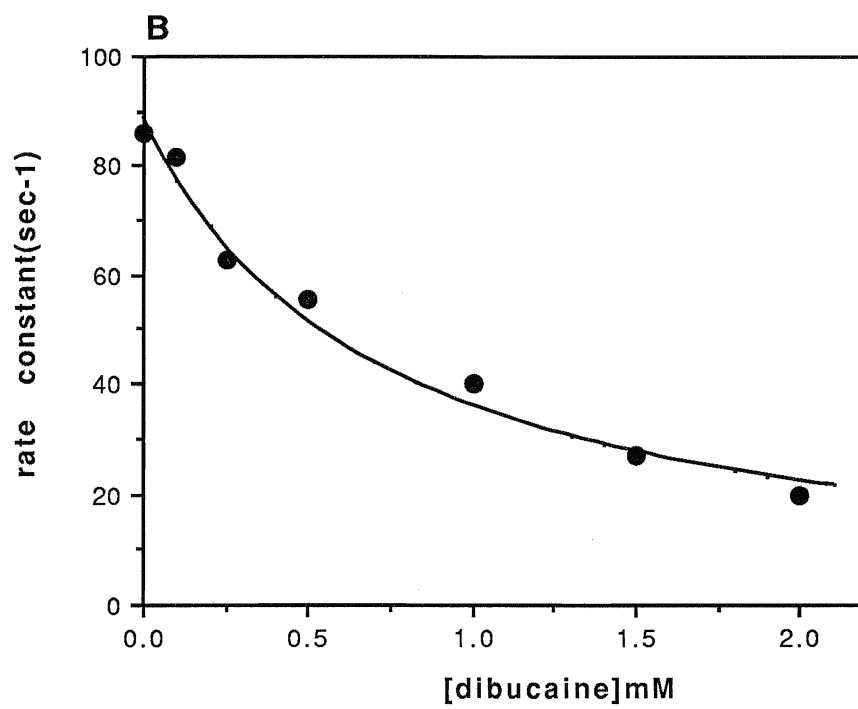
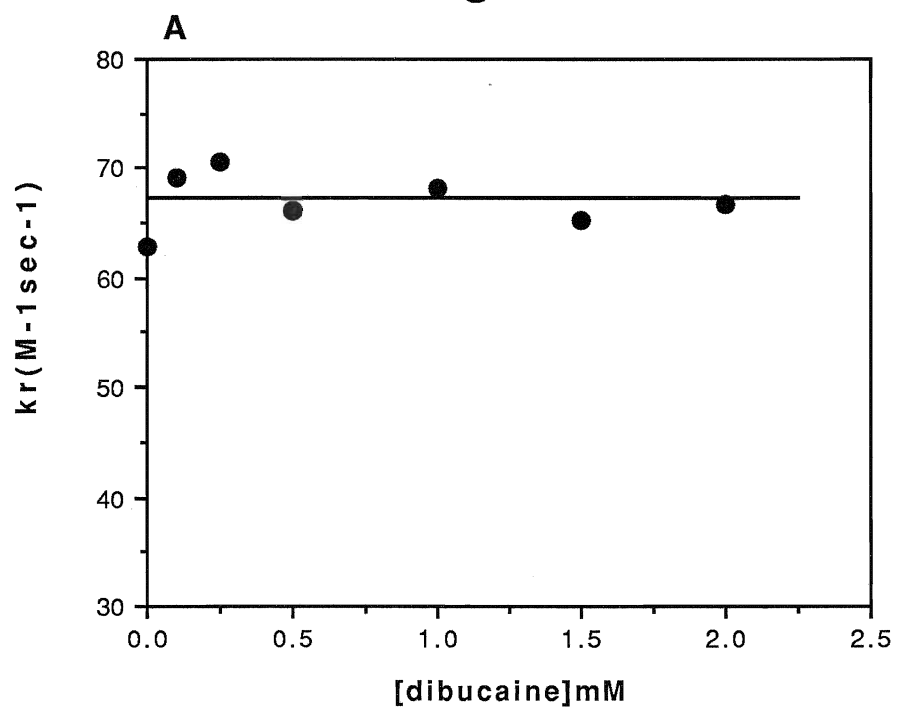


Fig. 26. Kinetic analysis of the effects of dibucaine upon the ascorbate-cytochrome *c*-cytochrome *aa₃*-O₂ steady state. 101

A. Reduction of cytochrome *c* by ascorbate.

The second order reduction rate constants were calculated from the steady state data of Fig. 25 according to the method described on p. 65 of the **Results**. The straight line is drawn for a constant k_r value of $68 \text{ M}^{-1} \text{ s}^{-1}$. Conditions are as in the legend of Fig.25. Error bars are not shown .

B. Enzymatic activity (turnover).

The turnover number k_o is the oxidation rate constant calculated according to the method described on p.65 of the **Results** . The theoretical curve is drawn for a K_d of 0.7mM and a residual activity of 20%. Conditions are as in the legend of Fig. 25. Error bars are not shown.

half of maximal inhibition is estimated as 0.7mM (see fitted 102 curve, Fig. 26B).

The rate constant for cyanide binding is greatly enhanced under enzymatic turnover conditions(Nicholls and Chance 1974). Does the presence of reducing equivalents have the same accelerating effect on dibucaine binding with the enzyme? Fig. 27(A) shows that under turnover conditions, dibucaine causes a biphasic increase of cytochrome *c* reduction in its steady state , with apparent rate constants of 0.08 sec⁻¹ and 0.0018 sec⁻¹ ; 73% of the rise is the fast phase, 27% is the slow phase. These data were obtained by fitting the data to a double exponential rise function in the OIis™ programme. These rate constants are four times greater and ten times greater respectively than the corresponding rate constants for the spectral shift. Since the steady state of cytochrome *c* reflects the percentage of the active enzyme (Nicholls and Chance 1974), the rise in the reduced cytochrome *c* steady state can be explained by gradual binding of dibucaine to the enzyme. The apparent rate constants obtained above can thus be treated as the apparent rate constants for dibucaine binding. So the presence of reducing equivalents indeed increases the rate of dibucaine binding , as in the case of cyanide . The corresponding logarithmic plot (Fig. 27B) supports the result of direct fitting. The maximal inhibition is 80%. The details of data transformation are in **Methods**.

The dibucaine effect upon electron transfer was investigated by following the steady state spectral change at the 445-470nm wavelength pair(Fig. 28). Whether the reducing

Fig. 27(A)

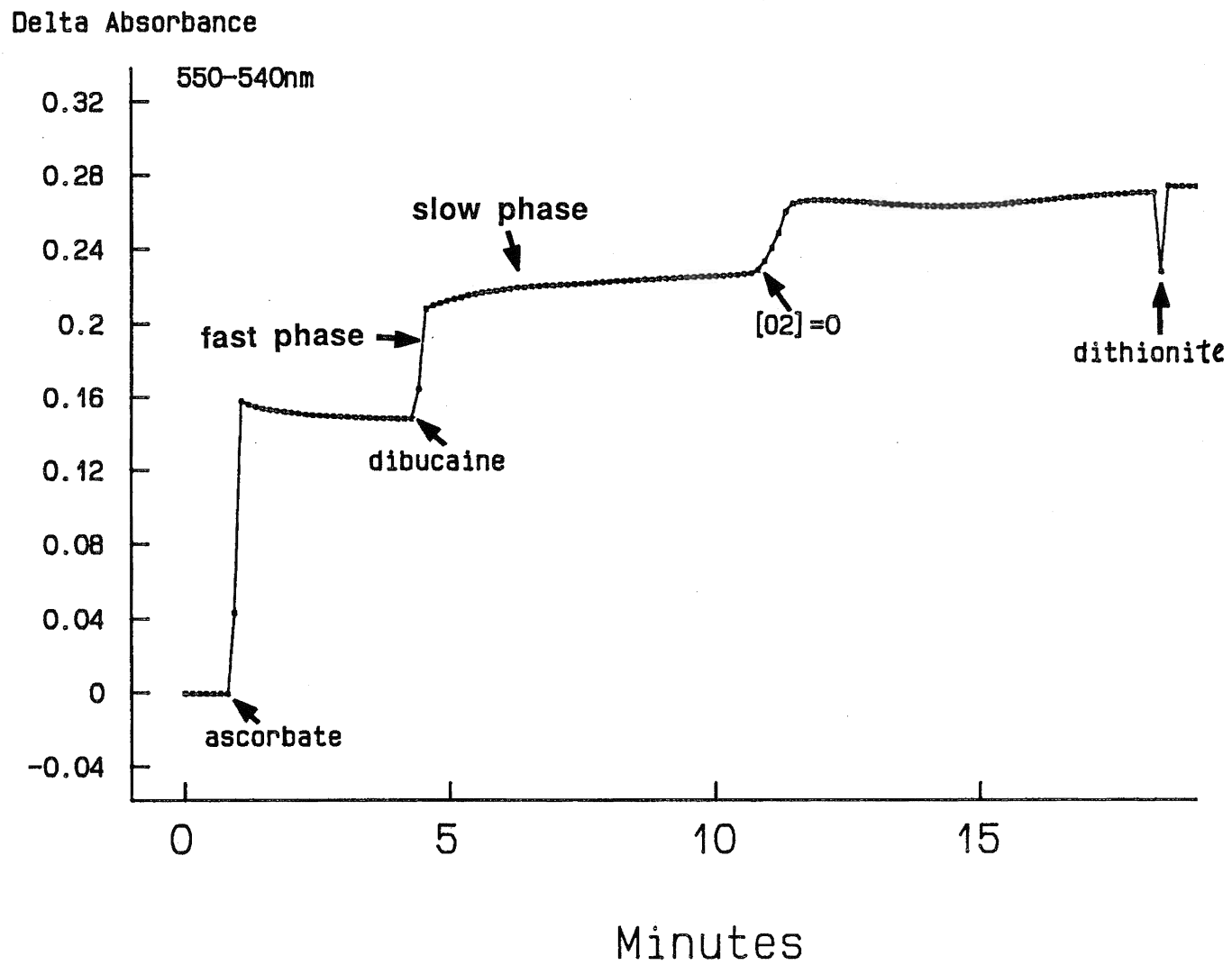


Fig. 27(A). **Fast and slow phases of dibucaine inhibition of cytochrome oxidase** 103

This experiment was carried out in 50 mM potassium phosphate, pH 7.4, 0.015% lauryl maltoside at 30°C with the DW-2 dual wavelength spectrophotometer. 7.4 mM ascorbate was added to a mixture of 85 nM *aa₃* and 13 μM cyt. *c* in a 1cm-lightpath, 1ml-volume quartz cuvette to start the reaction. 1.5 mM dibucaine was then added during the steady state as indicated . Measurements were made at the 550-540nm wavelength pair.

Fig. 27(B)

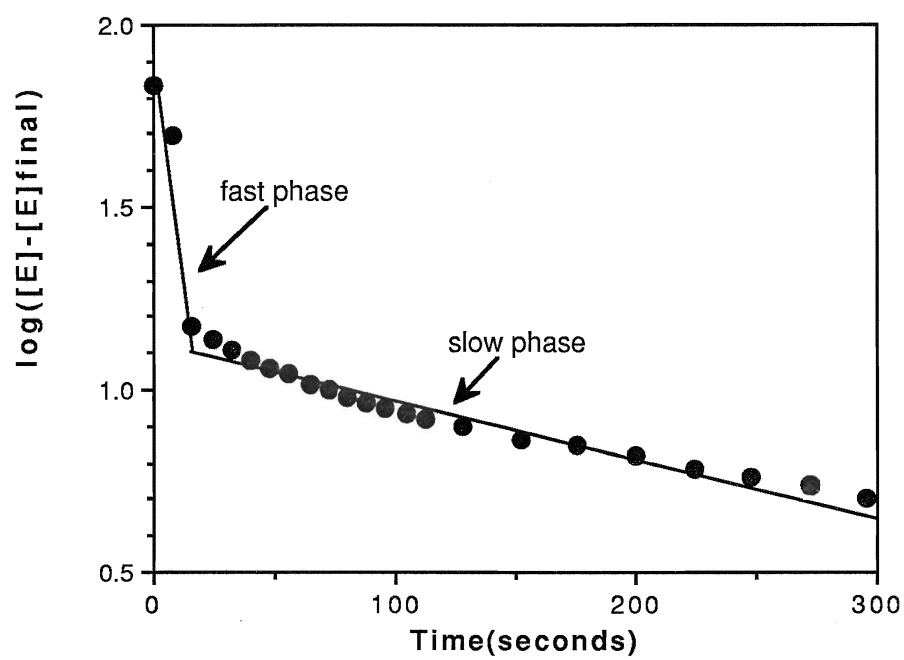


Fig. 27(B) **Kinetics of dibucaine inhibition monitored by the cytochrome c steady state.** 104

The experimental data are taken from the single set of results in Fig. 27(A). The end point (final steady state cytochrome c reduction) was estimated using the OIis™ fitting routine for a double exponential rise function (see **Methods**). The changes of uninhibited oxidase concentration ($[E]$, closed symbols) with time were calculated as described in **Methods**. The two straight lines were drawn by hand to indicate two phases. Conditions are as in the legend to Fig.27(A).

Fig. 28(A)

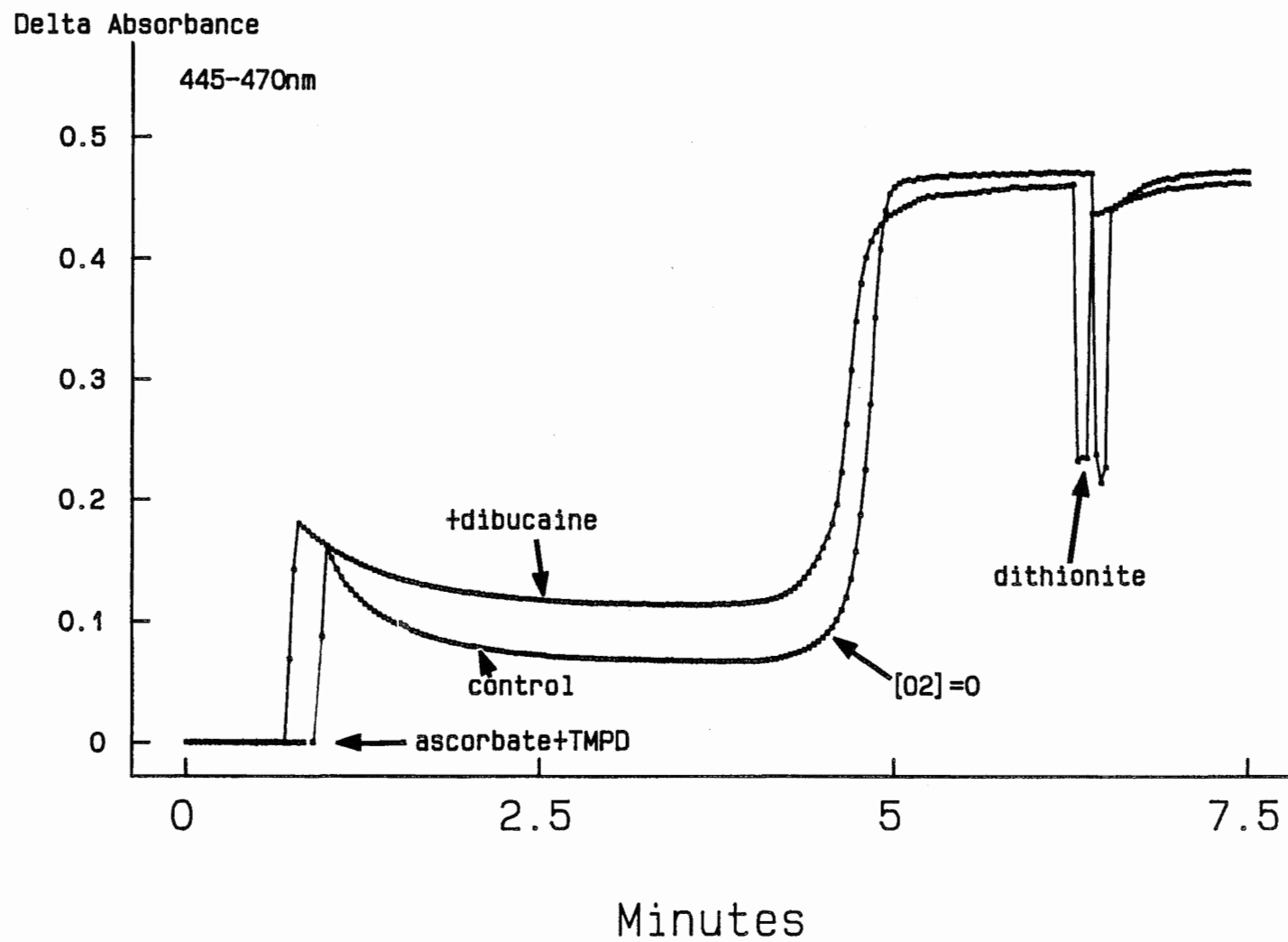


Fig. 28A Effect of dibucaine on the steady state of 105
cytochrome oxidase : ascorbate + TMPD as reductants

The experiments were conducted in 10mM potassium phosphate, pH 7.4, 0.015% lauryl maltoside at 30°C. 4μM enzyme was incubated in 2mM dibucaine for 30min before 10mM ascorbate plus 0.4mM TMPD were added to the enzyme solution to start the reaction. Measurements were made at 445-470nm wavelength pair. DW-2 dual wavelength spectrophotometer; 1cm-lightpath, 1ml-volume quartz cuvette .

Fig. 28(B)

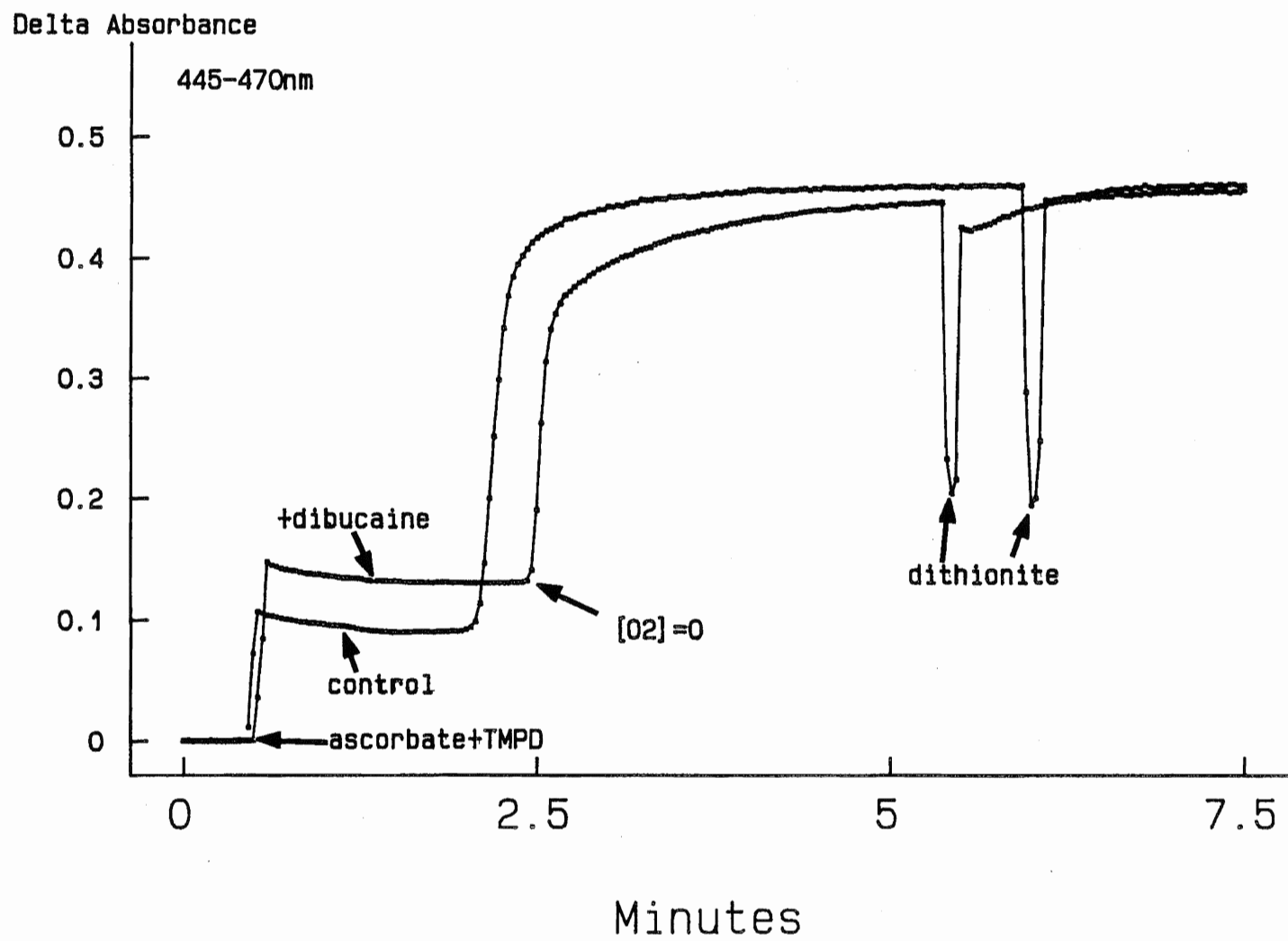


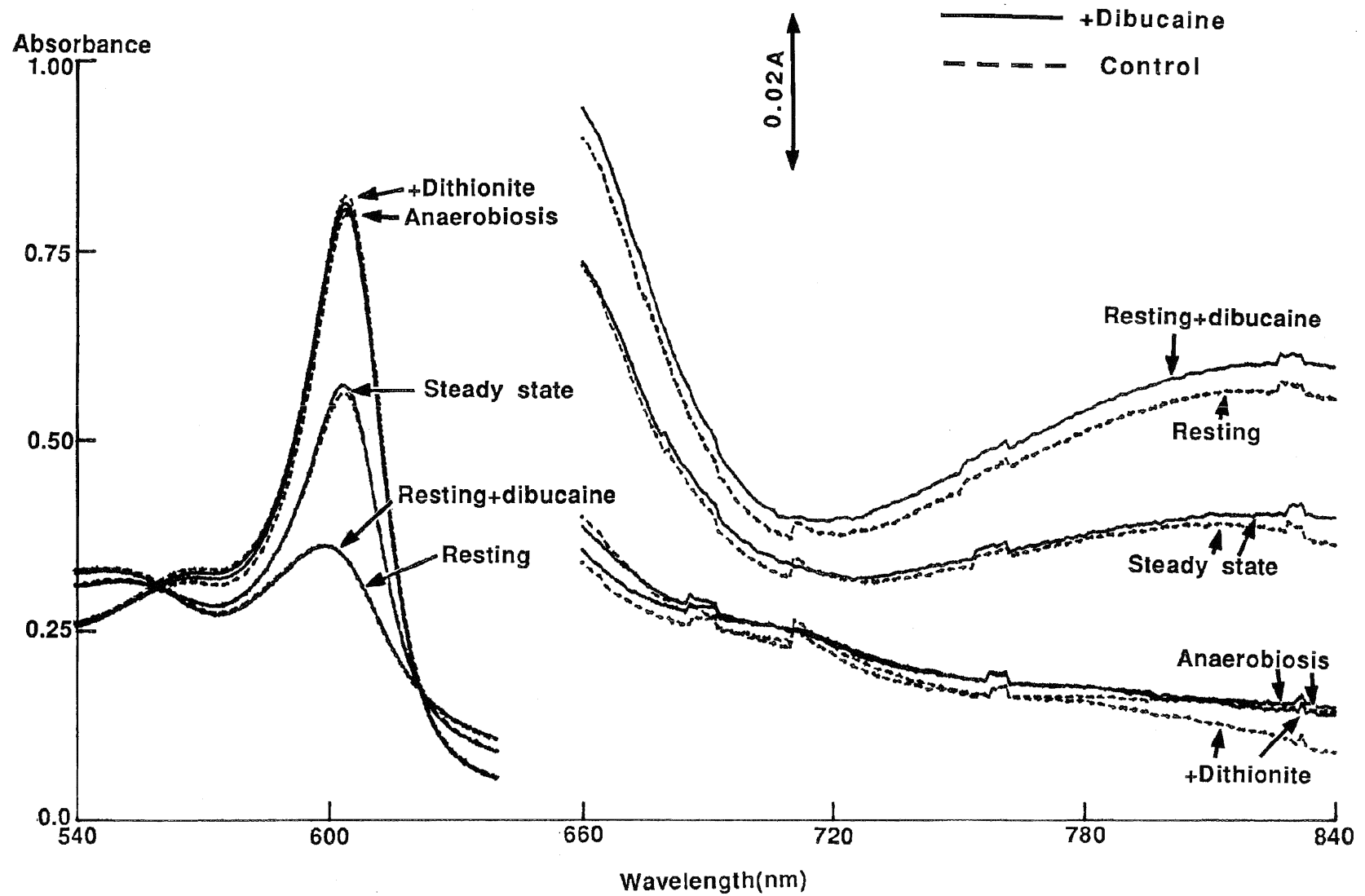
Fig. 28B Effect of dibucaine on the steady state of cytochrome oxidase : TMPD plus cytochrome c as reductants 106

The experiments were conducted in 10mM potassium phosphate, pH 7.4, 0.015% lauryl maltoside at 30°C. 4μM enzyme was incubated in 2mM dibucaine for 30min before 10mM ascorbate plus 40μM TMPD were added to the enzyme-cytochrome c mixture to start the reaction. The cytochrome c concentration was 5μM. Measurements were made at 445-470nm wavelength pair. DW-2 dual wavelength spectrophotometer; 1cm-lightpath, 1ml-volume quartz cuvette .

equivalents were ascorbate plus TMPD(Fig.28A), or cytochrome *c* (Fig.28B), the presence of dibucaine caused a substantial rise of steady state reduction at 445-470nm, indicating an increase in the steady state amount of reduced cytochrome *a* which in turn suggests an inhibition of electron transfer between cytochrome *a* and the binuclear center . But after anaerobiosis the spectral change in the presence of a high concentration of dibucaine($\approx 2\text{mM}$) was very close to that under control conditions. Adding dithionite had only a small additional effect. This indicated that both cytochromes *a* and *a₃* were fully reduced after anaerobiosis. In addition, unlike cyanide and formate (Nicholls and Chanady 1982, Nicholls 1976), there was no observable change of the reduction rate of *a₃* monitored at anaerobiosis. This result is contrary to the claim by Stringer and Harmon(1990) that dibucaine blocked the reduction of *a₃* completely but is compatible with the observation that the maximum percentage of inhibition by dibucaine is 80%(Fig. 26B).

No perturbation of Cu_A was seen(Fig.29). When ascorbate plus TMPD were the reducing equivalents(Fig.29A), Cu_A was partially reduced during the steady state, which was evidenced by a decrease of absorbance at 830nm, the absorption band attributed to cupric Cu_A (Nicholls and Chanady 1982). The higher steady state of cytochrome *a* and the prolonged anaerobiosis time(100 seconds in the presence of dibucaine, compared with 52 seconds in control conditions) indicated that the electron transfer between *a* and the binuclear center was inhibited. After anaerobiosis, both cytochrome *a* and Cu_A were fully reduced in the

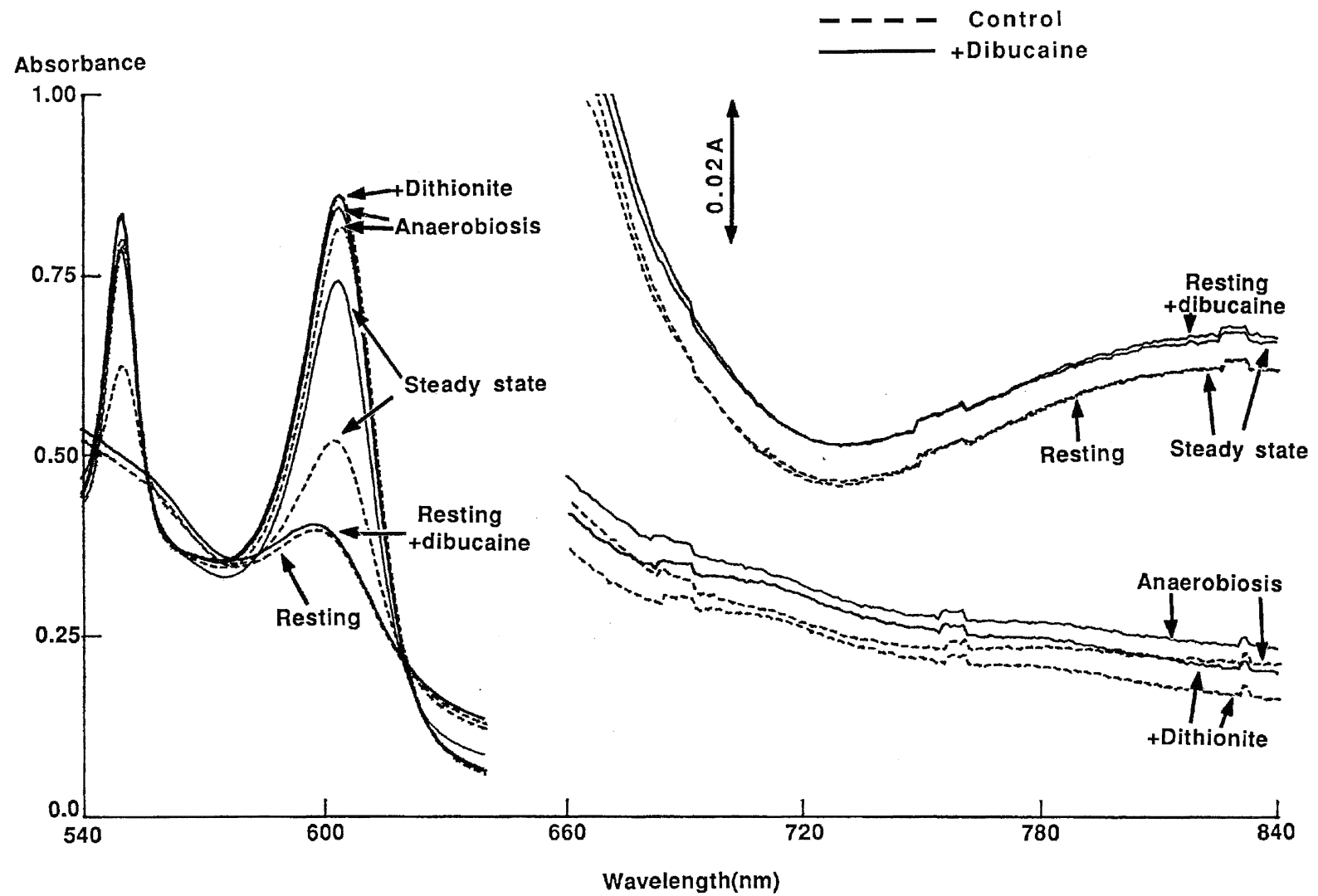
Fig. 29(A)



Cu_A: TMPD is the reductant

The experiments were carried out in 50 mM potassium phosphate, pH 7.4, 0.015% lauryl maltoside at 30°C. 11 mM ascorbate and 0.23 mM TMPD were added to 20μM resting enzyme or 20μM resting enzyme previously incubated in 1.0 mM dibucaine for 40 min. DW-2 dual wavelength spectrophotometer; 1cm-lightpath, 1ml-volume quartz cuvette.

Fig. 29(B)



Cu_A: cytochrome *c* is the reductant

The experiments were carried out in 50 mM potassium phosphate, pH 7.4, 0.015% lauryl maltoside at 30°C. 19.4 μM cytochrome *c* was mixed with 20μM resting enzyme or 20 μM resting enzyme previously incubated in 1.0 mM dibucaine for 40 min. Then, 11mM ascorbate was added to the mixture to start the reaction. DW-2 dual wavelength spectrophotometer; 1cm-lightpath, 1ml-volume quartz cuvette.

presence of dibucaine, and adding dithionite had little further effect. When cytochrome *c* was used(Fig.29B) , there was little spectral change at 830nm during the steady state both in control conditions and in the presence of dibucaine, indicating that Cu_A remained mostly oxidized during a steady state. This phenomenon was observed previously by Nicholls and Chanady (1982). On the other hand, dibucaine greatly increased the steady state reduction of cytochrome *a* , indicating a strong inhibition of electron transfer between *a* and the binuclear center. After anaerobiosis, Cu_A was again fully reduced in the presence of dibucaine, adding dithionite had little extra effect.

Based on the above observation, it seems that Cu_A is not the site of dibucaine attack as Stringer and Harmon(1990) suggested.

All the experiments described so far have involved the isolated enzyme, What about other forms of the enzyme? Is the conclusion drawn from the isolated enzyme still valid for the enzyme in its physiological environment? To answer this question, the dibucaine effect on cytochrome oxidase in submitochondrial particles was tested(Fig. 30). In submitochondrial particles, the substrate for the enzyme, cytochrome *c* , is inside the vesicles. Therefore TMPD, a membrane-permeable reductant, is chosen as the source of reducing equivalents. Ascorbate , the agent usually employed to keep TMPD reduced, cannot reduce the oxidized TMPD trapped in the membrane because it is membrane-impermeable. To solve this problem and avoid the absorption interference from oxidized TMPD(Wursters blue), the submitochondrial particles were first

Fig. 30(A)

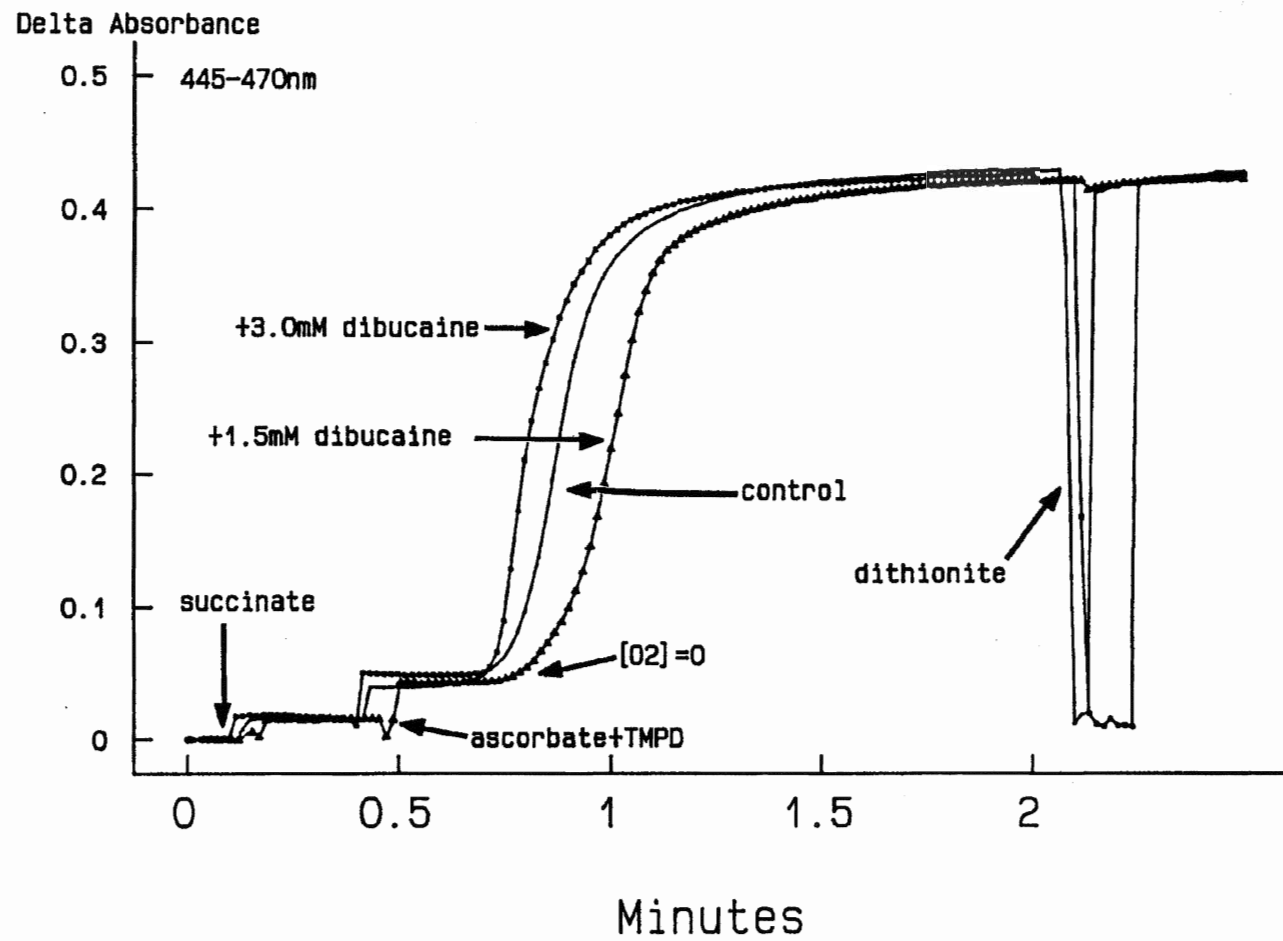


Fig. 30A Effect of dibucaine on the steady state behaviour of submitochondrial particles: 445-470nm 111

The experiments were conducted in 50mM potassium phosphate, pH 7.4 at 30°C .Submitochondrial particles were incubated in 24μM antimycin for 5 min before 25mM succinate and 3.33mM ascorbate plus 0.1mM TMPD were added to commence the reaction. Dibucaine concentrations varied from 0.0 to 3mM, and the incubation time was 30min. DW-2 dual wavelength spectrophotometer; 1cm-lightpath, 1ml-volume quartz cuvette.

Fig. 30(B)

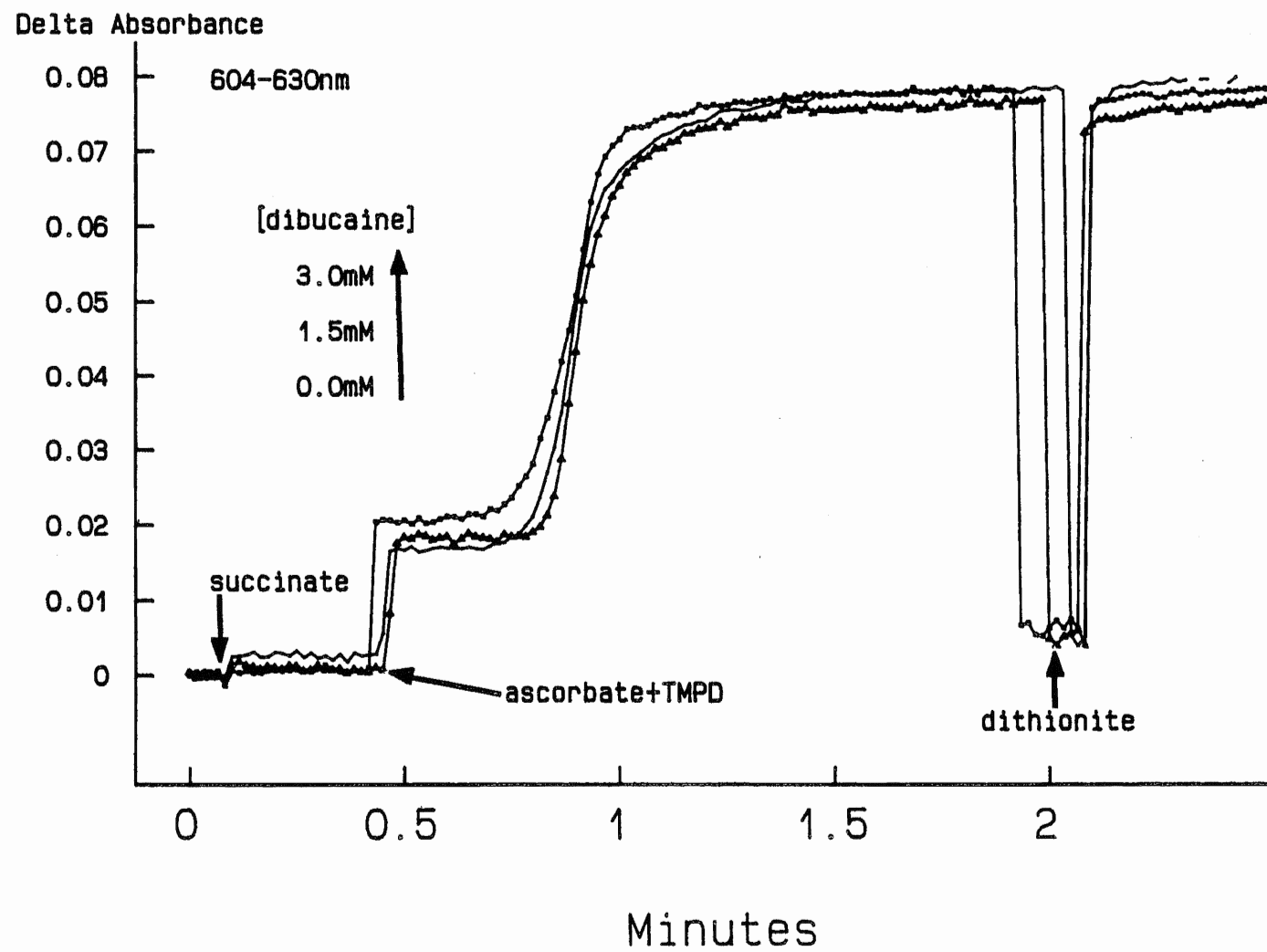


Fig. 30B Effect of dibucaine on the steady state behaviour of submitochondrial particles: 605-630nm 112

The steady state spectral change was monitored at 605-630nm instead of 445-470nm, other conditions are identical as those of Fig. 30A.

incubated with 24 μM antimycin(an inhibitor of cytochrome b/c_1 complex, Cramer and Knaff1991)to make sure that cytochrome c would not be reduced by cytochrome b/c_1 complex. An excess (25mM) of succinate, a membrane-permeable reducing agent, was then added to reduce the membrane bound TMPD. As it turned out, similar to the results with isolated enzyme, dibucaine increased the steady state of cytochrome a when monitored in both the 445-470nm(Fig. 30A) and 604-630nm(Fig. 30B) regions, suggesting an inhibition of electron transfer between cytochrome a and the binuclear center. Dibucaine had little effect upon the rate of a_3 reduction when monitored at anaerobiosis nor did it inhibit the reduction of a_3 . The similarity between this result and those of experiments with isolated enzyme suggests that dibucaine has a similar effect upon isolated enzyme and the enzyme in submitochondrial particles as well . Less marked steady state spectral changes in submitochondrial particles induced by dibucaine(Fig. 30) , as compared with the isolated enzyme(Fig. 28), is probably due to the fact that dibucaine can bind other components of the respiratory chain within submitochondrial particles as well as the oxidase (Chazotte and Vanderkooi 1981).

The severe scattering effects with submitochondrial particles and the low absorption at 830nm($\Delta E_{m830-740\text{nm}}=1.0$, Nicholls and Chanady 1982) make it very difficult to monitor the Cu_A steady state with the submitochondrial particles.

The dibucaine effect on the enzyme kinetics in both high and low ionic strength systems was also studied

Fig. 31

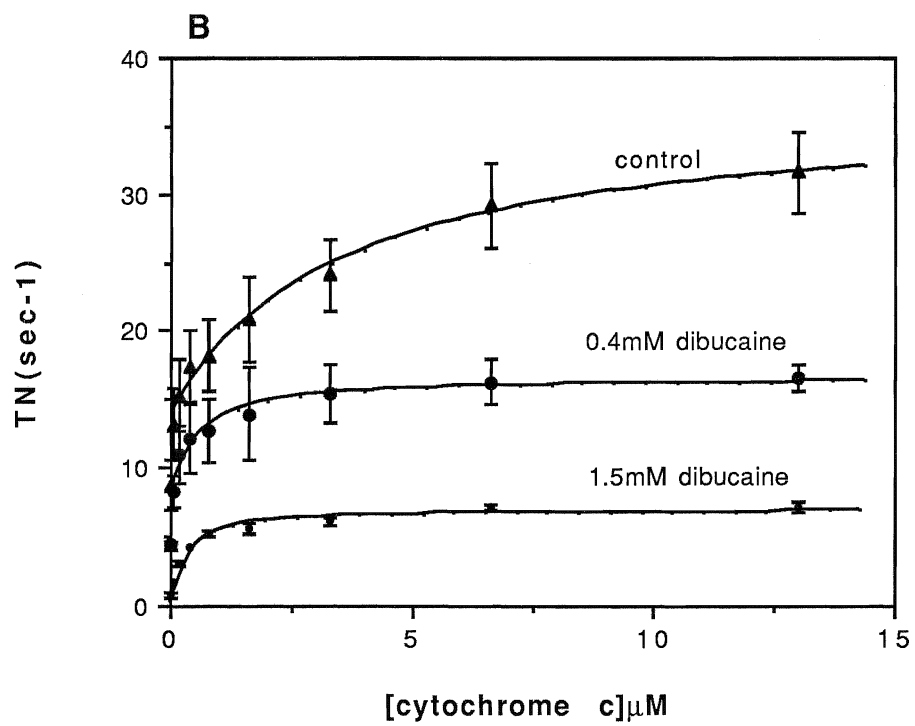
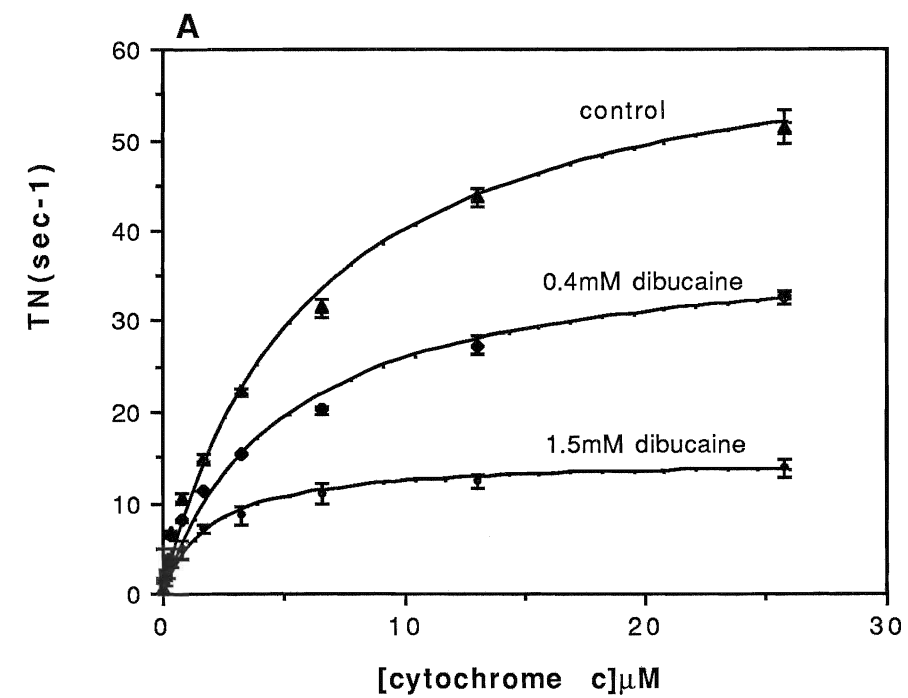


Fig.31 Effect of dibucaine on cytochrome oxidase turnover at high and low ionic strengths: Polarographic study 114

The experiments were carried out in 10mM KHEPES plus 70mM K₂SO₄ or 10mM KHEPES plus 4mM K₂SO₄, pH 7.37, 0.015% lauryl maltoside at 30°C with a Clark type oxygen electrode (Yellow Springs Instruments). 25.6μM EDTA, 3mM ascorbate, 0.174mM TMPD, 0-1.5mM dibucaine, 51 nM cytochrome oxidase and various concentrations of cytochrome c as indicated were added sequentially.

The turnover is calculated from the slope of the oxygen electrode traces. The mean turnover is shown with ± 1 standard deviation. (n=3).

- A. High ionic strength (10mM KHEPES plus 70mM K₂SO₄).
- B. Low ionic strength (10mM KHEPES plus 4mM K₂SO₄).

polarographically (fig. 31). To keep buffering constant, 10mM KHEPES plus 70mM K_2SO_4 or 4mM K_2SO_4 were used instead of the potassium phosphate buffer. Fig. 31 reveals that at a higher ionic strength, the turnover number of the enzyme increases hyperbolically with the cytochrome *c* concentration, while at a lower ionic strength, a biphasic, non-hyperbolic rise is seen. This general phenomenon has been explained by supposing that the enzyme has two binding sites for cytochrome *c* (Cooper 1990), one a "tight" site, and the other a "loose" site. At low ionic strengths, both sites are catalytically functional, while at high ionic strengths, only one binding site is catalytically functional. Fitting the data from Fig. 31 with a Double Michaelis function in the Multifit™ programme, the maximum velocities at the "tight" site V_{mT} and the "loose" site V_{mL} can be obtained. Fig. 32 shows that even at high ionic strength (10mM KHEPES plus 70mM K_2SO_4), there is some activity at both binding sites. Perhaps the ionic strength employed here was not high enough to eliminate fully the biphasicity. Dibucaine has little effect on the V_{mT} in both high and low ionic strengths, but it decreases the $V_{m(tot)} (=V_{mT} + V_{mL})$ substantially. Dibucaine does not affect K_{mT} and K_{mL} at either high or low ionic strengths (Fig. 33). So apparently dibucaine inhibits the "loose" binding site of the enzyme non-competitively, decreasing V_{mL} without affecting the kinetics of the "tight" site.

Uncompetitive, noncompetitive and mixed types of inhibition have been suggested for dibucaine-induced inhibition (Singer 1982 & 1983, Casanovas et al 1983). Here I report a

Fig.32

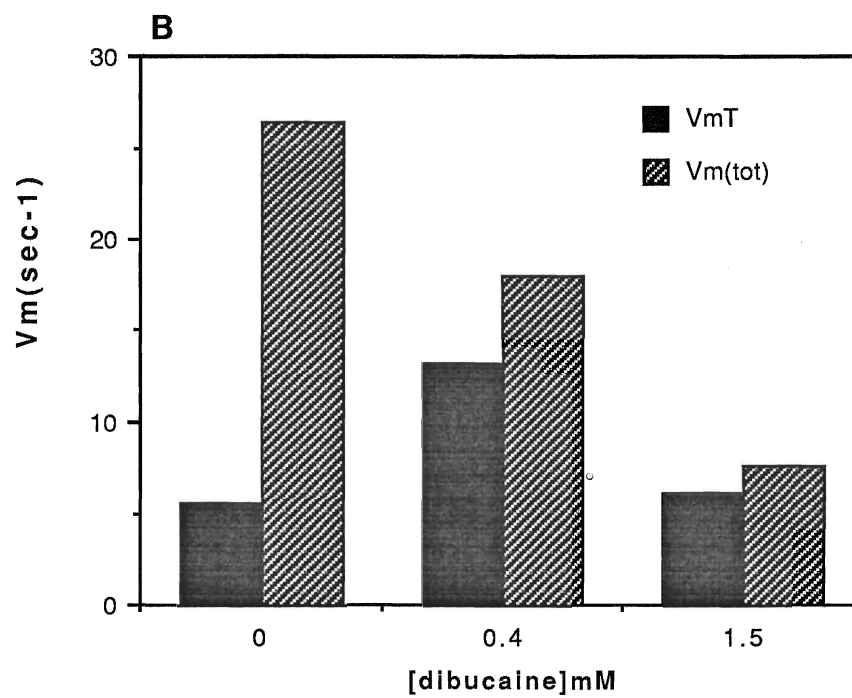
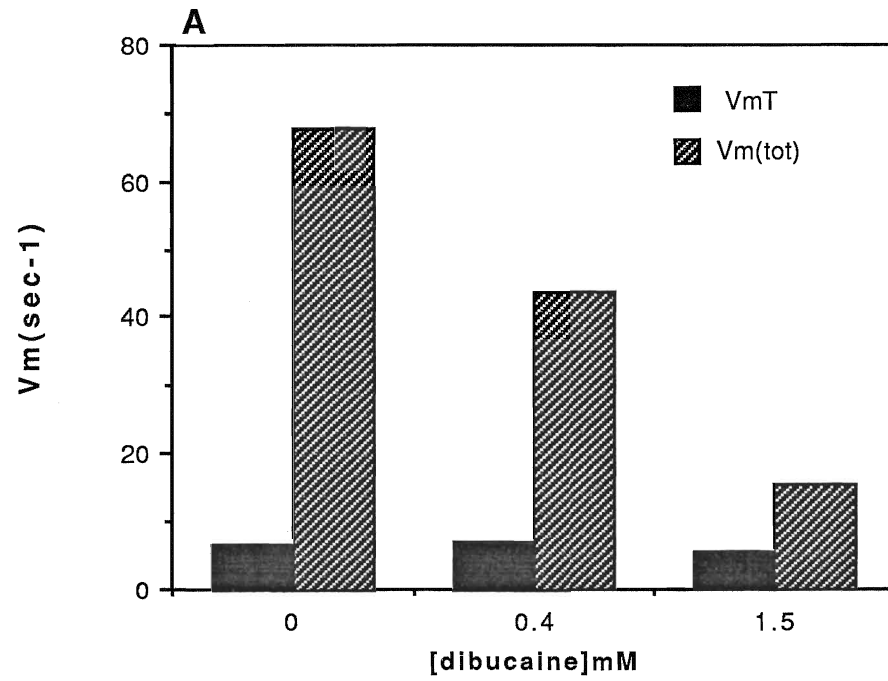


Fig.32 Dibucaine effect on V_{\max} values for cytochrome oxidase at high and low ionic strengths. 116

V_{\max} values were obtained by fitting the data in Fig.31 to a "Double Michaelis" function using the **Multifit™** programme. Error bars are not shown (but see Fig. 31).

Conditions as in Fig.31.

A. High ionic strength(10mM KHEPES plus 70mM K_2SO_4).

B. Low ionic strength(10mM KHEPES plus 4mM K_2SO_4).

noncompetitive inhibition of cytochrome oxidase activity by dibucaine. It may be noted that an apparent uncompetitive behaviour could be derived from results under biphasic binding conditions where only the second phase is dibucaine-sensitive. This may account for the earlier reports of uncompetitive and mixed inhibition patterns.

The dibucaine-reconstituted cytochrome oxidase interaction was also investigated polarographically (Fig. 34). When a low concentration ($< 1\text{mM}$) of dibucaine was added to the tightly controlled cytochrome oxidase-contained proteoliposomes (Fig. 34A), a stimulation of the respiration rate was seen. The dibucaine concentration causing half maximal stimulation is estimated to be 0.2mM . The respiration rate reached a saturating level of $70\mu\text{M}$ electron equivs. sec^{-1} when the dibucaine concentration exceeded 1mM . This can be best explained by the ΔpH -dissipating effect of dibucaine, since dibucaine is a membrane - permeable weak base. When the proteoliposomal respiration was released by ionophores (FCCP plus valinomycin), dibucaine caused a progressive decrease of the respiration rate with a $K_i = 0.4\text{mM}$, suggesting that in addition to the ionophore effect, dibucaine also had an inhibition effect. The ionophore effect of dibucaine is further supported by the decrease of the respiratory control ratio in the presence of dibucaine (Fig. 34B).

Fig.33

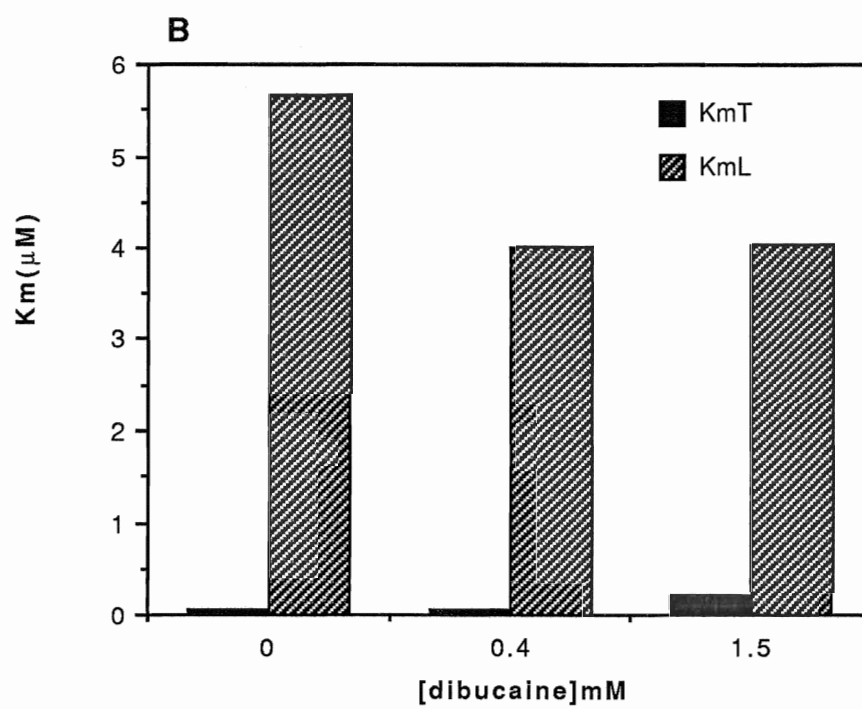
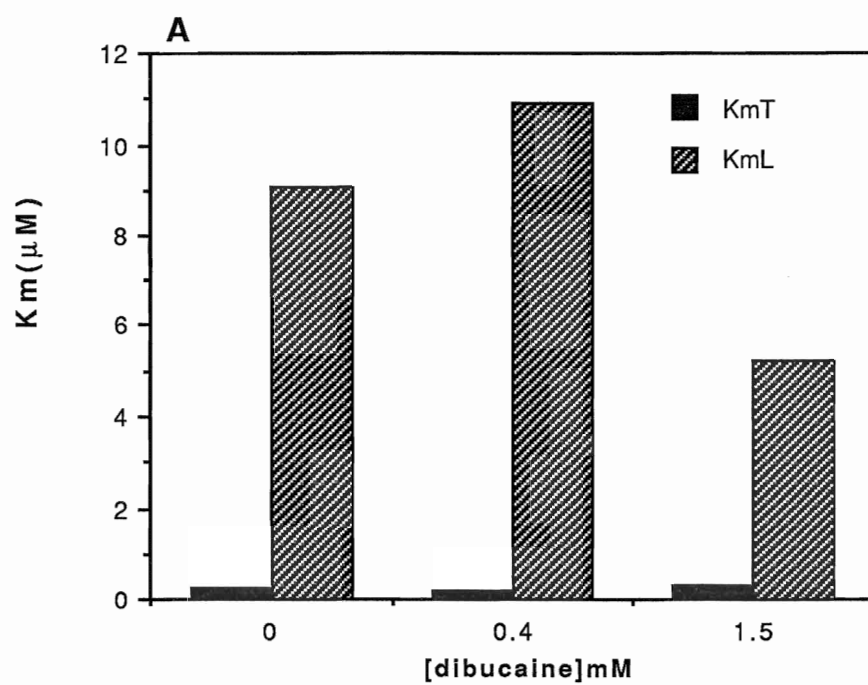


Fig. 33 Dibucaine effect on K_m values for cytochrome c and cytochrome oxidase at high and low ionic strengths. 118

K_m values were obtained by fitting the data in Fig.31 to a "Double Michaelis" function using the **Multifit**TM programme. Error bars are not shown (but see Fig. 31).

Conditions as in Fig.31.

A. High ionic strength (10mM KHEPES plus 70mM K_2SO_4).

B. Low ionic strength (10mM KHEPES plus 4mM K_2SO_4).

Fig. 34

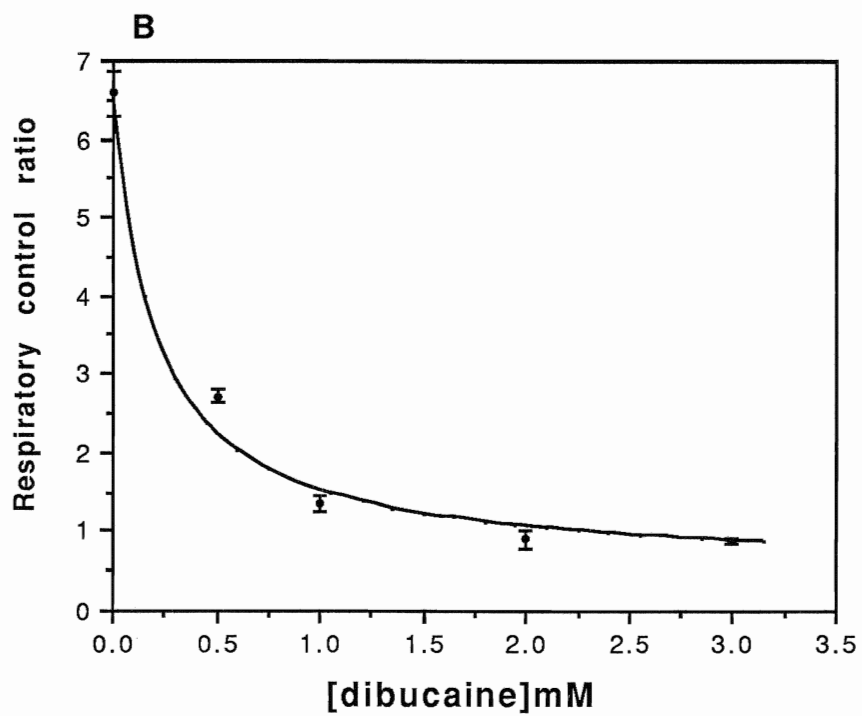
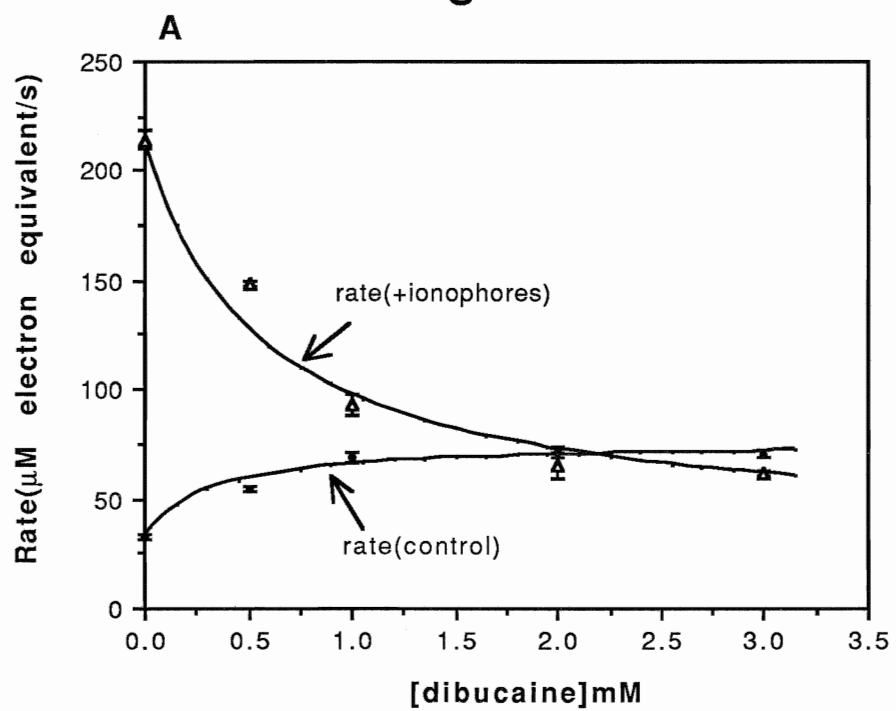


Fig. 34 The dibucaine effect on the respiration of reconstituted cytochrome oxidase . 119

Sets of experiments were carried out in 50mM potassium phosphate, pH 7.37, at 30°C with a Clark type oxygen electrode (Yellow Springs Instruments). 24 μ M EDTA, 5.4mM ascorbate, 0.18mM TMPD, 12 nM reconstituted cytochrome oxidase, and 24 μ M cytochrome *c* were added. Dibucaine was present at the indicated concentrations. The respiration rates were calculated from the slopes of oxygen electrode traces. The average respiration rates are shown \pm 1 standard deviation ($n = 3$). The respiratory control ratios were calculated as the ratios between the control respiration rate and the respiration rate after adding ionophores (1 μ M valinomycin plus 0.16 μ M nigericin).

A. Respiration rates plotted against dibucaine concentration.

Open triangles : uncontrolled rate(+ ionophores)

Closed circles : controlled rate (- ionophores)

Continuous lines: arbitrary exponential fits.

B. Respiratory control ratio plotted as a function of dibucaine concentration .

Closed circles : ratios of rates from Fig. 34A .

Continuous line : exponential fit assuming the respiratory control ratio equals 1 at high dibucaine concentrations.

Using spectrophotometric and oxygen electrode techniques, the effects of valinomycin and dibucaine upon isolated cytochrome *c* oxidase and cytochrome *c* oxidase in membrane systems are investigated here. It is found that valinomycin and dibucaine cause a similar but not identical red shift of the Soret peak in the enzyme spectrum. In addition to their inhibitory effects on the enzyme activity, valinomycin and dibucaine can also act as ionophores in cytochrome oxidase containing vesicle systems.

Valinomycin, in the form of its potassium complex, binds to the isolated enzyme in some hydrophobic region of the protein. This region may have some anionic character, as valinomycin- K^+ can form quite specific complexes with hydrophobic anions including the FCCP anion itself (O'Brien et al 1978). However, the dependence on the presence of K^+ is more likely due to a conformational change of the valinomycin molecule structure upon binding with K^+ than to a involvement of electrostatic forces (Fig. 9). The valinomycin molecule can assume different conformations in different media (Ovchinnikov 1974). In non-polar media, it assumes a compact symmetric structure with the six carbonyl oxygen atoms pointing away from the centre; in polar media, it assumes a flatter structure with the six carbonyl oxygen atoms locating on one plane, forming a triangle (Fig. 3B). Upon binding the K^+ ion, all the six carbonyl oxygen atoms become

liganded to the K^+ at the centre , forming an octahedral-like shape with the oxygen atoms from the peptide bonds pointing outwards. Probably these oxygen atoms from the peptide bonds as well as the hydrophobic side chains are responsible for binding to the enzyme. This site may be located somewhere near the binuclear centre, as its occupancy causes the Soret band red shift(an apparent high- to low- spin state change). The effect is distinct from that induced in 'pulsed' enzyme , and more similar to the cyanide-induced change, although of a smaller magnitude by about 60%. Like the cyanoenzyme, and unlike the 'pulsed' form, the valinomycin-enzyme complex is inhibited. But unlike the cyanide complex, the inhibition is incomplete. This inhibition occurs with both isolated and vesicular enzyme(Fig. 10, Fig. 13) at a valinomycin concentration in the micromolar range.

Two effects occur at lower valinomycin concentrations(Fig. 13). These are the stimulation of flux in the absence of other ionophores and the stimulation in the presence of nigericin. The former may be due to the action of valinomycin as a proton carrier(Hodarnau et al 1986). The latter is presumably due to the collapse of the controlling membrane potential (Wrigglesworth et al. 1990). It is not the same as the effect on the isolated oxidase. The stimulation occurs in the nanomolar range and is clearly distinguished from the direct and partially inhibitory effects (this thesis , Steverding and Kadenbach 1990, Prochaska and Wilson 1991).

The valinomycin-induced conformational change was also

studied by monitoring the protein fluorescence and phosphorescence. There are three amino acid residues(La^yrowicz 1983) which contribute to luminescence : tryptophan(trp), tyrosine(tyr) and phenylalanine(phe). The emission from phenylalanine is rarely observed because of its relatively low absorption in the usual protein excitation wavelength range. Tyrosine luminescence is also less common than that of tryptophan, one reason being that energy can be transferred from excited tyrosine residues to tryptophan residues. Above 295nm, the absorption is due primarily to tryptophan. So tryptophan can be selectively excited at 295nm-305nm. As I have shown in Fig. 14 , valinomycin has some quenching effect on the enzyme fluorescence , supporting the idea of a conformational change induced by valinomycin. In addition, the nitrite quenching behaviour was also altered in the presence of valinomycin for an excitation wavelength of 260nm(Fig. 16). I propose that when the excitation wavelength is 290nm, only tryptophan residues are excited, valinomycin has little effect. At an excitation wavelength of 260nm, some tyrosine residues are also excited. Valinomycin causes a conformational change of the protein structure that prevents the access to one part of these tyrosine residues by the quencher nitrite; this results in a decreased overall quenching of the phosphorescence signal(Table 3) . On the other hand, the quenching constant K_D itself increases in the presence of valinomycin , indicating that some residues become more accessible to nitrite because of this valinomycin-induced conformational change .

Comparison of the effects of dibucaine upon COV systems (Fig. 34) and upon the intact enzyme (Fig. 19 and 26) shows that like valinomycin $-K^+$, there are two different types of dibucaine effect. Proteoliposomal activation requires 0.1 to 0.5mM anaesthetic while inhibition involves 0.5 to 5mM levels. The rates are also different. The ionophore-like behaviour is rapid, while the enzyme binding is slow, requiring tens of minutes or even hours for completion in the absence of turnover (Fig.20A). Inhibition still requires significant times to develop in actively turning over system (Fig.27A). Most of my inhibitor studies involved preincubation of the enzyme and the inhibitor. Similar conclusions can be drawn from the results of Chazotte and Vanderkooi (1981) who recognized stimulatory and inhibitory concentration ranges.

Vanderkooi and Chazotte(1982) and Stringer and Harmon (1990), used dibucaine to probe the oxidase mechanism. The latter observed blockage of both ascorbate plus TMPD dependent cytochrome a_3 reduction and of Cu_A reduction with normal cytochrome c depleted beef heart mitochondria. Inhibitors that block cytochrome a_3 reduction, such as cyanide, promote reduction of Cu_A ; and inhibitors of Cu_A reduction normally have no effect upon the binuclear $a_3 Cu_B$ centre. In the present experiments, low concentrations of dibucaine(<5mM) were found to inhibit the enzyme by interfering with electron transfer between cytochrome a and the binuclear centre. The steady states of Cu_A were little affected by the presence of dibucaine,

and the anaerobic transition of the cytochrome *a₃* was 124 kinetically very similar to the transition in the controls. So the attack site of dibucaine apparently is the electron transfer between cytochrome *a* and the binuclear centre, not the CuA centre as Stringer and Harmon (1990) suggested.

That the dibucaine-cytochrome oxidase interaction is kinetically reversible has been demonstrated by several authors (Vanderkooi and Chazotte 1982, Grouselle et al 1990). Although I have not directly examined such reversibility spectroscopically, the results described here suggest that, like the kinetic effects, the spectroscopic ones are also reversible. On the other hand, there is no mention in the literature of the reversibility of valinomycin-cytochrome oxidase interaction, but, judged from its relatively small maximal effect upon the oxidase activity, and from its adherence to the binding equation, presumably this process is also a reversible one. Although valinomycin and dibucaine cause superficially similar spectral shifts of the enzyme to those caused by conventional ligands such as cyanide, the interactions are fundamentally different. The differences are: (i) both are large amphiphilic molecules which bind the protein structure instead of haem groups; (ii) the changes are less marked than with cyanide; (iii) unlike cyanide, only partial inhibition is achieved; and, (iv) no dramatic spectral changes are seen during steady state reduction in the presence of these substances (Fig. 23) while cyanide, azide and formate cause marked spectral changes during turnover.

Valinomycin K^{+} - and dibucaine-oxidase interactions are probably analogous (cf. Steverding and Kadenbach 1990). In both cases an amphiphilic monocation interacts with the enzyme in a region distinct from the binuclear centre and the cytochrome *c* binding site. Dibucaine does not affect formate binding, which occurs equally with free and dibucaine-bound enzyme; formate can bind to either resting or 'pulsed' enzyme to give a complex almost indistinguishable from the 'high-spin' resting form (Moody et al 1991; Schoonover and Palmer 1991). The final valinomycin or dibucaine complex has a modified Soret peak and shows diminished but not zero activity. The spectral change induced by valinomycin is the more marked, but valinomycin is less effective in inhibiting the enzyme. These spectral and kinetic effects identify an enzyme site which influences electron transfer between cytochrome *a* and the cytochrome *a₃* Cu_B centre. Somewhere between cytochrome *a* and the binuclear centre lies a hydrophobic and perhaps anionic site that can bind fairly large species so that the resting *a₃* Cu_B spectrum is modified and electron transfer slowed (cf. ATP binding, Bisson et al 1987). The exact location of this site is difficult to determine from currently available knowledge. Subunit III is known to be somehow related to proton pumping activity (Brunori et al 1987; Prochaska and Fink 1987), and it is easy to deplete the enzyme of subunit III (Cooper et al 1991). The depleted enzyme shows a red-shifted Soret peak (Tihova et al 1992). Sone and Nicholls (1984) reported that after heating the oxidase to 43.5°C , the

enzyme lost H^+ -pumping capability without affecting turnover. These authors could not rule out the possibility of a functional dissociation of subunit III. The Soret peak of heated cytochrome oxidase was also red shifted. Such red shifts of the Soret peak are related to dissociation or damage to subunit III. Dibucaine causes a partial dissociation of the F_1 complex (Chazotte, et al 1982). It is thus possible that dibucaine, and perhaps valinomycin as well, binds at the interface of Subunits I and III, causing a partial dissociation of subunit III from the rest of the enzyme, which in turn triggers a conformational change of the whole enzyme structure. The major aspects of valinomycin- and dibucaine- oxidase interactions are summarized in Table 5, to allow comparisons to be made.

I propose the scheme for valinomycin and dibucaine inhibition in Fig. 35, to compare with other inhibitors of cytochrome oxidase. Hill(1991) claims that the Cu_A site is probably the first acceptor of electrons entering from cytochrome c . Polylysine competes with cytochrome c for the binding site on subunit II, thus inhibiting the reduction of Cu_A by cytochrome c . Cyanide, azide and formate are ligands of the binuclear centre, so they inhibit entrance of electrons into that centre. Carbon monoxide occupies the dioxygen binding site (Nicholls and Chance 1974), thus inhibiting the reoxidation of the binuclear centre. Finally, valinomycin and dibucaine cause a conformational change of subunit I, diminishing the rate of the electron transfer between cytochrome a and the binuclear centre.

Table 5

Ligand	ΔE_{mM} 433-413nm (mM ⁻¹ cm ⁻¹)	K_d (with resting enzyme)	Inhibition type	K_i	Maximum inhibition	Ionophore effect concentration
Valinomycin	22	2.5-3.0 μ M	non- competitive	1.0 μ M	55%	< 0.05 μ M
Dibucaine	9.5	0.65mM	non- competitive	0.7mM	80%	0.1-0.5mM

**Table. 5 Comparison of valinomycin- and dibucaine-
cytochrome c oxidase interactions.** 127

The values listed summarize the results shown in Figs. 7, 11, 21 ,
and 26. The conditions in each case are listed in the legends to
these figures.

Fig. 35

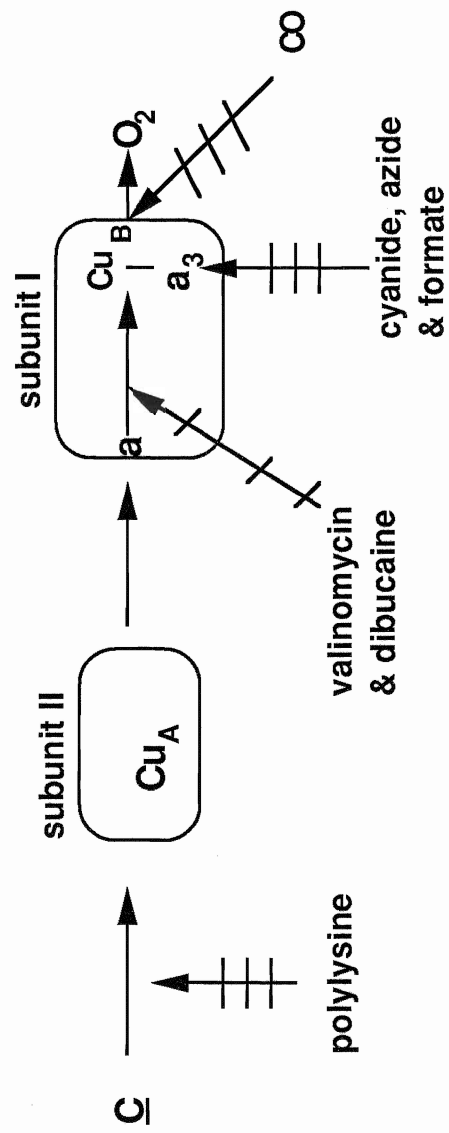


Fig. 35. A scheme for inhibition of electron transport through cytochrome c oxidase to molecular oxygen.

128

CONCLUSIONS

129

(1) Valinomycin- K^+ complex binds with the isolated cytochrome *c* oxidase with a K_D in the micromolar range, causing a red shift of the Soret peak in the enzyme spectrum and a maximal 55% inhibition of the enzyme activity.

(2) The membrane potential dissipating ability of valinomycin saturates at a much lower concentration ($< 0.05\mu M$) than required to cause an inhibition.

(3) Dibucaine binds with the isolated cytochrome *c* oxidase with a $K_D \approx 0.5mM$, causing a biphasic red shift of the Soret peak and a maximal 80% inhibition of the enzyme activity.

(4) Dibucaine acts as an ionophore in the concentration range of 0.1-0.5mM, and it acts as an enzyme inhibitor at the 0.5mM to 5mM levels.

(5) Both valinomycin and dibucaine inhibit cytochrome *c* oxidase non-competitively by causing a conformational change of the protein structure which modifies the spectrum of the $a_3 Cu_B$ centre and diminishes the rate of electron transfer between cytochrome *a* and the binuclear centre.

REFERENCES

130

Albracht, S.P.J., Van Verseveld, H.W., Hagen, W.R. and Kalkman, M.L.1980. A comparison of the respiratory chain in particles from *Paracoccus Denitrificans* and bovine heart mitochondria by EPR spectroscopy. Biochim. Biophys.Acta , **593** : 173-186

Azzi, A., Casey, R.P., and Nalecz, M.J. 1984. Effect of DCCD on enzymes of bioenergetic relevance. Biochim. Biophys. Acta, **768**: 209-226

Babcock, G. T., Vickery, L.E. and Palmer, G. 1976 . Electronic state of heme in cytochrome oxidase. I . Magnetic circular dichroism of the isolated enzyme and its derivatives. J. Biol. Chem. **251** : 7907-7919

Babcock, G. T., Callahan, P. M., Ondrias, M. R. and Salmeen, I. 1981. Coordination geometries and vibrational properties of cytochrome *a* and *a₃* in cytochrome oxidase from Soret excitation Raman spectroscopy. Biochemistry, **20**: 959-966

Babcock, G. T., and Wikstrom, M. 1992. Oxygen activation and the conservation of energy in cell respiration. Nature, **356** : 301-309

Bisson,R., Jacobs, B. and Capaldi, R.A. 1980 . Binding of arylazidocytochrome *c* derivatives to beef heart cytochrome *c* oxidase: Cross-linking in the high- and low-affinity binding sites. Biochemistry, **19** : 4173-4178

Bisson, R., and Montecucco,C. 1982. Different polypeptides of bovine heart cytochrome *c* oxidase are in contact with cytochrome *c*. FEBS lett. **150** : 49-53

Bisson,R., Schiavo, G., and Montecucco, C. 1987. ATP induced conformational changes in mitochondrial cytochrome *c* oxidase. J. Biol. Chem. **262** : 5992-5998

Brittain, T. and Greenwood, C. 1976. Kinetic studies on the binding of cyanide to oxygenated cytochrome *c* oxidase. *Biochem. J.* **155** : 453-455

Brodie, J. D. and Nicholls, P. 1970. Metabolism and enzymology of fluorosuccinic acid . I. Interaction with the succinate oxidase system . *Biochim. Biophys. Acta*, **198** : 423-437

Brunori, M., Antonini, G., Malatesta, F., Sarti, P., and Wilson, M. 1987 . Cytochrome *c* oxidase . Subunit structure and proton pumping. *Eur. J. Biochem.* **169** : 1-8

Brunori, M., Colosimo, A., Rainoni, O., Wilson, M. T. and Antonini, E. 1979. Functional intermediates of cytochrome oxidase . Role of "pulsed" oxidase in the pre-steady state and steady state reactions of the beef enzyme. *J. Biol. Chem.* **254** : 10769-10775

Buse, G., Hensel, S., and Fee, J.A. 1989. Evidence for cytochrome *c* oxidase subunit I and a cytochrome *c*-subunit II fused protein in the *c₁aa₃* of *Thermus thermophilus*. *Eur. J. Biochem.* **181** : 261-268

Casanovas, A.M. ,Labat, C. ,Courriere, P. and Oustrin, J. 1985. Model for action of local anesthetics with cytochrome oxidase . *Biochem. Pharma.* **34** : 3187-3190

Casanovas, A.M., Nebot, M.F.M. ,Courriere, P. and Oustrin, J. 1983. Inhibition of cytochrome *c* oxidase activity by local anesthetics. *Biochem. Pharma.* **32** : 2715-2719

Chan, S.I. and Li, P. M. 1990 . Cytochrome *c* oxidase : understanding nature's design of a proton pump . *Biochemistry*, **29** : 1-12

Chanady, G. A., Chang, E., and Proteau, G. A. 1985. Appendix : A program package linking the Beckman DU-7 spectrophotometer with an Apple IIplus microcomputer. *Canad. J. Biochem. Cell. Biol.* **63** : 160-161 .

Chazotte, B. and Vanderkooi, G. 1981. Multiple sites of inhibition of mitochondrial electron transport by local anesthetics . Biochim. Biophys. Acta, **636**: 153-161

Chazotte, B. , Vanderkooi, G. and Chignell, D. 1982. Further studies on F₁-ATPase inhibition by local anesthetics. Biochim. Biophys. Acta, **680** : 310-316

Colman, P.M. , Freeman, H.C., Gass, J.M., Murata, M., Norris, V.A., Ramshaw, J.A.M., and Venkatappa, M.P.1978 . X-ray crystal structure analysis of plastocyanin at 2.7Å resolution. Nature , **272** : 319-324

Cooper, C.E. 1990. The steady state kinetics of cytochrome c oxidation by cytochrome c oxidase. Biochim. Biophys. Acta, **1017** : 187-223

Cooper, C.E., Nicholls , P. and Freedman, J.A. 1991. Cytochrome c oxidase : structure , function and membrane topology of the polypeptide subunits . Biochem. Cell Biol. **69** : 586-607

Cramer, W.A. and Knaff. D.B. 1991. "Energy transduction in biological membranes ." (Cantor, C.R. , ed.) Springer-Verlag press, New York.

Crinson, M. and Nicholls , P. 1992. Routes of electron transfer in beef heart cytochrome c oxidase : is there a unique pathway used by all reductants ? Canad. J. Biochem. Cell. Biol. **70** : 301-308

Dabadie, P. , Bendriss, P. , Erny, P. and Mazat, J-P. 1987. Uncoupling effects of local anesthetics on rat liver mitochondria. FEBS Lett. **226**: 77-82

Eftink, M.R., Puri, R.K. and Ghahramani, M.D. 1985. The pH dependence of the binding of dibucaine to dimyristoylphosphatidylcholine vesicles. Biochim. Biophys. Acta, **813** : 137-140

Einarsdottir, O., and Caughey, W.S. 1984 . Zinc is a constituent of bovine heart cytochrome *c* oxidase preparations. *Biochem. Biophys. Res. Commun.* **124** : 836-842

Einarsdottir, O., and Caughey, W.S. 1985. Bovine heart cytochrome *c* oxidase preparations contain high affinity binding sites for magnesium, as well as for zinc, copper and heme iron. *Biochem. Biophys. Res. Commun.* **129**: 840-847

Erecinska, M. 1977 . A new photoaffinity-labelled derivative mitochondrial cytochrome *c* . *Biochem. Biophys. Res. Commun.* **76** : 495-501

Erecinska, M. and Wilson, D.F. 1978. Cytochrome oxidase : a synopsis. *Arch. Biochem. Biophys.* **188** : 1-14

Fukumori, Y., and Yamanaka, T. 1984. Two K_m values for cytochrome *c* of *aa₃*-type two-subunit cytochrome oxidase of *Nitrobacter agilis*. *FEBS lett.* **170** : 301-304

Gornall, A. G. , Bardawill , G. J. and David, M.A. 1949. Determination of serum proteins by means of the Biuret reaction. *J. Bio. Chem.* **177** : 751-766

Grouselle, M. Tueux, O. Dabadie, P. Georgescaud, D. and Mazat, J-P. 1990. Effect of local anesthetics on mitochondrial membrane potential in living cells . *Biochem. J.* **271**: 269-272

Haltia, T., Finel, M., Harms, N., Nakari, T., Raitio, M., Wikstrom, M., and Saraste, M. 1989 . Deletion of the gene for subunit III leads to defective assembly of bacterial cytochrome *c* oxidase. *EMBO J.* **8** : 3571-3579

Hartzell, C.R., Beinert, H., Babcock, G.T. , Chan, S. I. , Parlmer, R.A. and Scott, R.A. 1988. Heterogeneity in an isolated membrane protein. Has an "authentic" cytochrome *c* oxidase been identified ? *FEBS Lett.* **236** : 1-4

Hill , B.C. 1990. The reaction of the electrostatic cytochrome *c* - cytochrome oxidase complex with oxygen. *J. Biol. Chem.* **266**, 2219-2226

Hodarnau, A., Elsdén, J., Steenson, T. I. and Wigglesworth , J. M. 1986. Proton permeability of large unilamellar vesicles. *Biochem. Soc. Trans.* **14** , 1218-1219

Hoppe, J., and Sebald , W. 1984 . The proton conducting F_0 -part of bacterial ATP synthetases. *Biochim. Biophys. Acta*, **768** : 1-27

Ishizuka, M., Machida, K., Shimada, S., Mogi, A., Tsuchiya T., Ohmori, T., Souma, Y., Gonda, M., and Sone, N. 1990. Nucleotide sequence of the gene coding for four subunits of a cytochrome *c* oxidase from the thermophilic bacterium PS3. *J . Biochem.(Tokyo)***108** : 866-873

Jones, M.G., Bickar, D., Wilson, M. T., Brunori, M., Colosimo, A. and Sarti, P. 1984. A re-examination of the reactions of cyanide with cytochrome *c* oxidase. *Biochem. J.* **220** : 57-66

Kadenbach, B. 1986. Regulation of respiration and ATP synthesis in higher organisms : Hypothesis . *J. Bioenerg. Biomemb.* **18** : 39-54

Kadenbach, B., Jarausch, J., Hartmann, R., and Merle, P. 1983. Separation of mammalian cytochrome *c* oxidase into 13 polypeptides by a sodium dodecyl sulfate-gel electrophoresis procedure. *Anal. Biochem.* **129** : 517-521

Kadenbach, B., and Stroh, A., 1984 . Different reactivity of carboxylic groups of cytochrome *c* oxidase polypeptides from pig liver and heart. *FEBS lett.* **173** : 374-380

Keilin,D., and Hartree, E.F. 1939. Cytochrome and cytochrome oxidase . *Proc. Roy. Soc. B*, **127** : 167-191

Kuboyama, M., Yong, F.C., and King, T. E. 1972. Studies on cytochrome oxidase . VIII: Preparation and some properties of cardiac cytochrome oxidase. J. Biol. Chem. **247** : 6375-6383

Lakowicz, J. R. 1983. " Principles of fluorescence spectroscopy" . Plenum Press, New York.

Ludwig, B. 1982. In "Electron Transport and Oxygen Utilization" (Ed.C. Ho), Elsevier North Holland , Amsterdam, pp 293-296

MacDonald, A.G. and Wann, K. T. 1978. "Physiological aspects of anesthetics and inert gases", Academic Press, London

Mathews, C.K. and van Holde, K.E. 1990. "Biochemistry". Benjamin/Cummings Publishing Co. Ltd. New York .

Minnaert, K. 1961. The kinetics of cytochrome *c* oxidase. I. The system : cytochrome *c*-cytochrome oxidase-oxygen. Biochim. Biophys. Acta, **50** : 23-34

Mitchell, P. 1966a. "Chemiosmotic coupling and energy transduction." Glynn Research Ltd. Bodmin, U. K.

Mitchell, P. 1966b. "Chemiosmotic coupling in oxidative and photosynthetic phosphorylation." Glynn Research Ltd. Bodmin, U.K .

Mitchell, R., Brown, S., Mitchell, P. and Rich, P. R. 1992. Rates of cyanide binding to the catalytic intermediates of mammalian cytochrome *c* oxidase, and the effects of cytochrome *c* and poly-(l)-lysine . Biochim. Biophys. Acta, **1100**: 40-48

Moody, A.J. , Cooper, C.E., and Rich, P.R. 1991 . Characterisation of 'fast' and 'slow' forms of bovine heart cytochrome *c* oxidase . Biochim. Biophys. Acta, **1059** : 189-207

Musatov, A., and Konstantinov, A.A. 1988. Conformational change of cytochrome *a*₃ induced by oxidized cytochrome *c* . FEBS Lett. **238** : 295-299

Nicholls , P. 1975. Formate as an inhibitor of cytochrome *c* oxidase . Biochem. Biophys. Res. Comm. **67** : 610-616 136

Nicholls , P. 1976. The effect of formate on cytochrome *aa₃* and on electron transport in the intact respiratory chain. Biochim. Biophys. Acta, **430** : 13-29

Nicholls, P. 1978. A carbon monoxide induced complex of cytochrome *c* oxidase. Biochem. J. **173** : 1147-1150

Nicholls , P. 1983. " Biochemical research techniques ". (Wrigglesworth, J.M . ed.) John Wiley & Sons , New York.

Nicholls , P. , and Chanady, G.A. 1982. Titration and steady-state behaviour of the 830nm chromophore in cytochrome *c* oxidase. Biochem. J. **203** : 541-549

Nicholls , P. , and Chance, B. 1974. in " Molecular mechanisms of oxygen activation " (O. Hayashi, ed.). Academic Press, New York. pp479-534

Nicholls , P. , and Hildebrandt, V. 1978a. Binding of ligands and spectral shifts in cytochrome *c* oxidase. Biochem. J. **173**: 65-72

Nicholls , P. , and Hildebrandt, V. 1978b. Redox state of the partially reduced cytochrome *aa₃*-cyanide complex. Biochim. Biophys. Acta, **504** : 457-460

Nicholls , P. , and Sone, N. 1984. Kinetics of cytochrome *c* and TMPD oxidation by cytochrome *c* oxidase from the thermophilic bacterium, PS3. Biochim. Biophys. Acta, **767** : 240-247

Nicholls, P., Hildebrandt, V. and Wrigglesworth, J. M. 1980. Arch. Biochem. Biophys. **204** : 533-554

Nicholls , P. , Petersen, L.C., Miller, M. and Hansen, F.B. 1976. Ligand-induced spectral changes in cytochrome *c* oxidase and their possible significance. Biochim. Biophys. Acta, **449**: 188-196

O'Brien, T. A., Nieva-Gomez, D., and Gennis, R. B. 1978. Complex formation between the uncoupler carbonyl cyanide *p*-trifluoromethoxy phenylhydrazone (FCCP) and valinomycin in the presence of potassium. *J. Biol. Chem.* **253** : 1749-1751

Ovchinnikov, Y. A. 1974. Membrane active complexones. *Chemistry and biological function.* *FEBS Lett.* **44** : 1-21

Papp, S. , King, T. E. and Vanderkooi, J. M. 1991. Intrinsic tryptophan phosphorescence as a marker of conformation and oxygen diffusion in purified cytochrome oxidase. *FEBS Lett.* **283** : 113-116

Papp, S. and Vanderkooi, J. M. 1989. Tryptophan phosphorescence at room temperature as a tool to study protein structure and dynamics. *Photochem. Photobio.* **49** : 775-784

Penttila, T., Saraste, M., and Wikstrom, M. 1979. The number of subunits in bovine cytochrome *c* oxidase . *FEBS lett.* **101**, 295-300

Poole, R.K. 1988. Bacterial cytochrome oxidase in " Bacterial Energy Transduction " (Anthony , C. ed) Academic Press, New York, pp.231-249

Prochaska, L. J., Bisson, R., Capaldi, R.A., Steffens, G.C.M. , and Buse, G . 1981. Inhibition of cytochrome *c* oxidase function by dicyclohexylcarbodiimide. *Biochim. Biophys. Acta*, **637**: 360-373

Prochaska, L. J. , and Fink, P. S. 1987. On the role of subunit III in proton translocation in cytochrome *c* oxidase . *J. Bioenerg. Biomembr.* **19** : 143-166

Prochaska, L. J. and Wilson, K.S. 1991. Phospholipid vesicles containing bovine heart mitochondrial cytochrome *c* oxidase exhibit proton translocating activity in the presence of gramicidin. *Arch. Biochem. Biophys.* **290** : 179-185

Proteau, G. , Wrigglesworth, J.M. and Nicholls, P. 1983. Protonmotive functions of cytochrome *c* oxidase in reconstituted vesicles . Biochem. J. **210** : 199-205.

Reed, C. A. and Landrum, J. T. 1979. Structural models for the heme *a*₃ / copper active site of cytochrome *c* oxidase. FEBS Lett. **106**: 265-267

Saraste, M. 1990. Structural features of cytochrome oxidase. Quart.Rev. Biophys. **23**: 331-366

Saraste, M. , Penttila, T., Coggins, J.R., and Wikstrom, M. 1980. Structure of bovine cytochrome oxidase . FEBS lett. **114**, 35-38

Schoonover, J.R. and Palmer, G. 1991. Reaction of formate with the fast form of cytochrome oxidase : a model for the fast to slow conversion. Biochemistry, **30**: 7541-7550

Shaw, R.W., Hansen, R.E. and Beinert, H. 1978. Responses of the *a*₃ component of cytochrome *c* oxidase to substrate and ligand addition. Biochim. Biophys. Acta, **504**: 187-199

Singer, M. A. 1980. Interaction of drugs with a model membrane protein. Effects of four local anesthetics on cytochrome oxidase activity. Biochem. Pharm. **29**: 2651-2655

Singer, M. A. 1982. Interaction of drugs with a model membrane protein. Effect of dibucaine on cytochrome oxidase proteoliposomes. Biochem. Pharm. **31**:527-534

Singer, M. A. 1983. Interaction of drugs with a model membrane protein. Effects of local anesthetics on electron transfer and hydrogen uptake in ionophore stimulated cytochrome oxidase proteoliposomes. Biochem. Pharm. **32** : 1619-1625

Sone , N. and Nicholls, P. 1984. Effect of heat treatment on oxidase activity and proton-pumping capability of proteoliposome-incorporated beef heart cytochrome *aa₃* . Biochemistry, **23** : 6550-6554

Steffens, G.C.M., Biewald, R., and Buse, G. 1987. Cytochrome *c* oxidase is a three-copper, two-heme-A protein. Eur. J. Biochem. **164** : 295-300

Steverding, D. and Kadenbach, B. 1989. Valinomycin binds stoichiometrically to cytochrome *c* oxidase and changes its structure and function. Biochem. Biophys. Res. Comm. **160** : 1132-1139

Steverding, D. and Kadenbach, B. 1990. The K⁺-ionophores nonactin and valinomycin interact differently with the protein of reconstituted cytochrome *c* oxidase . J. Bioener. Biomem. **22** : 197-205

Stringer, B. K. and Harmon, H. J. 1990. Inhibition of cytochrome oxidase by dibucaine. Biochem. Pharmacol. **40**: 1077-1081

Thompson, D.A., Gregory, L., and Ferguson-Miller, S. 1985. Cytochrome *c* oxidase depleted of subunit III : proton-pumping , respiratory control, and pH dependence of the mid-point potential of cytochrome *a* . J. Inorg. Biochem. **23** : 357-364

Tihova, M., Tattrie , B., and Nicholls, P. 1992. (personal communication)

Trivedi, A. , Fantin, D.J., and Tustanoff, E.R. 1986. Role of phospholipid fatty acids on the kinetics of high and low affinity sites of cytochrome *c* oxidase . Biochem. Cell Biol. **64** : 1195-1210

Tweedle, M.F., Wilson, L.J., Garcia-Iniguez, L., Babcock, G.T. and Palmer, G. 1978. Electronic state of heme in cytochrome oxidase III. The magnetic susceptibility of beef heart cytochrome oxidase and some of its derivatives from 7-200 K. Direct evidence for an antiferromagnetically coupled Fe(III)/Cu(II) pair. J.Biol. Chem. **253** : 8065-8071

Van Buuren, K.J.H. , Nicholls, P. and Van Gelder, B.F. 1972. Biochemical and biophysical studies on cytochrome *aa₃* . VI. Reaction of cyanide with oxidized and reduced enzyme. Biochim. Biophys. Acta, **256** : 258-276

Vanderkooi, G. and Chazotte, B. 1982. Cytochrome *c* oxidase inhibition by anesthetics . Thermodynamic analysis. Proc. Natl. Acad. Sci. USA. **79** : 3749-3753

Wikstrom, M. 1977 . Proton pump coupled to cytochrome *c* oxidase in mitochondria. Nature(London), **266** : 271-273

Wikstrom, M. , Krab, K., and Saraste, M. 1981. Cytochrome oxidase , a synthesis, Academic Press, London.

Wikstrom, M. , Krab, K., and Saraste, M. 1981. Proton-translocating cytochrome complexes. Annu. Rev. Biochem. **50**: 623-655

Wilson , D. F. , Erecinska, M. and Owen, C.S. 1976. Some properties of the redox components of cytochrome *c* oxidase and their interactions. Arch. Biochem. Biophys. **175** : 160-173

Wilson , D. F. and Leigh, J. S. , Jr. 1972. Heme-heme interaction in cytochrome *c* oxidase in *situ* as measured by EPR spectroscopy. Arch. Biochem. Biophys. **150**: 154-163

Wilson , K. S., and Prochaska, L.J. 1990. Phospholipid vesicles containing bovine heart mitochondrial cytochrome *c* oxidase and subunit-III deficient enzyme : analysis of respiratory control and proton translocating activities. Arch. Biochem. Biophys. **282** : 413-420

Wrigglesworth, J. M., Cooper , C. E. , Sharpe , M., and Nicholls , P. 1990. The proteoliposomal steady state. Biochem. J., **270** : 109-118

Wrigglesworth, J. M., Ioannidis, N. and Nicholls, P. 1988. Spectrophotometric characterization of intermediate redox states of cytochrome oxidase. Ann. N. Y. Acad. Sci. **550** : 150-160.

Yewey, G.L., and Caughey , W.S. 1987. Metals and activity of bovine heart cytochrome *c* oxidase are independent of polypeptide subunits III, VII, a and b. Biochem. Biophys. Res. Commun. **148** : 1520-1526

Yonetani, T. 1960. Studies on cytochrome oxidase. J. Biol. Chem. **235**: 3138-3143